
Validation and Optimization of In Vitro Hepatocyte Systems and Physiologically Based Pharmacokinetic Modelling for Translation of Drug Metabolism to Human

Inauguraldissertation

zur

Erlangung der Würde eines Doktors der Philosophie

Vorgelegt der

Philosophisch-Naturwissenschaftlichen Fakultät

der Universität Basel

Von

Luca Docci

Basel, 2021

*Originaldokument gespeichert auf dem Dokumentenserver der Universität Basel
edoc.unibas.ch*

Genehmigt von der Philosophisch-Naturwissenschaftlichen Fakultät

auf Antrag von

Erstbetreuer: Dr. Stephen Fowler

Zweitbetreuer: Prof. Dr. Stephan Krähenbühl

Externer Experte: Prof. Dr. Michael Arand

Basel, den 30.03.2021

Prof. Marcel Mayor

Dekan der Philosophisch-
Naturwissenschaftlichen Fakultät

1 CONTENTS

2	Acknowledgements	6
3	High Level Summary	8
4	Abbreviations	10
5	Introduction	14
5.1	Drug Metabolism and Pharmacokinetics.....	14
5.1.1	Drug Development in the Pharmaceutical Industry	14
5.1.2	Drug Metabolizing Enzymes.....	17
5.1.3	UDP-Glucuronosyltransferases	21
5.2	In Vitro Hepatocyte Systems.....	27
5.2.1	Subcellular Fractions and Recombinant Enzymes	27
5.2.2	Hepatocyte Systems	29
5.2.3	Microphysiological Systems	31
5.3	Computational Approaches in Drug Research	33
5.3.1	Predictions of Drug Properties	33
5.3.2	Physiologically Based Pharmacokinetic Modelling	35
5.4	Outline and Aims of the Studies.....	45
6	Results	48
6.1	Paper 1.....	50
6.2	Paper 2.....	52
6.3	Paper 3.....	54
6.4	Preview Paper 4.....	56
7	Summary and Future Investigations.....	74
8	Conclusion.....	80
9	References	82

2 ACKNOWLEDGEMENTS

I am truly grateful that I was offered the opportunity to devote my time on a very exciting field of research within a company that is always seeking for new ways of delivering cutting-edge treatments to the patients. The years of my PhD project at Roche were very educative and prepared me for the future steps of my career. Yet, the project would not have been the same without the support from many of my professional and personal environment.

I want with utmost respect thank Stephen Fowler and Neil Parrott which were mentoring the PhD project. Stephen is a true expert in the field of enzymology and Neil a true expert in physiologically based pharmacokinetic modelling and simulation. I will always appreciate your dedication and how you made the project successful with your valuable skills and inputs. I also want to thank Stephan Krähenbühl for his supervision of the project. He always provided helpful support during the meetings and was a great aid in bringing the project forward. Then, I would like to acknowledge all my colleagues at Roche: Nicolás Milani, Aynur Ekiciler, Florian Klammers, Birgit Molitor, Kenichi Umehara, Björn Wagner, Na Hong Qiu, Eva Aparicio, and Lilian Richter. Your support in the laboratory and for other activities was crucial for me and I could not have finalized the project without your help.

My personal environment always gave me strength to go through the project. Amongst many, I would like to highlight my family: Brigitte Docci-Tschudin, Mauro Docci, Carmen Docci, Nando Docci, Gabriela Docci, and the newest member: Sergio-Mauro Docci; and my flat mates: Olivia Fischer and Kilian Erbacher. True friends on my side were Fabian Wenger and Nicolas Eichenberger, which always had an open door for me to find relaxation.

Finally, I would like to truly thank Nadine Schmidt Sanchez to whom I dedicate this work. She had way more difficult, yet distinct challenges to face during the period of my PhD project, for which I want to give her all my respect.

3 HIGH LEVEL SUMMARY

In the last few decades, great strides were made in predicting pharmacokinetic drug properties to reduce attrition rates of drug projects in the clinical phase due to unfavorable pharmacokinetic characteristics. Nonetheless, capability gaps still remained and emerged during the past years. Optimization of the metabolic stability of drugs to avoid metabolism by the cytochrome P450 enzymes led to increasing relevance of alternative drug metabolizing enzymes and routes of clearances. On a related note, the importance of UDP-glucuronosyltransferases as metabolizing enzymes for new chemical entities increased, which formed the challenge of determining and translating the metabolism of a less well-established enzyme family. Furthermore, novel *in silico* and *in vitro* test systems are constantly adopted in the pharmaceutical industry with the promise to improve the quality of the pre-clinical data, whereas the systems must be fundamentally evaluated and assessed before routine application during the drug development.

The aims of the PhD project was to address current capability gaps to enhance the confidence in the prediction of human clearance and to evaluate a novel *in vitro* hepatocyte system. We investigated the translatability of UGT-mediated drug clearance by using a promising hepatocyte co-culture and physiologically based pharmacokinetic modelling and simulation. In addition, we aimed to advance the adoption of novel *in vitro* hepatocyte system that potentially offers new capabilities of determining more complex research questions during the drug development. These studies resulted in three published manuscript and in one on-going work that is planned to be finalized and submitted in the near future:

1. **In Vitro to In Vivo Extrapolation of Metabolic Clearance for UGT Substrates Using Short-Term Suspension and Long-Term Co-Cultured Human Hepatocytes**
2. **Construction and Verification of Physiologically Based Pharmacokinetic Models for Four Drugs Majorly Cleared by Glucuronidation: Lorazepam, Oxazepam, Naloxone, and Zidovudine**
3. **Application of New Cellular and Microphysiological Systems to Drug Metabolism Optimization and Their Positioning Respective to In Silico Tools**

4. Optimization of a Liver-on-Chip System for DMPK Application and Combination with Modelling and Simulation

We demonstrated for the first time that an improvement is achieved upon the application of a hepatocyte co-culture for the in vitro to in vivo extrapolation of metabolic clearance. We could further identify and discuss current limitations for physiologically based pharmacokinetic modelling and simulation based on well-constructed models. With the review, we reported the state of the art for the application of conventional and more advanced hepatocyte systems as parts of the value chain during drug development in relation to computational approaches. Finally, we evaluated a microphysiological system (i.e. liver-on-chip device) for the application of DMPK determination. Overall, the studies have a positive impact on the decision-making process during the pre-clinical drug development and increase the confidence in the application of the hepatocyte co-culture and PBPK modelling for UGT substrates.

To the structure of the thesis: The introduction will familiarize the reader to the elements that were key to the PhD program: metabolic clearance and factors affecting the drug metabolizing enzymes, in vitro hepatocyte systems for the determination of DMPK properties, and physiologically based pharmacokinetic modelling (i.e. computational approaches) and its relevance in the pharmaceutical industry. The introduction will further highlight the current gaps and limitations that exist in the field and elaborates on the outline and plans of the studies conducted during the project. The results section contains the manuscripts that report the core studies conducted in the past three years. Finally, the “Summary and Future Investigations” section summarizes the work with an emphasis on the impact of the studies for the pharmaceutical industry and complements the thesis with next investigations that should be conducted in order to extend the work.

4 ABBREVIATIONS

ADME	Absorption, Distribution Metabolism, Excretion
AhR	Aryl hydrocarbon receptor
AKR	Aldo-keto reductase
AO	Aldehyde oxidase
APR	Albumin production rate
AUC	Area under the curve
BCRP	Breast cancer resistance protein
BCS	Biopharmaceutic classification system
Caco-2	Colon carcinoma cell line
CADD	Computer-aided drug design
CAR	Constitutive androstane receptor
CES	Carboxylesterases
CL_{int}	In vitro intrinsic clearance
C_{max}	Maximum plasma concentration
CYP	Cytochrome P450
DDI	Drug-drug interactions
DME	Drug metabolizing enzymes
DMPK	Drug metabolism and pharmacokinetics
ECCS	Extended clearance classification system
EIH	Entry into human
EMA	European Medicines Agency
EPH	Epoxide hydrolase
ER	Endoplasmic reticulum
F	Bioavailability
f_a	Fraction absorbed into enterocytes
FDA	U.S. Food and Drug Administration
f_{DP}	Fraction of drug entering the portal vein
FIH	First in human
FMO	Flavin-containing monooxygenase

$f_{u,p}$	Fraction unbound in plasma
GFR	Glomerular filtration rate
GST	Glutathione-S-transferase
HLM	Human liver microsomes
IM	Intermediate metabolizers
IVIVE	In vitro to in vivo extrapolation
K_I	Inhibition constant
K_M	Michaelis constant
K_p	Tissue-to-plasma partition coefficient
LC-MS	Liquid chromatography-mass spectrometry
logD	Distribution coefficient
logP	Partition coefficient
M&S	Modelling and simulation
MAO	Monoamine oxidase
MBDD	Model based drug development
MPS	Microphysiological System
MRP	Multi-drug resistance-associated protein
MW	Molecular weight
NAT	N-acetyltransferase
NCE	New chemical entity
NDA	New drug application
OATP	Organic anion transporting polypeptide
OoC	Organ-on-Chip
PBPK	Physiologically based pharmacokinetic modelling
PD	Pharmacodynamic
P-gp	P-glycoprotein
PK	Pharmacokinetics
pKa	Acid dissociation constant
PM	Poor metabolizer
PXR	Pregnane X receptor
rhCYP	Recombinant human cytochrome P450
rhUGT	Recombinant human UDP-glucuronosyltransferase
SULT	Sulfotransferase

T_{max}	Time of maximum plasma concentration
UDPGA	Uridine diphosphate glucuronic acid
UGT	UDP-glucuronosyltransferase
URM	Ultra-rapid metabolizer
V_{max}	Maximum velocity
V_{ss}	Steady state volume of distribution
XO	Xanthine oxidase

5 INTRODUCTION

5.1 DRUG METABOLISM AND PHARMACOKINETICS

5.1.1 Drug Development in the Pharmaceutical Industry

The process from drug discovery to entry into market of a drug takes several years and is very costly (Figure 1). A high interest and expense is therefore invested into the refinement of predictive tools with the tenet “to fail early and fail cheap” to avoid late attrition of a drug candidate. Discontinuance of the drug development is mostly due to poor efficacy of the therapy, observed toxicity in animals, adverse events in human, commercial reasons, or inappropriate human pharmacokinetics (PK) (1). Latter was with 39.4% of the attritions the most frequent source of drug failure between 1964 and 1985 (2). Nevertheless, this has been substantially improved in the following decades and the number of drug attritions due to pharmacokinetics was reduced to 10% in the years from 1991 to 2000 (3). This improvement came from the standard incorporation of pharmacokinetics assessments into early drug discovery, a better knowledge of the underlying mechanisms based on enzymes involved in the disposition of the drug, a better knowledge of the differences between subjects and species, and finally, the improvement of pharmacokinetic properties optimization as strategy during drug discovery and development (4).

Information about the time course of drug concentrations at different sites in the body and the design of an appropriate dosing regimen to evoke the desired therapeutic effect requires expertise from pharmacokinetics. In the best case, the therapeutic drug is at sufficiently high concentrations in order to attain the desired effect but remains at the same time at low enough concentrations to avoid any toxic effects (Figure 2). This therapeutic concentration range is usually described as ‘therapeutic index’ or ‘therapeutic window’ and is substantially determined by the pharmacokinetics of a drug. Hence, drug metabolism and pharmacokinetics (DMPK) properties have to be reliably assessed as early as possible during the preclinical drug development process and were recognized as vital elements for the progression of a drug candidate to ensure appropriate pharmacokinetics and, in addition, to design the dosage regimen for entry into human (EIH) clinical studies (5-7). Although progress was made in the

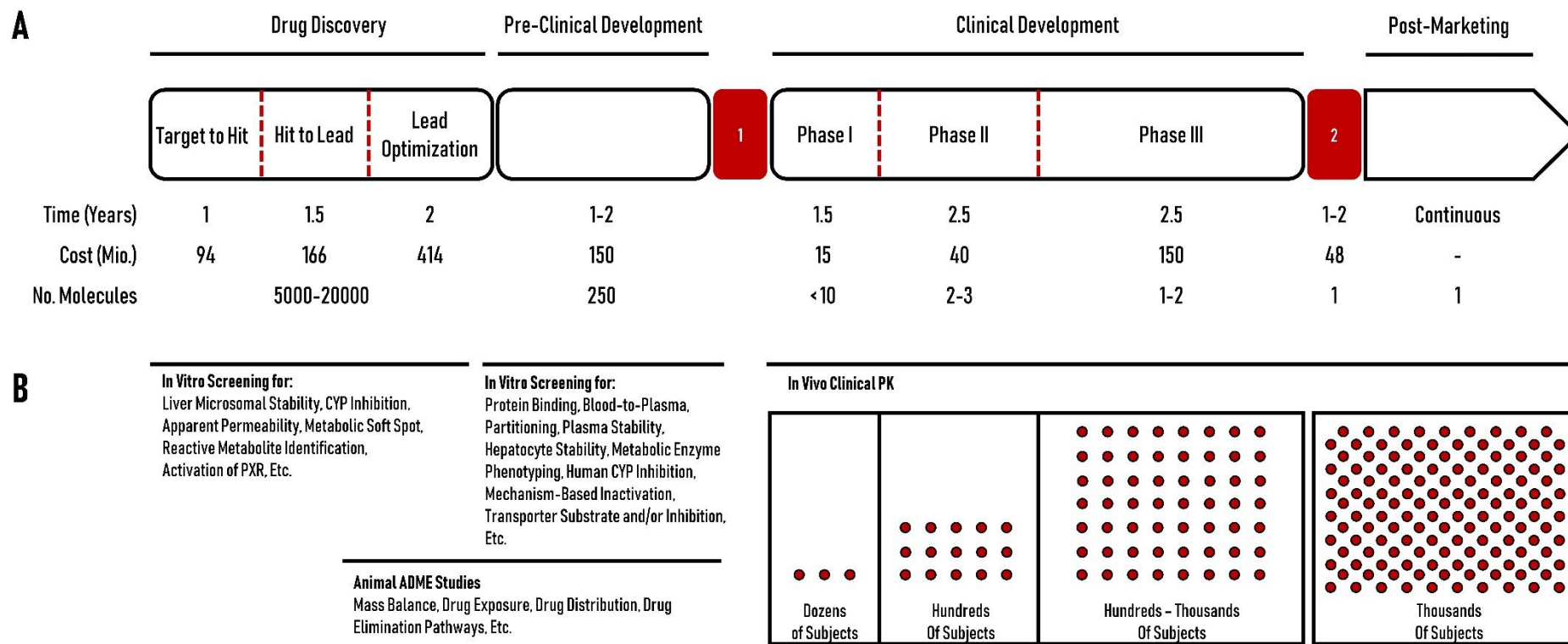


Figure 1 - Drug Development in the Pharmaceutical Industry. A) Timeline showing different stages of the drug development and the associated cycle time, cost per launch, and number of molecules included in the screening. After target discovery and validation, the ability of molecules to bind to the target is assessed in a high-throughput screening in the target to hit stage. Hit to lead is the process of creating a short-list of most promising candidates among the hit series based on ‘drug-like’ characteristics. Lead optimization is the stage where lead compounds are selected by iteratively testing and modifying the chemical structure of the compounds. Safety and pharmacokinetic/pharmacodynamics testing and determination of the initial human dose are the main investigations in the preclinical drug development stage. The objective of Phase I trials are the assessment of the tolerable dose limit and the PK/PD characteristics. Phase II trials involve the demonstration of efficacy and the optimal use in the target population. Phase III trials is employed to demonstrate safety and efficacy for the clinical use. Red areas mark “1” filing of an investigational New Drug Application (IND) with the FDA for safety review and “2” submission of New Drug Application (NDA) to the FDA for market approval. B) Important DMPK screenings conducted for small molecules and number of participants in the clinical trials per phase. Data and descriptions are based on (4, 8-11).

last decades, predictions of DMPK properties during the preclinical drug development is yet a monumental task for the project teams since the behavior of a drug as determined in the preclinical models is only a modest and often one-dimensional description of the actual complexity of drug behavior in the human body. This is also true for in vivo animal studies (e.g. mice, rats, rabbits, dogs, or monkey), which are similarly complex like humans, but where the translation might still be limited by inter-species variability. For example, Cao and colleagues reported poor correlation of observed bioavailability in human and in rat due to inter-species differences in the intestinal enzyme expression (12). A similar finding was made by Akabane and colleagues for the translation of bioavailability, which was significantly lower in monkeys compared to human (13). In addition to the limited translatability, animal models cannot be deployed at earlier stages of the drug development because studies are cost intensive and not ethical. Hence, a big effort is made to introduce and evaluate preclinical in vitro models with high translational value.

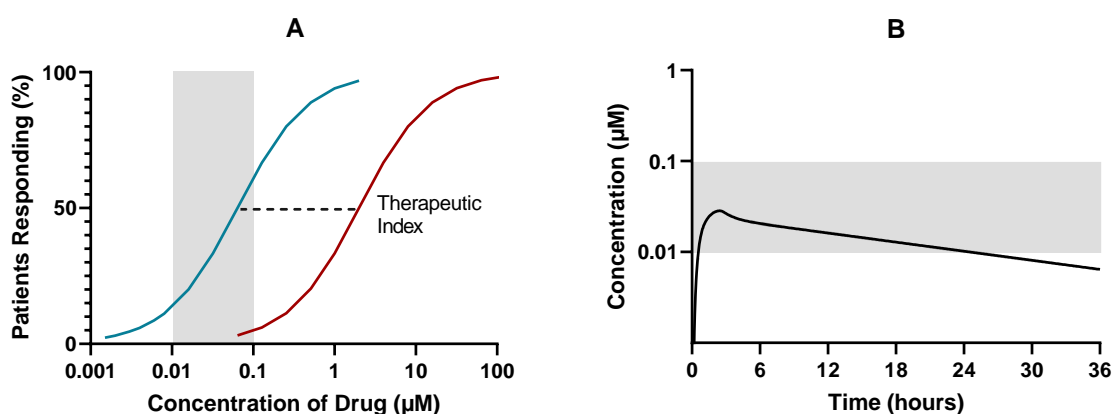


Figure 2 - Therapeutic Index and Therapeutic Window. The grey area indicates the therapeutic window of a drug in which the drug elicits its therapeutic effect without toxicological response. A) Description of the therapeutic index showing the pharmacological (blue) and toxicological (red) response plotted against the plasma drug concentration. B) Plasma concentration-time profile of an orally administered drug within the therapeutic window.

Important DMPK in vitro studies during the pre-clinical drug development investigate metabolic stability, metabolite identification, reaction phenotyping, and drug-drug interactions for which mostly hepatocyte-derived tissues are required. Furthermore, transporter activity and permeability studies using either hepatocyte-derived tissues or transfected cell lines (e.g. Caco-2), protein binding studies using

plasma, as well as studies to determine physico-chemical properties such as the acid dissociation constant (pKa), distribution coefficient (logD), and aqueous solubility are necessary (4).

5.1.2 Drug Metabolizing Enzymes

About 73% of marketed drugs undergo metabolism as primary route of clearance (14), hence, a key study of pharmacokinetics is the in vitro assessment of drug metabolism to determine the type of metabolizing enzymes and to predict the rate and site of drug clearance. The screening for the assessment of drug metabolism and the interpretation of the results prerequisites a fundamental understanding about the metabolizing enzymes involved in the metabolism.

Metabolic transformation is relevant to detoxify the organism from xenobiotic drugs and to modify the structures for subsequent elimination via renal or biliary clearance. In addition to facilitated excretion, the drugs are usually reduced in the biological activity (e.g. lower affinity to target protein) during biotransformation, whereas in some cases, the drug is converted to a more potent drug or a highly reactive metabolite. Examples are the 100-fold higher affinity of morphine-6-glucuronide to the μ -opioid receptor compared to unchanged morphine (15) or the formation of the acyl glucuronide of gemfibrozil which induces idiosyncratic hepatic injury (16). The transformation process can also be exploited by the design of so-called prodrugs, where the prodrug has beneficial properties e.g. for oral absorption (i.e. increased bioavailability) with subsequent transformation to the pharmacologically active drug. This is exemplified by the ester prodrug mycophenolate mofetil, which is almost completely metabolized by carboxylesterases 1 and 2 to the pharmacologically active mycophenolic acid. The utilization of the prodrug enhances the oral bioavailability of mycophenolic acid (17-19).

Common biotransformation reactions of drug metabolizing enzymes (DMEs) are oxidation, reduction, hydrolysis, and conjugation of and at functional groups of the molecule (14). Enzyme families that catalyze the introduction of functional groups to reduce the lipophilicity via oxidation are cytochrome P450 (CYP), aldehyde oxidase (AO), xanthine oxidase (XO), monoamine oxidase (MAO), and flavin-containing monooxygenase (FMO). DMEs involved in the reduction reactions are the aldo-keto reductase (AKR), azo-reductase, or nitro-reductase, and DMEs catalyzing the hydrolysis reactions are the epoxide hydrolase (EPH), carboxylesterases (CES), or peptidases. Conjugation reactions of the drug with a polar moiety to increase its hydrophilicity is mediated by UDP-glucuronosyltransferases (UGT),

Table I – Common Drug Metabolizing Enzymes

Drug Metabolizing Enzymes	Common Abbreviation	Reaction	Main Cofactor	Examples of Chemical Classes	Examples of Xenobiotic Substrates
Cytochrome P450	CYP	Oxidation	Nicotinamide adenine dinucleotide phosphate (NADPH)	alkanes, furans, aromatic hydrocarbons, aromatic amines, thiocarbonyls	Phenacetin, Efavirenz, Midazolam, Caffeine, Tolbutamide, Omeprazole
Flavin-containing monooxygenase	FMO	Oxidation	Nicotinamide adenine dinucleotide phosphate (NADPH)	Secondary amines, tertiary amines, hydrazines, thiols, sulfides, thiones	Cimetidine, Ranitidine, Benzydamine, Albendazole
Monoamine oxidase	MAO	Oxidation	H ₂ O	Primary, secondary, and tertiary amines (e.g. phenethylamine or benzylamine)	Citalopram, Sumatriptan, Milacemide
Aldehyde oxidase	AO	Oxidation	H ₂ O	Amides, xanthines, putines, phthalazines	Carbazeran, Zoniporide, O ⁶ -Benzylguanine
Xanthine oxidase	XO	Oxidation	H ₂ O	Purines, xanthines, acetaldehydes, benzaldehydes, pteridines	Caffeine, Theophylline, 6-Mercaptopurine
Carboxyl esterase	CES	Hydrolase	H ₂ O	Carboxylic esters	Temacapril, Cocaine, Doxazolidine
Uridine diphospho-glucuronosyltransferase	UGT	Conjugation	Uridine diphosphate glucuronic acid (UDPGA)	Phenols, arylamines, alcohols, carboxylic acids	Estradiol, Trifluoperazine, Propofol, Morphine, Naloxone, Zidovudine
Sulfotransferase	SULT	Conjugation	3'-phosphoadenosine-5'-phosphosulfate (PAPS)	Phenols, alcohols, heterocyclic amines, arylamines	Acetaminophen, minoxidil, 1-Naphtol
N-acetyltransferase	NAT	Conjugation	Acetyl coenzyme A (Acetyl-CoA)	Amines, alcohols, thiols	Isoniazid, Procainamide, Hydralazine, Dapsone, Sulfasalazine
Glutathione S-transferase	GST	Conjugation	Glutathione (GSH)	Epoxides, aldehydes, halogens, organic peroxides	Ethacrynic Acid, Chlorambucil

Information is based on (20)

sulfotransferases (SULT), N-acetyltransferase (NAT), and glutathione S-transferase (GST). Table I lists common enzymes for drug metabolism, the catalyzed reactions, involved cofactors, and example drugs. The enzyme families are further subdivided into sub-families and isoforms. Based on the percent amino acid sequence identity, the CYP super-family in human is divided into 14 families (>40% amino acid identity) and 20 subfamilies (>55% amino acid identity). In total, 57 genes are encoded in the human genome that express different CYP isoforms with varying relevance for drug metabolism (21, 22). Families CYP1, CYP2, and CYP3 are responsible for 70-90% of all phase I drug metabolism with CYP1A2, CYP3A4/5, CYP2C9, CYP2C19, CYP2D6, and CYP2E1 as most important isoforms (23). A compound can be a specific substrate of a single enzyme isoform or metabolized by multiple enzyme isoforms. For example, dextromethorphan is mainly metabolized by CYP2D6 with only minor contribution from CYP3A4 or other CYP isoforms (24). Contribution to metabolism can also be more evenly distributed to different enzyme isoforms as observed for diclofenac which is metabolized mainly by UGT2B7 and CYP2C9 (25) or for tramadol which is metabolized by a combination between different CYP enzymes (26, 27).

Several factors affect the function and phenotype of drug metabolizing enzymes. DMEs can be inhibited or induced by perpetrator drugs and dietary chemicals that impacts the systemic or oral clearance of a victim drug due to increased or decreased metabolic activity. These drug-drug interactions (DDIs) can have a significant impact on drug exposure and therefore on the efficacy or toxicity of a therapy. Inhibition of metabolizing enzyme can be reversible (competitive, uncompetitive, and non-competitive, mixed inhibition), quasi irreversible, or irreversible (e.g. time-dependent inhibition) and leads to the decrease in reaction velocity and/or the reduction in the affinity of the substrate to the enzyme (28). As a consequence, less drug is metabolized per unit of time that leads to a decrease in systemic or oral clearance and an increase in drug exposure. A severe example is the interaction between terfenadine, which is rapidly and completely metabolized by CYP3A4 in the intestinal wall, and ketoconazole, a potent inhibitor of CYP3A. Terfenadine is a prodrug and not intended to reach systemic circulation. However, inhibition of CYP3A4 in the intestine by ketoprofen causes systemic availability of terfenadine, potentially resulting in fatal torsade de pointes due to inhibition of the potassium ion channel in the heart (29, 30). In contrast, enzyme induction reduces the drug exposure due to an increase in

enzyme expression in the body. An inducing agent causes de novo synthesis of DMEs via binding and activation of nuclear receptors including the aryl hydrocarbon receptor (AhR), pregnane X receptor (PXR), and the constitutive androstane receptor (CAR) that control the expression of DMEs (31). The onset of enzyme induction is not an acute process like enzyme inhibition and requires several days to elicit the full effect. An example for this type of DDI is the induction of CYP3A4-mediated clearance of verapamil by rifampicin. After daily administration of 600 mg rifampicin for 24 days, the bioavailability of the S-enantiomer of verapamil was 25-fold lower compared to the non-induced state, which was due to a 32-fold increase in the apparent oral clearance of the drug by CYP3A4. As a consequence, the pharmacological effect of verapamil is almost completely abolished (32).

Another clinically relevant factor for DME activity are enzyme polymorphisms, which are based on differences in genotypes due to one or several mutant alleles and can have a marked effect on the observed metabolic clearance. Different phenotypes due to polymorphisms are defined that divides a population into poor metabolizers (PM), intermediate metabolizers (IM), extensive metabolizers (EM), and ultra-rapid metabolizers (URM) (33). The prevalence and occurrence of polymorphisms are strongly depending on the demographic composition and the ethnicity (34). The CYP2D6 enzyme is well-known as a highly polymorphic enzyme for which about 70 variant alleles have been identified that cause up to 200-fold variability in drug metabolism (34, 35). The frequency of variant alleles of CYP2D6 correlated with ethnic groups: Polymorphisms resulting in lack of metabolic activity are more prevalent in Caucasians (5-10%) compared to Asians (ca. 1%) (36). As an example, polymorphisms of the CYP2D6 enzyme has an important clinical implication for the treatment with codeine which is enzymatically transformed to its active metabolite morphine. Individuals that are lacking CYP2D6 activity (i.e. PMs) experience a poor analgesic effect since no or almost no morphine is formed, while ultra-rapid metabolizers experience exaggerated or at worst critical opioidergic effects (37). Polymorphisms are, however, not only limited to the CYP2D6 isoform, but further affect other CYP isoforms (34, 38) or other enzyme super-families (33, 39-41).

The section above highlights inter-individual differences in DMEs due to inherited sequence variation. Nevertheless, inter-individual variability is also a result of variations in enzyme expression that is driven by different gene expression due to exposure to endogenous and exogenous regulatory factors (Figure

3). Exogenous regulatory factors can be enzyme inducing drugs, as discussed in the DDI section, environmental factors, or diet/nutrition. Endogenous factor describes the varying expression and function of DME as a function of age, sex, natural physiological cycles, pregnancy, as well as diseases and/or organ impairment (42-44).

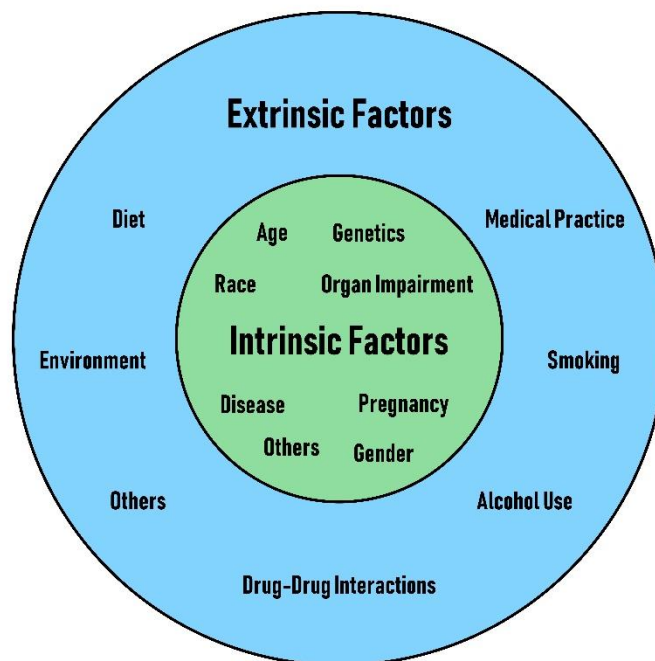


Figure 3 - Factors for Inter-Individual Variability of Drug Metabolizing Enzymes. Different extrinsic and intrinsic factors that affect drug metabolism in human. Diagram is based on (44).

5.1.3 UDP-Glucuronosyltransferases

About 50% of therapeutic drugs are metabolized via oxidative metabolism by CYP enzymes, among which the CYP3A4 isoform is most frequently involved in the metabolism of marketed drugs (14). In the past decades, however, the aim in pharmaceutical industry was to increase the metabolic stability and, thus, to reduce the rate and extent of metabolism. The higher metabolic stability of the drug has beneficial effects on the frequency of administration (i.e. avoiding short duration of action) and on the oral bioavailability (i.e. avoiding extensive first-pass metabolism) (45). In order to meet the desired pharmacokinetic properties, the metabolic stability of new chemical entities (NCEs) is optimized during drug discovery with high throughput screening to avoid vulnerable moieties within the structure, with a focus on reducing oxidative metabolism mediated by CYP enzymes (46). Hence, chemical structures proceeding in the drug development have little to no oxidative metabolism, but are instead more prone

to alternative transformation reactions.

Enzymes that are increasingly important and mediate the primary metabolism of a growing number of drugs are the UGT enzymes. UGTs typically catalyze the conjugation of a glucuronic acid to a suitable functional group utilizing uridine diphosphate glucuronic acid (UDPGA) as a cofactor. Other sugars like UDP-xylose, UDP-N-acetylglucosamine, UDP-galacturonic acid, UDP-galactose, or UDP-arabinose might serve as cofactors as well (47). The reaction with the UDPGA is depicted in Figure 4. The conjugation reaction prepares the xenobiotic substrate for subsequent excretion via urine or bile mediated by active transport, e.g. organic anion transporting polypeptide (OATP) or multi-drug resistance-associated protein (MRP) (48). The types of substrates undergoing UGT-mediated conjugation reaction typically contain electron-rich nucleophiles such as phenols, alcohols, carboxylic acids, amines, or N-containing heterocycles. Most common reactions are O- and N-glucuronidation (41). Substrates are versatile and involve many endogenous molecules (e.g. bilirubin, bile acids, steroid hormones, or fatty acids), non-drug xenobiotics (e.g. environmental and nutrition chemicals), as well as xenobiotic drugs from many therapeutic areas (49).

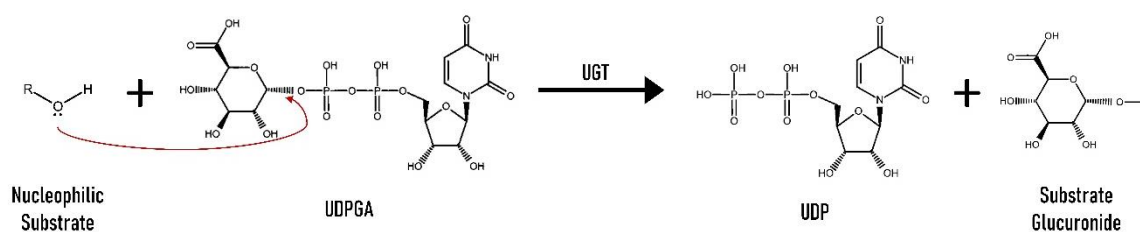


Figure 4 - Chemical Reaction mediated by UGT Enzymes. Schematic representation shows the enzyme reaction mediated by UGT enzymes. The conjugation reaction of the nucleophilic substrate and the sugar moiety follows a bimolecular substitution (S_N2) mechanism to form the substrate glucuronide and uridine diphosphate as reaction products. The description and illustration are based on (41) and chemical structures were drawn using Chemspace (www.chem-space.com).

The enzyme superfamily is highly conserved in the evolution and can be found in animals, plants, fungi, and bacteria (50). UGTs are transmembrane enzymes located at the membrane of the endoplasmic reticulum (ER) where the luminal domain constitutes the major part of the polypeptide chain and contains the metabolically active site (51). The simplified topology of UGT enzymes at the membrane is depicted in Figure 5. Although the complete crystalline structure of a mammalian UGT is not available

yet, a topological model is generally accepted where the N-terminal of the protein is responsible for substrate binding and the C-terminal is responsible for binding of the UDP-glucuronic acid (52).

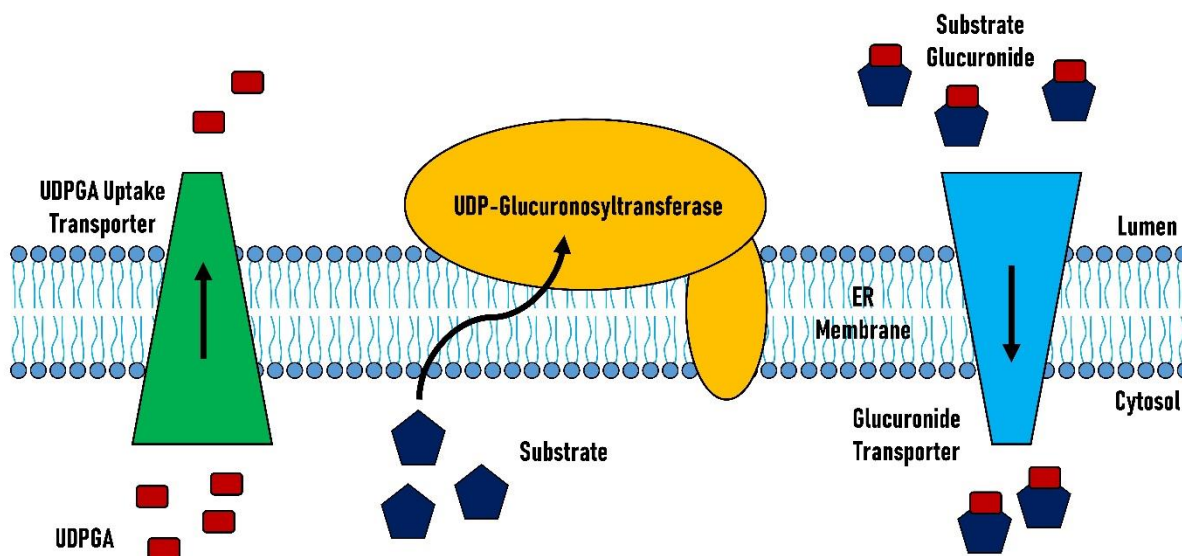


Figure 5 - Topology of UGT Enzymes in the Endoplasmic Reticulum. Endogenous and exogenous substrates permeate through the membrane of the endoplasmic reticulum (ER), while UDPGA is transported into the ER via active transport. Conjugation reaction occurs in the ER mediated by UGT enzymes and substrate glucuronides are actively transported out of the ER. Figure and description are based on (41, 53-55).

In human, UGT enzymes are classified in four families (UGT1, UGT2, UGT3, and UGT8) based on the gene sequence. The families UGT1 and UGT2 enzymes are most important for the detoxification of xenobiotics (56, 57). Cases are present where the UGT3 family is involved in the metabolism of xenobiotics (with a negligible role), whereas no xenobiotic substrates are known for UGT8 (54, 58). The gene for the UGT1 family is located on chromosome 2q37 and encodes nine distinct UGT isoforms (1A1, 1A3, 1A4, 1A5, 1A6, 1A7, 1A8, 1A9, 1A10), which are variants due to alternate splicing of the exon at the N-Terminal domain of the sequence (57, 59). In contrast, UGT isoforms of the UGT2 family are encoded in separate genes located on the chromosome 4q13 and are further divided into two subfamilies comprised of ten different isoforms (A1, A2, A3 and B4, B7, B10, B11, B15, B17, B28) (57) (Figure 6). Among these 19 different UGT isoforms in the families UGT1 and 2, seven isoforms are clinically most relevant for the metabolism of drugs (1A1, 1A3, 1A4, 1A6, 1A9, 2B7, and 2B15), whereas other UGT isoforms (e.g. UGT1A10, UGT2B4 or UGT2B10) are also often involved in drug metabolism (60).

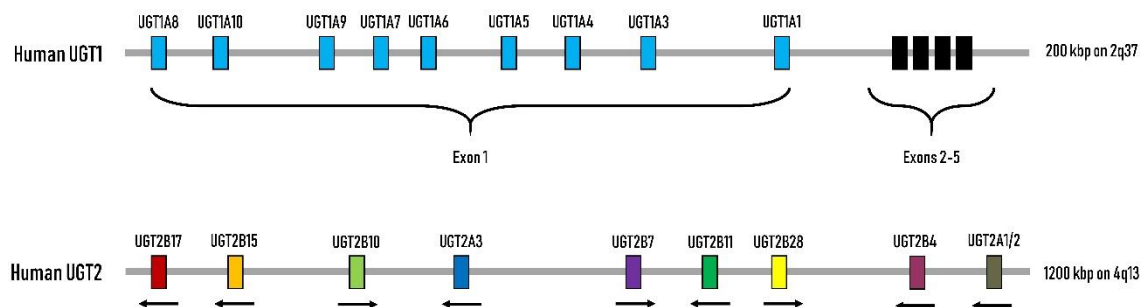


Figure 6 - Schematic Representation of Human UDP-Glucuronosyltransferase Enzymes Gene Loci and Encoded UGT Proteins. UGT1 enzymes are encoded on chromosome 2, share four common exons (Exons 2-5), and differ due to alternative splicing of the first exons. In contrast, different genes encode UGT2 enzymes. All UGT enzymes have a conserved region at the C-terminal for the UDPGA binding domain and a transmembrane domain for the protein, but differ in the substrate-binding domains at the N-terminal. The graphics and description are based on (41, 52)

Almost all enzymes in the UGT1A and UGT2B families are expressed to a greater or lesser extent in hepatic tissue with exception of a few UGT isoforms (UGT1A5, 1A7, 1A8, and 1A10) (41, 57). UGT2B7, which is most frequently involved in the glucuronidation of drugs (56) has the highest abundance in hepatic tissue (61, 62). Glucuronidation in renal tissue is predominantly due to the UGT isoforms 1A9, 2B7, and 1A6, creates an important extra-hepatic site of clearance in the systemic circulation (63). An example for a compound undergoing excessive extra-hepatic glucuronidation is propofol which is a substrate of UGT1A9 (64) and for which the contribution from renal glucuronidation almost accounts to 40% of total clearance (65). Glucuronidation activity is also present in the gastrointestinal tract due to expression of UGT1A1, 1A3, 1A5, 1A6, 1A7, 1A8, 1A9, 1A10, 2B7, 2B15, and 2B17 (66, 67). UGT enzymes in the stomach, small intestine, and/or colon are relevant for the first-pass metabolism and potentially lower the bioavailability of a drug. An example here is the very poor bioavailability of raloxifene, which is a result of gut metabolism by UGT1A1, 1A8, 1A9, and 1A10 (68, 69). UGT expression is also found in many other tissues such as lungs, skin, or reproductive organs and contribute to local metabolism of UGT substrates in these tissues (66).

It is well recognized that, although the qualitative expression patterns of UGT enzymes in the body are quite well defined, quantitative data about protein abundance is yet limited (62, 70). Traditional quantitative methods to determine enzyme expression levels, like Western blotting and enzyme-linked immunosorbent assay (ELISA), only provide variable and imprecise measurements. This is due to the inherently high sequence homology between UGT enzymes which results in cross-reactivity in the

assays (70). More recently, the liquid chromatography-mass spectrometry (LC-MS) isotope-labelled standard targeted method was developed as more quantitative methodology for the determination of protein abundance (71). Nevertheless, heterogeneity is still observed between studies with quite variable enzyme expression levels reported in hepatic and/or other tissues (62, 70).

Strong polymorphisms have been observed for UGT enzymes with clinical relevance in drug therapy (41, 72). Polymorphisms of the UGT1A1 isoform are probably the most extensively studied since the UGT1A1*28 (mainly among Caucasians) and UGT1A1*6 (mainly among Asians) polymorphism have severe consequences. The UGT1A1 isoform is responsible for conjugation and detoxification of bilirubin. Complete or almost complete deficiency observed for the two mutant alleles leads to the fatal Crigler-Najjar's syndrome due to reduced bilirubin clearance (73). Other cases are reported where polymorphisms of UGT1A1 have a critical impact on the clinical outcome after drug dosing. Irinotecan is a prodrug of the topoisomerase I inhibitor 7-ethyl-10-hydroxycamptothecin (SN-38) used for anti-cancer treatment. SN-38 can cause diarrhea and myelosuppression at higher doses, whereas the compound is usually detoxified by the UGT1A1 isoform (74). However, poor metabolizers due to UGT1A1*28/UGT1A1*6 polymorphism might experience life-threatening side effects, since the detoxification by UGT1A1 is inactive (75, 76). UGT1A1 polymorphism does further affect the pharmacokinetics of other drugs like etoposide (anticancer drug) or raltegravir (HIV integrase inhibitor) (72). Polymorphisms are also reported for other enzymes that belong to the UGT1A family (73, 77). The UGT1A4*2 variant is associated with a higher and the UGT1A4*3 variant is associated with a lower serum concentration of lamotrigine, while polymorphisms of the UGT1A3 isoform have an effect on the pharmacokinetics of e.g. telmisartan and atorvastatin (78). Among the UGT2B family, polymorphisms have been reported for UGT2B7, UGT2B10, UGT2B15, and UGT2B17 (72, 79-84). The polymorphism of the UGT2B15 enzyme has a major impact on the pharmacokinetics of oxazepam and caused relatively high inter-individual variability (79). The importance of considering (UGT) polymorphism during drug development can be demonstrated with two studies, which both obtained significant impact of the polymorphisms on the drug clearance. Fowler and colleagues reported 136-fold above average systemic exposure to the parent drug in a subject of African origin during the first clinical trial and finally detected reduction in metabolic clearance due to UGT2B10 polymorphism as

main cause (80). Wang and colleagues (84) investigated the genetic polymorphism of UGT2B17 in a first-in-human (FIH) study and found that homozygous carriers of the UGT2B17*2 allele had a 25-fold higher drug exposure compared to carriers of the wild type.

For CYP enzymes, selective inhibitors (e.g. furafylline for CYP1A2, montelukast for CYP2C8 or ketoconazole for CYP3A4/5) and substrates (bupropion hydroxylation by CYP2B6, S-mephenytoin 4'-hydroxylation for CYP2C19, or midazolam 1'-hydroxylation by CYP3A4) have been identified and are widely established and evaluated (85). Contrarily, UGT substrates are usually metabolized by multiple isoforms, while inhibitors miss specificity for individual UGT isoforms (86). Nevertheless, appropriate substrates have been proposed for UGT1A1 (ezetimibe, SN-38, β -estradiol), UGT1A3 (telmisartan, desacetylcinobufagin, chenodeoxycholic acid), UGT1A4 (trifluoperazine, midazolam/1-hydroxymidazolam), UGT1A6 (serotonin, 5-hydroxytryptophol, deferiprone), UGT1A9 (propofol, mycophenolic acid), UGT1A10 (dopamine), UGT2B4 (canagliflozin), UGT2B7 (zidovudine, morphine, gemfibrozil), UGT2B10 (amitriptyline, cotinine), UGT2B15 (S-oxazepam), UGT2B17 (testosterone) (54, 56, 60, 87-89). Similarly, selective inhibitors have been identified for UGT1A1 (atazanavir, erlotinib, nilotinib, regorafenib), UGT1A4 (hecogenin), UGT1A9 (niflumic acid, magnolol), UGT2B7 (fluconazole), and UGT2B10 (desloratidine) (54, 60, 90-92). Selective substrates and inhibitors are yet unknown or only poorly defined for other UGT isoforms (56, 88).

Characterization of oxidative metabolism by CYP enzymes is relatively advanced in contrast to the uncertainties present for the UGT-mediated metabolism due to the predominant role in the metabolism of small molecules. The low evaluation state of UGT-mediated metabolism is a general issue and requires increasing focus on the functions and characteristics of UGT enzymes to improve confidence in the progression throughout all drug development stages. A successful example about adaptation to in vitro testing of UGT substrates is the improved incubation methodology with liver microsomes: The luminal location of the active site of UGT enzymes causes a latency of the activity, because substrates and cofactors first need to pass the ER membrane. This was overcome with the addition of alamethicin, a pore-forming peptide, which increases the reaction rate by several fold compared to untreated microsomes (93). In addition, it was demonstrated that fatty acids inhibit some UGT isoforms (e.g. UGT2B7 and UGT1A9) which consequently led to under-prediction of the metabolic clearance. The

problem could be resolved by addition of bovine serum albumin (BSA) that bind the inhibitory fatty acids which ultimately lowers the apparent unbound K_m for substrates of UGT1A9 and UGT2B7 (94). Nevertheless, other knowledge gaps remain and have a significant impact on the in vitro to in vivo extrapolation of drug metabolism mediated by UGT enzymes. Shortage of well-defined and validated inhibitors and substrates for the UGT isoforms negatively impacts the quality of reaction phenotyping (86), while under-prediction of the drug metabolism for UGT substrates has been reported using primary human hepatocytes and/or human liver microsomes (46).

5.2 IN VITRO HEPATOCYTE SYSTEMS

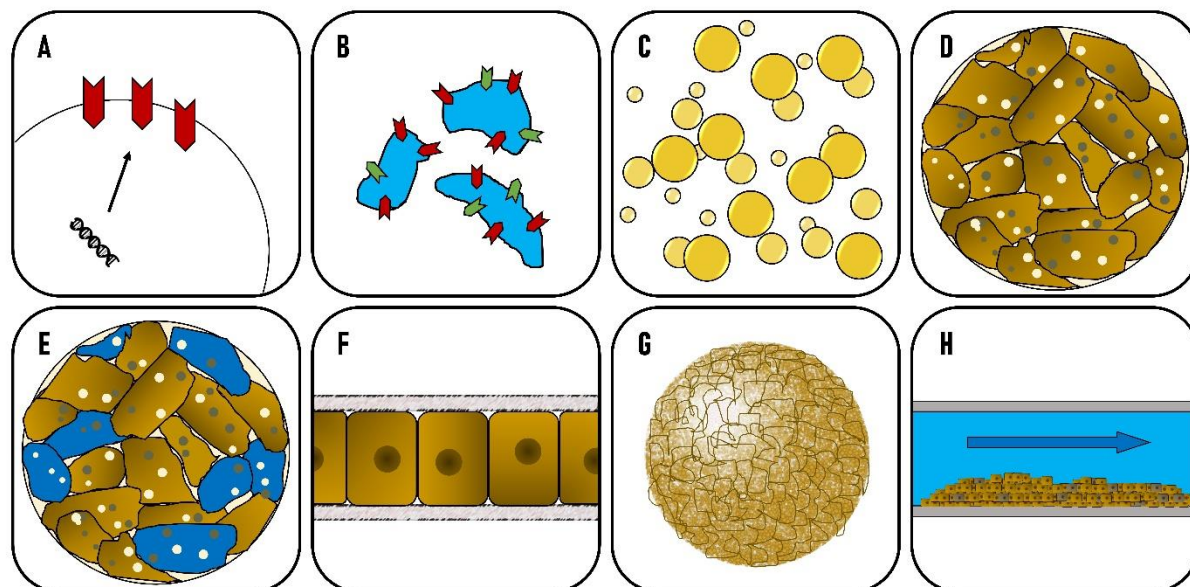
5.2.1 Subcellular Fractions and Recombinant Enzymes

Human liver microsomes (HLM) are a convenient in vitro tool with low cost and simple handling (Figure 7B). The presence of UGT and CYP enzymes in the incubation allows for the high-throughput screening of the metabolic activity by the clinically most important drug metabolizing enzymes during drug discovery (4, 95). Alternatively, cytosol or S9 fractions could be deployed in addition to complement the investigations with DMEs that are not expressed in the microsomal incubations. Besides the screening for metabolic stability, HLMs are applied to identify the types of enzymes involved in the metabolism of the drugs and to assess DDIs due to enzyme inhibition. Microsomal incubations can further derive from other species to evaluate the translatability of the drug metabolism from in vitro to the in vivo animal models or can be applied to investigate the metabolism in other tissues such as the intestine (human intestine microsomes) or the kidneys (human kidney microsomes).

Quantitative identification of enzymes responsible for drug metabolism is usually conducted with reaction phenotyping that relies on the deployment of combined studies using microsomes and heterologously expressed recombinant enzymes. Recombinant human CYP enzymes (rhCYP) or UGT enzymes (rhUGT) (Figure 7A) are produced with expression of transfected cDNA coding for the enzyme of interest using cells from bacteria, yeast, insects, or mammalian cells (96). The reaction phenotyping approach involves the examination of the drug metabolism in the absence and presence of specific enzyme inhibitors, detection of drug metabolism using isolated recombinant enzymes, and the

correlation between rate of metabolism between HLM and rhCYP/rhUGT using a specific marker reaction (i.e. specific substrate) (86).

Figure 7 - Hepatic In Vitro Test systems.



In Vitro Test System	Purpose	Subcellular/Cellular	Incubation Term	Throughput	Validation
A Recombinantly Expressed DMEs	Kinetic Analyses and Reaction Phenotyping	Subcellular	Minutes	High	
B Liver Microsomes	Metabolic Stability, Drug-Drug Interactions (Inhibition)	Subcellular	Minutes	High	
C Suspended Hepatocytes	Metabolic Stability, Active Transport, DDI Studies (Inhibition)	Cellular	Hours	High	
D 2D-Plated Hepatocytes	Metabolic Stability, DDI Studies (Induction)	Cellular	Days	Intermediate	
E Co-Cultured Hepatocytes	Metabolic Stability (Low Clearance), DDIs (Induction)	Cellular	Weeks	Low	
F Sandwich-Culture Hepatocytes	Active Transport, Biliary Clearance	Cellular	Weeks	Low	
G Liver Spheroids	Multiple Endpoint Studies, Toxicological Response	Cellular	Weeks	Low	
H Microfluidic Liver-On-Chip Devices	Multiple Endpoint Studies	Cellular	Weeks	Low	

Although HLM and recombinantly expressed enzymes are relatively convenient and very useful for the dedicated purpose, a disadvantage is the lack of a complete cell complement. However, during the

candidate selection and characterization, more comprehensive PK properties of drug candidates will be determined, including protein binding, blood-to-plasma partitioning, hepatocyte stability, drug-drug interactions, mechanism-based inactivation, and metabolite identification. Whole cell systems like primary human hepatocytes are systems of choice for some of these studies since primary cells include all relevant hepatic uptake/efflux transporters, metabolizing enzymes and signaling cascades (97).

5.2.2 Hepatocyte Systems

Historically, experiments with hepatocytes could only be conducted with freshly prepared cells. This had the strong disadvantage that fresh hepatocytes are not readily available from humans and that the liver preparation could only be used once, leading to low flexibility for the experimenter and high inter-occasion variability since different experiments were based on different organ donors. A breakthrough was achieved when the cryopreservation technique was developed that allows to store the samples over a long time period, to use the hepatocytes “on-demand”, and to avoid cells with poor quality. It was shown that the metabolic function of cryopreserved hepatocytes resembles that of freshly thawed hepatocytes (98). Although primary hepatocytes are most frequently cultivated as suspension (Figure 7C), different cultivation techniques were developed in the last few decades with remarkable progress in the understanding of the underlying mechanisms to form viable and physiologically relevant hepatocytes. Nonetheless, hepatocytes in suspension have the advantage of convenient and immediate utilization after the thawing process and provide already a decent system for the investigation of drug metabolism and active transport for most of the drugs tested in an intermediate-high throughput screening. A major limitation of the suspended hepatocytes is the quite rapid loss of activity which limits the incubation time to 2-4 hours (99). First of all, this does not allow to investigate long-term processes such as enzyme induction, which is a process that shows full effect only after about three days, and secondly, the application of suspended hepatocytes could not keep pace with the trend of developing compounds with a higher metabolic stability.

The fast decrease of activity is owed to the unnatural environment present for the hepatocytes (100). The liver is a complex organ composed of different types of cells in a highly organized structure, whereas hepatocytes constitute only about 60% of the cells (which is 85% of liver mass) (97, 100). The remaining 40% are non-parenchymal cells that are responsible for several tasks such as secondary

response upon an initial damage to hepatocytes. Furthermore, hepatocytes are spatially organized in the so called liver lobules in a hexagonal shape, encompassing the arteries, veins and the bile ducts (97). On a cellular level, hepatocytes are tightly connected and have a polarized structure where the basolateral membrane faces the liver sinusoidal endothelial cells and the apical membranes form the bile canaliculi. Upon isolation, primary human hepatocytes lose intercellular connections and their polarity, leading to dedifferentiation and finally to a loss of phenotype/activity (101). In addition, recovered hepatocytes in suspension undergo apoptosis and necrosis, which is demonstrated in a decrease of viable cells (101). One approach to prolong the activity of hepatocytes is to seed the cells in a collagen-coated plate (Figure 7D), where the cells adhere to the surface of the plate to re-aggregate and to establish intercellular contacts after a few hours (99, 102). This cultivation technique prolongs the activity of the cells to at least 24 hours, allowing for more advanced investigations like the determination of enzyme induction. However, a substantial loss in baseline enzyme activities was observed for plated hepatocytes already after 24 hours (99, 103). Another approach with the aim to mimic physiological condition is to cultivate the cells in a two-dimensional co-culture together with non-parenchymal cells (Figure 7E), which prolongs the activity of the hepatocytes up to four weeks, depending on the incubation conditions (104, 105). Examples for such systems are H μ REL and HepatoPac, which are a co-culture between human hepatocytes and stromal cells. Latter is introduced in more detail in Figure 8. Similarly, long-term activity over several weeks can be attained when the hepatocytes are seeded in a three-dimensional format as demonstrated with spheroids (Figure 7G), which is in addition often combined with co-cultivation (106, 107).

The augmented physiological-like conditions for the hepatocytes with the cultivation techniques introduced novel possibilities to investigate drug candidates and to conduct mechanistic studies. Enough resolution could be achieved in recent studies to test the metabolic clearance of metabolically stable drugs in some example studies (108, 109). Furthermore, in a study from Kratochwil et al. 2018 (110), a hepatocyte co-culture was successfully applied to simultaneously assess compound clearance, metabolism, and DDIs. Finally, by the application of primary human hepatocyte cultivated as spheroids, Mizoi and colleagues observed CYP1A2-mediated metabolic toxicity from dacarbazine metabolism

(111). These studies demonstrate the usefulness of more advanced hepatocyte cultivation techniques, which slowly established in the value chain of drug development in the past years.

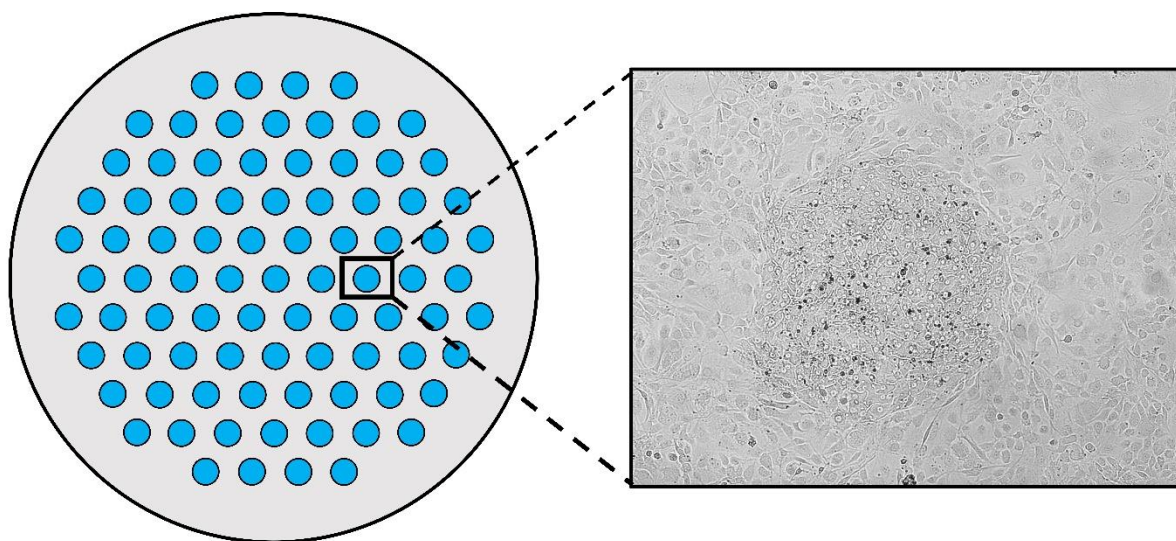


Figure 8 – HepatoPac® Co-Culture. The co-culture between human hepatocytes (blue area) and stromal 3T3-J2 mouse fibroblasts (grey area) in a micro-patterned arrangement supports the hepatocytes to maintain its phenotypic functions for several weeks. Microscope picture (right) shows a single hepatocyte island surrounded by the fibroblasts. Description and schematic are based on (105), picture was taken in our laboratory.

5.2.3 Microphysiological Systems

The next advancement is to cultivate the hepatocytes (or any other tissue type) in so called microphysiological systems (i.e. organ-on-chip, body-on-chip) which are designed to recapitulate functional units of human organs (112) (Figure 7H). The systems often involve a microfluidic model that has a positive effect on the polarization by introducing a shear stress to the cells and has further the advantage that different tissues can be interconnected to mimic the systemic circulation. Using such an approach creates the possibility to trigger organ-specific features such as bile canaliculi formation (113) or zonation (114) in the liver, absorption in intestinal epithelial cells (115, 116), malignant tumor invasion in mammary epithelial cells (117), or the epithelial barrier function in corneal epithelial cells (118) to mention only a few. The promise of the organ-on-chip systems is that the more sophisticated in vitro methodologies, mimicking organs, tissues, or whole organisms, might be deployed to resolve questions where current in vitro systems are limited (119). The potential of microphysiological systems (MPS) is appealing and led to a progressive adaptation by the pharmaceutical industry and to an increasing number of publications that provide examples of promising applications for the systems.

A merit might be achieved with the combination of gut and liver tissues as exemplified by Tsamandouras

and colleagues in 2017 (120). They developed a fluidic platform that integrates both tissues to investigate the organ crosstalk on the pharmacokinetics, where the drug was administered at the apical side of the gut trans-well to mimic oral administration or directly into the centrally circulating medium to mimic intravenous administration. The same group tried to quantitatively investigate population variability using a liver-on-chip device (121). Another example is the assessment of toxicity due to complex immune responses as investigated by Sarkar and colleagues in 2017 (25). By co-cultivation of primary human hepatocytes and cryopreserved human Kupffer cells, they simultaneously studied the metabolic profile of diclofenac and the toxicological responses of the metabolites. The examples are numerous and not only limited to pharmacological investigations, but further include other applications such as investigations of pathogenesis of neurodegenerative diseases (122), assessment of organ impairments (123, 124), or even in vitro modelling of human disease progression in microgravity (125). Although the applications of these newly evolving in vitro systems are manifold and sometimes sensational, the application of MPS is yet in the proof-of-concept phase and several challenges have to be resolved before the implementation into drug development – also for assessments of DMPK properties of drug candidates (126). A clear merit has to be shown for single cell systems (i.e. hepatocytes) over standard cellular tools compared to the conventional in vitro methodologies which are established/accepted by the pharmaceutical industry and the regulatory agencies (127). For multi-organ devices, where two or more tissues are combined within one chip, a big challenge is to optimize incubation condition (e.g. relative organ sizes, flow distribution among organs, or liquid-to-cell ratios) that allows for a stable activity and phenotype over time for all tissues involved (128-130). In addition, reproducibility and translatability of the results have to be shown in order to increase the confidence in the systems (129). From the perspective of a pharmaceutical industry, the application of these sophisticated in vitro systems is probably not feasible for investigations during the drug discovery since the number of substrates require a high-throughput screening for DMPK properties, whereas the MPS lack high-throughput capability in favor of high quality. Nevertheless, such high-quality systems elicit the higher potential at later stages of the drug development where the clinical candidate has to be selected from a reduced number of lead compounds and where pre-clinical animal testing might be partly replaced in future.

Finally, the data generated in MPS are more complex compared to results generated in microsomal incubations or other straightforward in vitro system. Hence, data analysis might require the support from more sophisticated computational approaches to interpret the results and translate the findings to the expected outcome in human (128, 131, 132). The before mentioned study from Tsamandouras and colleagues (120) demonstrates the combination between an integrated gut and liver MPS and computational model-based analysis to derive the intrinsic parameters such as intestinal permeability and hepatic metabolism. Other examples exist that used a similar approach of capturing the complexity of multi-organ MPS by the application of mathematical modelling and simulation (133-135).

5.3 COMPUTATIONAL APPROACHES IN DRUG RESEARCH

5.3.1 Predictions of Drug Properties

Predictions can be made based on classification systems where physico-chemical properties are defined and applied to have first estimates of a drugs behavior. The classification tools can be quite simple like the extended clearance classification system (ECCS) which classifies chemical structures into 6 different classes and subclasses to assign metabolism (Class 1A and 2), hepatic uptake (Class 1B and 3B), and renal clearance (Class 3A, 3B, and 4) as most likely rate-determining routes of clearance (136, 137). The assignment is based on the permeability, the molecular weight, and the ionic class of the compounds (Figure 9A). Another useful classification system is the biopharmaceutic classification system which classifies compounds based on their aqueous solubility and intestinal permeability into four different classes (Figure 9B) (138, 139). Depending on the classification, a strategy for the development of the oral dosage form can be designed where e.g. surfactants are most likely required in the formulation for compounds in Class 2 that have a high permeability and low solubility.

Other prediction tools come with a much higher complexity and require the deployment of a computer-based approach. This intersection to cheminformatics aims towards the extraction and processing of drug properties based on a chemical structure and a learning process based on past observations. In silico predictions offer valuable information during drug discovery with the merit to reduce the financial expenditure and valuable time on later testing stages, e.g. for in vitro and in vivo experiments, and

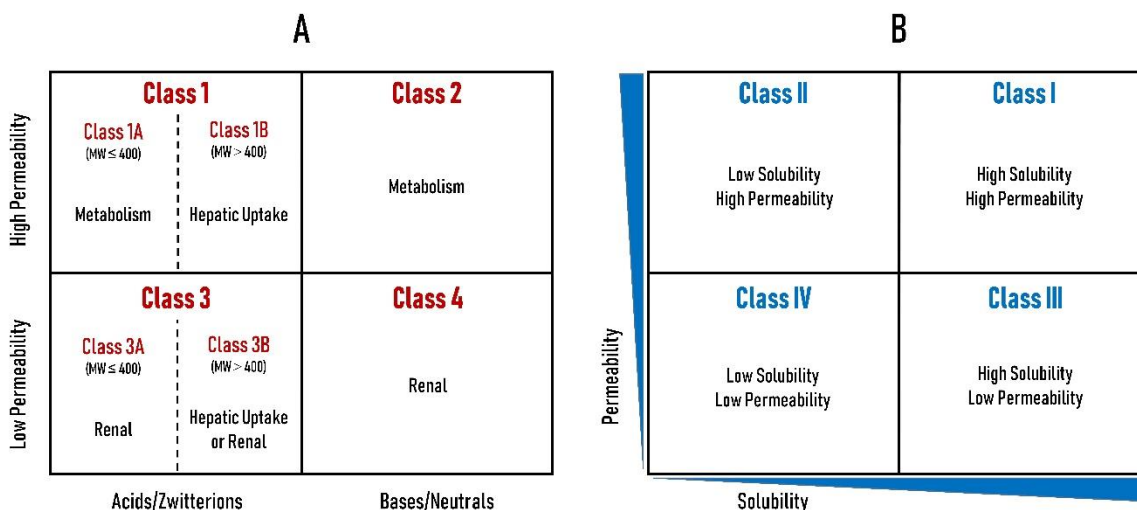


Figure 9 - ECCS and BCS Classifications. A) Extended clearance classification system (ECCS). B) Biopharmaceutical Classification System. Diagram is based on (136-139).

provide insights for compounds not yet synthesized (140). This computer-aided drug design (CADD) is deployed to reduce large molecule libraries into smaller and more promising sets of active molecules for the therapeutic target, to optimize ADME properties, and to avoid safety risks (141). The methodology for the in silico predictions can either be ‘molecular modeling’, where the predictions are made based on the three-dimensional structure of proteins together with the ligand, or ‘data modelling’, where the predictions depend on a statistical approach based on molecular descriptors (142). Latter uses molecular descriptors of numerous structures and their defined properties to generate a statistical model to predict the respective properties of novel compounds (142). An application is shown in a publication of Zhang and colleagues from 2009 (143) in which they constructed a statistical model for solubility and lipophilicity with a large ‘training set’ of structures ($n = 1202$ for solubility and $n = 7324$ for lipophilicity) with known properties to generate the model. Using a ‘test set’ of structures to validate the prediction model, they could demonstrate high prediction accuracy for both parameters. Another example is the prediction of renal clearance rate as conducted by Paine and colleagues in 2010 (144). They developed an in silico model using a human renal clearance data set of 349 drugs and concluded, after validation of the predictions with the test set, that the model delivers at least approximations of the human clearance.

Those prediction models are widely established in the pharmaceutical industry and are valuable as supporting tools during drug development. However, it has to be considered that these models rely on

the quality and quantity of the data used to develop the models. In addition, the appropriateness of the models is limited in case where the structures of interest are outside the chemical space that was used to train the models (142).

5.3.2 Physiologically Based Pharmacokinetic Modelling

5.3.2.1 Compartmental Modelling and Simulation

Another *in silico* approach applied during the drug development process is the modelling of the kinetic processes underlying the compounds pharmacokinetics and pharmacodynamics in so-called pharmacokinetic- (PK) or pharmacokinetic/pharmacodynamics- (PK/PD) modelling and simulation (M&S). PK and PK/PD models are, among other types of models (e.g. disease models), an integral part of the model-based drug development (MBDD) approach that is adopted by the pharmaceutical industry and is recommended by regulatory agencies (145, 146). The overall objectives of modelling and simulation in the preclinical stage of drug development are manifold and involve the guidance of the developmental strategy, the design of PK/PD experiments in preclinical species, the prediction of human PK based on *in vivo* and *in vitro* data, and/or the integration of ADME, efficacy, and toxicology measures for projection of first-in-human dose. At the clinical stages, the models are applied to quantify the variability of PK and PD between individuals and populations (i.e. assessing the impact of covariates), to optimize the study designs of the clinical trials (i.e. design dosing and sampling schemes), and to establish dose-response relationships in the target population (8). Ultimately, M&S approaches can help to reduce costs and cycle times during drug development and to improve success rates of the development projects (147).

Traditional PK and PK/PD-models usually consist of compartments as basic elements which are conceptual representation of the system designed without any physiological or anatomical relevance (148-151). On a mathematical basis, the models are described by differential equations to simulate the rate of change for the drug concentrations and/or effects over time. Figure 10 introduces different types

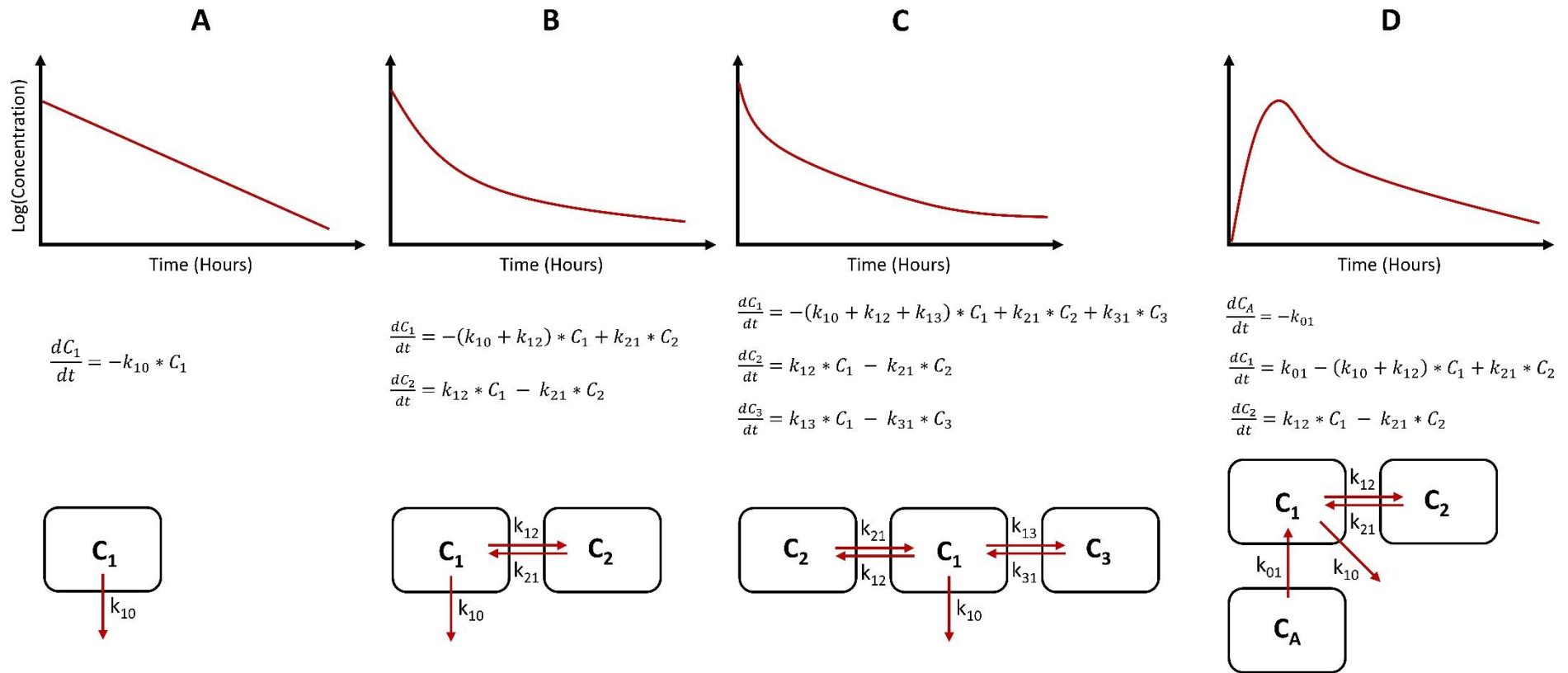


Figure 10 - Compartmental Models. The models consist of compartments as basic elements, which are a representation of the system designed. The mass transfer between the compartments is described with differential equations to simulate changes in drug concentration over time. A) Mono-exponential concentration-time profile after IV administration (no apparent distribution phase) is described with a one-compartmental model. B) Bi-exponential concentration-time profile (with initial distribution phase) after IV administration of a drug. The central (C1) and peripheral (C2) can be regarded as systemic circulation combined with tissues where the drug distributes immediately and the sum of tissues where compound distribution is not immediate, respectively. C) In case the concentration-time profile shows a tri-exponential decay after IV administration, a three-compartmental model might be most feasible. D) An additional compartment is usually integrated for models to describe oral administration of a drug to account for the drug absorption and bioavailability. PK/PD models (not shown) complement an effect compartment that is used to describe the time course of a drug's pharmacodynamics and to link the effect to the pharmacokinetic profile. C₁: central compartment; C₂: first peripheral compartment; C₃: second peripheral compartment; C_A: absorption compartment; k: rate constant of transfer between different compartments (e.g. k₁₂ → transfer from C₁ to C₂; k₁₀ → clearance rate). Based on (152).

of compartmental PK models, as well as their structures and mathematical representation. Given that a PK/PD profile of a study population (human or preclinical species) is present, PK/PD parameters and information about population variability can be derived from the observed data – a process often referred to as ‘top-down’ fitting.

Compartmental models as described in Figure 10 are mainly empirical and descriptive. Although quite pragmatic and helpful for the intended purpose, application of such models are only of limited translational value, since the underlying mechanistic processes causing differences between species and individuals are not considered, which forces the operator to use empirical scaling factors and/or allometric scaling (e.g. scaling based on the bodyweight of the different species) to project the PK/PD properties (147). The lack of mechanistic insight with the PK- and PK/PD-models as well as the growing knowledge about biological processes and tissue compositions led to a more advanced in silico approach: the physiologically based pharmacokinetic modelling and simulation.

5.3.2.2 Introduction to PBPK Modelling

Physiologically based pharmacokinetic (PBPK) models consist of different compartments similar to the PK- and PK/PD-models. The difference is the higher level of complexity of PBPK modelling, where the compartments have a physiological relevance and are usually representations of body organs and tissues. As an example: GastroPlus™, a commercial PBPK modelling and simulation platform, assumes in the standard model thirteen different systemic tissues (lung, liver, spleen, adipose, muscle, heart, brain, kidney, skin, reproductive organs, red bone marrow, yellow bone marrow, and rest of body) which are interconnected by the systemic circulation (Figure 11).

The main merit of PBPK over PK and/or PK/PD modelling and simulation is the predictive power and the mechanistic nature that allows conferring the optimized PBPK model from one species to another species of interest by replacing physiological parameters (147, 153). Consequently, application of PBPK modelling and simulation is of high value for the prediction of human PK/PD based on pre-clinical species to aid designing first-in-human studies (154-157). An example of a FIH dose prediction supported by PBPK modelling and simulation is provided by a cholesteryl ester transfer protein (CETP)

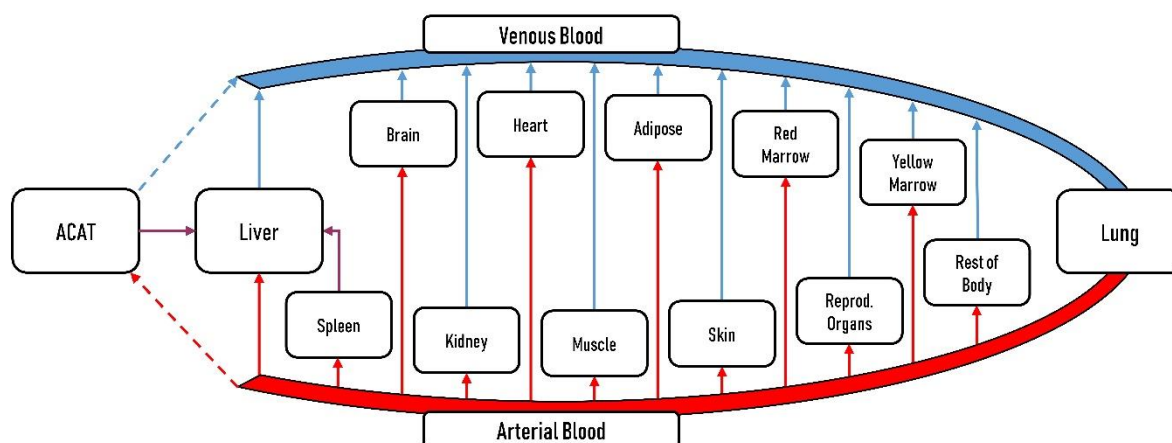


Figure 11 - Compartments in Physiologically Based Pharmacokinetic Models. Different Compartments describe individual (or merged) tissues in the body. The red and blue areas represent the arterial and venous blood, respectively. The ACAT model simulates the drug absorption process.

inhibitor developed by Bayer: PBPK modelling was applied to estimate the effective dose in human, which was used as a basis for the FIH dose-escalation study (158). The appropriateness of the selected doses (5 – 50 mg) could be demonstrated in the subsequent FIH studies (159). Besides FIH dose predictions, PBPK modelling is employed for several other applications during the development that involve (but are not limited to): 1) decision making in during the lead optimization stage to estimate the potential of a drug based on predicted PK properties, 2) evaluation of subpopulations of risk (e.g. due to enzyme polymorphisms or organ impairment) prior to clinical trials, 3) preclinical and clinical DDI predictions, and 4) simulations and assessments of alternative routes of administration (160).

The drawback of PBPK modelling and simulation is that the mechanistic approach is relatively data-hungry, requiring numerous system- and drug-specific parameters. System-dependent data involves a large number of physiological measures such as the tissue volume, tissue compositions, blood flows in the respective tissues, enzyme and transporter expression levels in various organs, pH in different segments of the gastro-intestinal tract, and many more. Compound-specific data include physico-chemical properties such as pKa, logP, solubility, molecular weight (MW), permeability, as well as other drug properties like metabolic clearance inhibition properties, rates of metabolite formation and involvement of active transport processes. In addition to the strong requirement for model input, only sparse data about the drug are present in the early discovery stage, which initially limits the appropriateness of the PBPK model. During the development process, newly generated data can be

integrated into the model to improve the simulations. As a consequence, PBPK models usually progress iteratively during the development process, involving multiple cycles of ‘predict, learn, confirm’ as newly generated data are available and can be integrated into the model (161).

The development itself can be based on the bottom-up, middle-out, or top-down approach. Bottom-up PBPK modelling makes use of knowledge about pharmacological mechanisms to predict in vivo pharmacokinetics of a drug and relies on the quality of data generated in vitro and in pre-clinical species. Contrarily, top-down approach involves the fitting of the model parameters based on observed in vivo data. In most cases, the PBPK modelling approach resembles the middle-out approach which is a combination between bottom-up predictions and top-down fitting. This includes the preclinical stage of drug development where the model predictions are verified with observed data from preclinical species to assess potential mismatches and to refine the model based on the model assumptions and the accuracy of input parameters as well as the clinical phases where the PBPK model is optimized based on observed clinical data in human (162, 163).

Over the last two decades, PBPK modelling has been developed and established in the pharmaceutical industry and reached acceptance by the regulatory agencies. The U.S. Food and Drug Administration (FDA) and the European Medicines Agency (EMA) both suggest the application of PBPK modelling to support the drug development (164). An increasing number of submissions for new drug applications (NDA) are complemented with analyses from PBPK simulations with a total of 110 submissions to the FDA from 2008 to 2017. Of these analyses in the submissions, 60% were about DDIs of metabolizing enzymes, 15% about simulation of pediatric populations, 7% about DDIs based on transporter activities, 6% about hepatic impairment, 4% about renal impairment, 4% about absorption and/or food effect, 2% about pharmacogenetic assessments, and 2% about other aspects (164). Examples of PBPK investigations that informed the prescription drug labeling are: the effect of a strong inhibitor on intravenous sildenafil exposure, the significance of OATP1B1/3 transporter on the simeprevir disposition was assessed, or the effect of alectinib and its metabolites on the pharmacokinetics of CYP2C8 substrates (164).

5.3.2.3 Theoretical Considerations and Simulations of PBPK Modelling

The assumptions and calculations of PBPK modelling are based on the core elements of pharmacokinetics: Absorption, Distribution, Metabolism, and Excretion (ADME) (Figure 12).

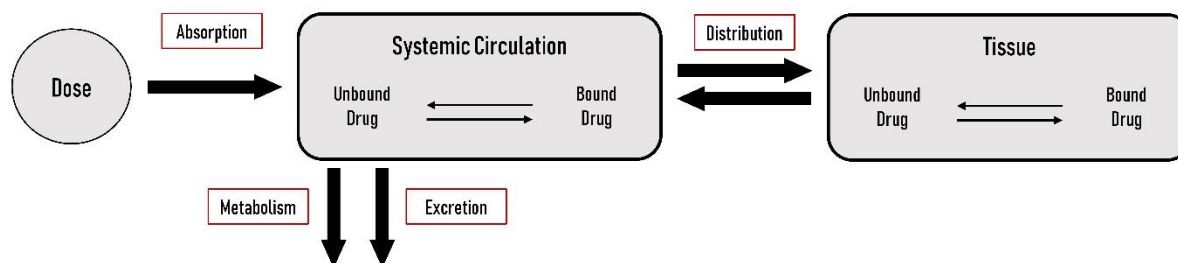


Figure 12 - Absorption, Distribution, Metabolism, and Excretion (ADME). ADME is a fundamental concept of pharmacokinetics and mechanistically describes the route of the drug in the body. Absorption describes the transfer of the compound and its metabolites from the site of absorption to the systemic circulation and is relevant for drugs that are not administered by the intravenous route (e.g. oral, nasal, or subcutaneous administration). Distribution is the process by which absorbed compound and its metabolites partition between blood and various tissues in the body. Metabolism is the process by which a drug is transformed by metabolizing enzymes, while excretion of unchanged drug or the metabolites is the elimination process via the liver, kidneys or other minor excretory organs such as the lung or skin. Figure and description are based on (152).

Since a drug is most frequently administered via the oral route, implementation of an absorption model in PBPK modelling is essential. The model should be capable of simulating and predicting the fractions and time courses of the compound absorbed into enterocytes (f_a), entering the portal vein (f_{DP}), and finally entering the systemic circulation (i.e. bioavailability). The transfer of the compound to different compartments (e.g. stomach, duodenum, jejunum, ileum, caecum, and colon) as depicted in Figure 13 is simulated under consideration of varying physiological conditions such as transit times, volumes, pH values, and bile salt concentrations (165, 166). In combination with formulation and drug-specific input (e.g. pH-dependent ionization state, solubility, particle size radius, permeability, etc.), the absorption model is able to simulate the dissolution of the drug and its transfer into enterocytes. Once permeated into the enterocytes, the drugs can subsequently proceed to the portal vein or might be subject to first-pass metabolism in enterocytes or can be actively transported back to the gut lumen by efflux transporters, e.g. by P-glycoprotein (P-gp). The advantage of implementing this mechanistic model into PBPK is the possibility to simulate different scenarios such as the food effect on drug absorption, the impact from different formulations on bioavailability (i.e. bioequivalence studies), or the extent and impact from first-pass metabolism, transporter activity including DDIs (167-170).

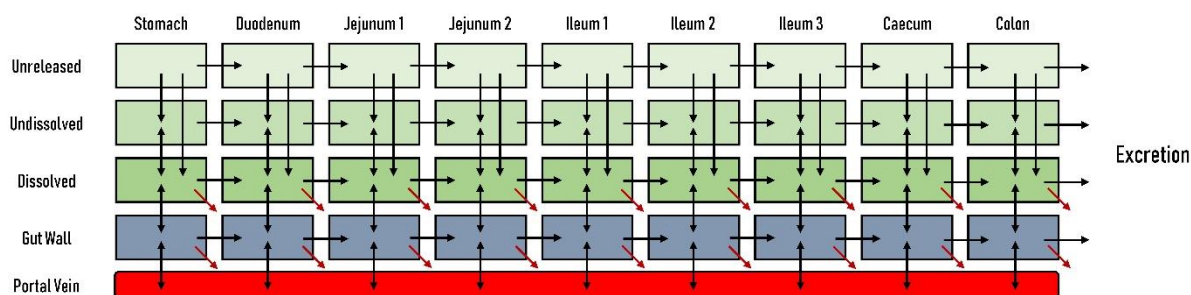


Figure 13 - Advanced Compartmental Absorption and Transit Model (ACAT). The ACAT model mathematically describes key processes present in the gut for simulation of absorption after oral administration of a drug. The compartments describe sections through the gastro-intestinal tract and different states of the drugs from the unreleased form to the dissolved form. Red arrows indicate luminal degradation of the dissolved drug and metabolic clearance of drug absorbed into the gut wall. Unabsorbed drug is subject to excretion via feces. The diagram is adapted from SimulationPlus®.

The fraction of the drug entering the systemic clearance from any site of administration undergoes distribution into the different tissues (mathematically: compartments), which is taken into account in the PBPK model (171). Different tissues have different properties such as tissue composition, volume, membrane permeability, or transporter expression patterns and the distribution is therefore regarded for each tissue individually. The steady state volume of distribution is the result of the sum of all individually calculated distribution volumes (plus the volume of the systemic circulation). The basic measures for the partitioning of the compound into the compartment are the tissue-to-plasma partition coefficients (K_p) which depend on tissue- and plasma protein binding of the drug, tissue composition and the ionization state, lipophilicity and pKa of the drug and might be driven by active uptake or efflux by transporter proteins (Figure 14) (172-175). It is further considered that the partitioning into tissues is limited by the blood flow for compounds with a high permeability (mostly lipophilic molecules) and limited by the permeability for compounds with low permeability (mostly hydrophilic and/or large molecules) (171).

Compound clearance can be integrated into the PBPK model if the clearance and the responsible DME(s) and transporter proteins are defined and, in addition, expression levels in the eliminating tissues are known. Total plasma clearance of a compound is the result of the combination between the metabolic clearance in respective tissues, drug excretion in the kidneys and biliary clearance in the liver. Hepatobiliary clearance is mediated by active transport of the parent drug (or metabolites) by efflux transporters, e.g. P-gp, breast cancer resistance protein (BCRP), or MRP2. Upon incorporation of biliary

clearance, the models might be extended to simulate enterohepatic recycling (176), which occurs when the compound after excretion from the bile pocket into the gut is reabsorbed into the enterocytes and finally reaching again the systemic clearance (177). The mechanistic model for renal excretion is a combination between filtration clearance, fraction unbound in plasma ($f_{u,p}$) * glomerular filtration rate (GFR), and active transport into the tubule under consideration of passive permeability from the capillary to the tubule and/or reabsorption to the capillary.

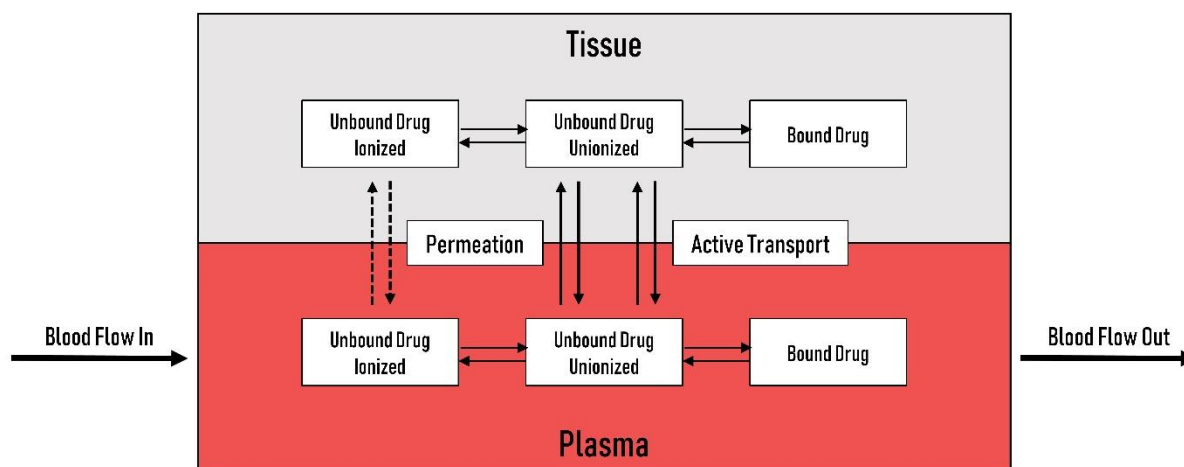


Figure 14 - Tissue to Plasma Partitioning of a Drug. The diagram shows a simplified scheme of the partitioning of a drug from the plasma into the tissue that is used as a basis for predictions of steady state volume of distribution. Only unbound drug in the unionized state can permeate through the membrane, whereas ionized drug might passively diffuse depending on the degree of ionization and the potential difference across the membrane. The ionization of a drug is depending on the pKa and on the pH of the respective tissues. Besides passive diffusion, compounds can be subject of active uptake or efflux. Descriptions and diagram are based on (173, 174).

The advantage of this mechanistic approach of estimating drug distribution and clearance is that drug concentrations in excretory tissues and at sites of action can be simulated at varying conditions (e.g. changes in blood flow, organ impairment, DDIs, etc.) and related to compound clearance and the observed therapeutic effect, respectively (171, 178-180). The input for enzyme kinetics of drug metabolizing enzymes and transporter proteins is usually a saturable process that follows a Michaelis-Menten kinetics described by the reaction velocity achieved at saturating concentrations of the drug (V_{max}) and the Michaelis-constant (K_M), which is the concentration of the substrate at half of the maximum velocity. This allows for the assessment of non-linearity due to DMEs or transporter proteins with PBPK modelling (181, 182).

5.3.2.4 Specific Applications of PBPK Models

Besides FIH dose predictions, evaluation of DDI risk is essential for the application of PBPK models in the pharmaceutical industry with a high regulatory impact (164). The mechanisms underlying the DDI effects are complex and time-dependent. A PBPK model is capable of stimulating the complex and time-dependent mechanisms underlying the DDI effects of the perpetrator on the victim drug, which makes it valuable for the drug development for the simulation of DDI risk assessments. Especially useful are prospective DDI predictions after FIH clinical studies: After FIH PK data give confidence in modelling the effect of clearance modifications due to DDIs, the simulations can be used as a waiver of clinical studies (162, 183). A case study where PBPK modelling was used for simulation of DDI due to inhibition is provided by Chen and colleagues (184). They demonstrated the use of PBPK modelling to predict the formation of and the inhibition by the inhibitory metabolite of amiodarone, mono-desethyl-amiodarone, on the PK of simvastatin, dextromethorphan, and warfarin. Yee and colleagues published in 2020 (185) a PBPK model to simulate the effect of CYP3A induction mediated by rifabutin on the doravirine and its major metabolites. Based the model simulations, they were able support the common dose adjustment performed in the clinical practice from 100 mg doravirine once daily to 100 mg twice daily when co-administered with rifabutin. Another, more complex model shows the attempt to simultaneously predict the effect of CYP3A/CYP2C9 induction and OATP inhibition due to rifampicin and using glibenclamide as probe substrate (186). The simulated results with the PBPK model were in accordance with the observed data, which shows the utility of using the approach for quantitative predictions of complex DDIs.

Another application for PBPK modelling is the simulation of PK (or PD) in different populations. Populations or subpopulations can be healthy volunteers/diseased patients for which the impact of the disease or other co-morbidities on the pharmacokinetic is simulated, different ethnicities with a different genotype/phenotype, subject of different ages which impacts the PK of a drug, or subjects of different gender. In a clinical setting, PK analysis of different populations and sub-populations require a large number of subjects which is consuming time and money. Therefore, PBPK modelling can be used to complement the population analysis by the simulation of a virtual population specified in the model. Zhou and colleagues (187) generated a model to assess PK differences in Caucasian and East Asian

populations with distinct CYP2C19 genotypes and successfully predicted the observed exposures in 84.4% of the cases. A model for a pediatric population with renal failure was generated by Ye and colleagues in 2020 (188) in which they simulated a significant increase in the AUC after oral administration of ertapenem in children with renal impairment to suggest a dose adjustment for this population. Also interesting is the application of PBPK modelling for the selection of an optimal mefloquine dose for young Caucasian children as conducted by Johnson and colleagues (189) which had to account for the developmental physiology and enzyme ontogeny and finally proposed a weekly dose of 62.5 mg for the prevention of malaria (in infant population from 5-10 kg). The impact of hepatic impairment was assessed for the PK of alectinib by Morcos and colleagues (190) which supports the dose adjustment in a population with severe hepatic impairment.

PBPK models are often combined with an effect compartment to simulate the fundamental relationship between drug concentration and pharmacodynamics effect in a physiologically based pharmacokinetic-pharmacodynamics (PBPK-PD). Knowing the pharmacokinetics of a drug and the pharmacodynamics effect, the time course of the therapeutic effect can be simulated. The combination of PBPK and PD is advantageous due to the mechanistic and quantitative derivation of the effect, which allows for better extrapolation capability and hypothesis testing and offers a valuable opportunity to explore the impact of physiological or drug-specific variability on the effect of the treatment. In addition, potential delay of the effect compared to the drug concentration that results in hysteresis in an effect concentration plot can be mechanistically assessed with a PBPK-PD model where e.g. distributional delay into the target tissue causes a lag time of activity. Application of a PBPK-PD models is demonstrated in a publication of Chetty and colleagues in 2014 (191), which linked PBPK and PD models to investigate the impact of variable PK on drug response. They successfully predicted the observed changes in drug response due to variations in phenotypes of metabolizing enzymes, drug formulations, drug receptor binding, and ethnic differences.

5.4 OUTLINE AND AIMS OF THE STUDIES

The introduction specifies the importance of predicting the hepatic clearance based on in vitro hepatocyte tools. Conventional and well-established in vitro tools with less complexity (e.g. human liver microsomes or suspended hepatocytes) lack sufficiently long incubation times and could not keep pace with the trend of developing drugs with a higher metabolic stability. This limitation was overcome with the adoption of a co-cultured hepatocyte system (HepatoPac) which offered the possibility to measure the in vitro intrinsic clearance for metabolically stable drugs and which showed in addition improved prediction of hepatic clearance. However, the studies that investigated the performance of the in vitro to in vivo (IVIVE) extrapolation with the system, mainly focused on CYP-mediated clearance, which leaves an important gap to the current drug development process: An increasingly high number of compounds is primarily biotransformed by UGT enzymes and not by CYP enzymes, hence, it was not known whether the findings for CYP substrates could be transferred to UGT substrates. We hypothesized that we can achieve improved predictions using the hepatocyte co-culture likewise for UGT enzymes, but further reflected that the scaling of glucuronidation clearance is connected to certain challenges owed to particularities of the UGT enzyme family such as extra-hepatic glucuronidation in the intestine and renal tissue, or the enterohepatic recirculation. To test and prove our hypothesis, we aimed to determine the performance of the hepatocyte co-culture for UGT enzymes and were keen on identifying possible sources of outlier behavior. Important to the significance of the study was a solid methodology throughout the work that included 1) multiple independent measurements of the in vitro intrinsic clearance for selected UGT substrates, 2) current state-of-the-art methodology for clearance scaling by accounting for the unbound fraction, and 3) thorough literature search for observed values of the hepatic clearance in human for the comparison to predicted values. The study resulted in the publication with the title “In Vitro to In Vivo Extrapolation of Metabolic Clearance for UGT Substrates Using Short-Term Suspensions and Long-Term Co-Cultured Human Hepatocytes”.

We also aimed on extending the work to the application of PBPK modelling for UGT substrates. As introduced in previous sections, the difficulty for UGT-mediated clearance is to define well-validated specific substrates and inhibitors which, as a result, impede the quantification of the contribution of individual UGT enzymes to the overall compound clearance. Furthermore, reported UGT expression

levels are yet connected to a high uncertainty. Based on the knowledge and on the expected quality of in vitro intrinsic clearance data determined in the hepatocyte co-culture, we concluded that we might use the in vitro intrinsic clearance as input in the PBPK models to achieve reasonable simulations. Hence, we were interested in learning about the potential of the HepatoPac system as a system for high quality input in the mechanistic modelling approach. Furthermore, we scrutinized the impact of extrahepatic glucuronidation on the oral and systemic clearance and wanted to demonstrate the current limitations and possibilities of PBPK modelling and simulation in regard of the uncertainties associated with UGT-mediated clearance. This thorough assessment is reported in-depth in the publication with the title “Construction and Verification of Physiologically Based Pharmacokinetic Models for Four Drugs Majorly Cleared by Glucuronidation: Lorazepam, Oxazepam, Naloxone, and Zidovudine”.

While having a special focus on UGT-mediated clearance, we also intended to advance in the adoption of novel hepatocyte in vitro systems. A big number of in vitro hepatocyte systems is meanwhile established and well-validated for assessments of ADME properties of compounds that differ in characteristics such as complexity, cost, throughput rate, and quality of the generated data. Furthermore, the repository is increasingly complemented with novel and potentially more sophisticated in vitro tools. In order to sort out the question: ‘at what development stage should which in vitro system be deployed’, we aimed to access and summarize the current strategy of using the value chain of in vitro systems. We also recognized the opportunity of using the HepatoPac co-culture to demonstrate potential merits that can be achieved with more sophisticated cultivation techniques by adding data about in vitro intrinsic clearance determinations, induction, and time-dependent inhibition as demonstration example. This thorough literature research accessorized with own in-house generated data resulted in the review with the title: “Application of New Cellular and Microphysiological Systems to Drug Metabolism Optimization and Their Positioning Respective to In Silico Tools”.

As next part, we aimed to evaluate a micro-physiological system which we purchased from the CN Bio Company. The system is a microfluidic liver-chip platform which has the advantage that shear stress on the hepatocytes can be generated that might have a beneficial effect on the metabolic stability and viability of the cells. Hence, the promise of the MPS is that it can be deployed for long-term incubations and to study complex research questions. Nevertheless, we first required to conduct a basic evaluation

of the system in which we demonstrate the capability of the system to maintain the fundamental phenotype of hepatocytes in order to allow for more advanced studies. We also acknowledged the higher sophistication of the system by combining the MPS with modelling and simulation approaches. The work is yet ongoing, whereas the modelling and simulation part needs to be finalized. Hence, the report with the working title “Optimization of a Liver-on-Chip System for DMPK Application and Combination with Modelling and Simulation” demonstrates the first part of the evaluation process which was conducted to assess the metabolic stability of the cells and which proposes an approach of quantifying the data generated on the liver-chip.

6 RESULTS

6.1 PAPER 1

Application of New Cellular and Microphysiological Systems to Drug Metabolism Optimization and Their Positioning Respective to In Silico Tools

Luca Docci, Neil Parrott, Stephen Krähenbühl, and Stephen Fowler

6.2 PAPER 2

In Vitro to In Vivo Extrapolation of Metabolic Clearance for UGT Substrates Using Short-Term Suspension and Long-Term Co-Cultured Human Hepatocytes

Luca Docci, Florian Klammers, Aynur Ekiciler, Birgit Molitor, Kenichi Umehara, Isabelle Walter, Stephan Krähenbühl, Neil Parrott, and Stephen Fowler

6.3 PAPER 3

Construction and Verification of Physiologically Based Pharmacokinetic Models for Four Drugs Majorly Cleared by Glucuronidation: Lorazepam, Oxazepam, Naloxone, and Zidovudine

Luca Docci, Kenichi Umehara, Stephan Krähenbühl, Stephen Fowler, and Neil Parrott

6.4 PREVIEW PAPER 4

Optimization of a Liver-on-Chip System for DMPK Application and Combination with Modelling and Simulation

Luca Docci and Nicolás Milani

Mentored and Supported by:

- **Stephen Fowler** (F. Hoffmann – La Roche; Basel)
- **Neil Parrott** (F. Hoffmann – La Roche; Basel)
- **Michael Gertz** (F. Hoffmann – La Roche; Basel)
- **Aleksandra Galetin** (University of Manchester; Manchester)
- **Patricio Godoy** (F. Hoffmann – La Roche; Basel)
- **Daniela Ortiz Franyuti** (F. Hoffmann – La Roche; Basel)

Introduction

Investigations of the pharmacokinetics are key studies during the drug development and rely on several *in vitro* systems that are routinely deployed to investigate and translate DMPK properties of a drug (4). Well established *in vitro* tools are optimized for the intended purposes, but still leave a gap that have to be addressed by the introduction of novel cell culture techniques (126). Microphysiological systems (MPS) are incrementally introduced in the pharmaceutical industry as novel cutting-edge *in vitro* systems that hold a high promise in addressing more complex questions due to the possibility of mimicking specific organ functions and organ-organ crosstalk (192-194). The promise in the field of ADME (absorption, distribution, metabolism, excretion) is to use the chips for assessments of first-pass after oral drug administration, for investigations of drug-drug interactions (DDIs), for studies about metabolite-driven toxicity, disease modelling, and/or special populations (126). In addition, multiple time points can be integrated into the *in vitro* experiments based on long-term incubations as achieved with microphysiological systems and used as high quality input for physiologically based pharmacokinetic modelling and simulation or other computational approaches (195).

However, integration of the MPS is yet in an exploratory stage and requires evaluation of adequate systems where the engineered platforms need to meet predefined specifications (e.g. low non-specific binding of lipophilic drugs and/or low volume loss due to evaporation and/or sampling) and the cultivated cells need to prove a physiological-like and stable phenotype (126, 196). For cultivating hepatocytes in a MPS, minimum prerequisites are active and stable activities of clinically relevant DMEs (e.g. CYP, UGT, AO) and transporter proteins (e.g. P-gp, OATP) (126). The fourth manuscript, which is currently in preparation, aims towards the evaluation of a promising microfluidic MPS, the CN Bio system (Figure 15).

The CN Bio system (Figure 15) is a microfluidic MPS that is currently undergoing proof-of-concept studies in which the merit of the system over conventional *in vitro* hepatocyte systems has to be demonstrated. However, before the application for complex *in vitro* studies, the system has to show stable metabolic activity towards probe substrates in order to qualify as adequate hepatocyte *in vitro* system for DMPK studies. In addition, certain challenges have to be resolved along the way: 1)

quantification of in vitro DMPK data is currently limited by the unknown number of hepatocytes residing the scaffold after the seeding and the pre-incubation of the cells, and 2) demonstration of the approach of combining the in vitro experiments with modelling and simulation techniques to overcome the complexities associated with the system (i.e. evaporation over longer incubation periods).

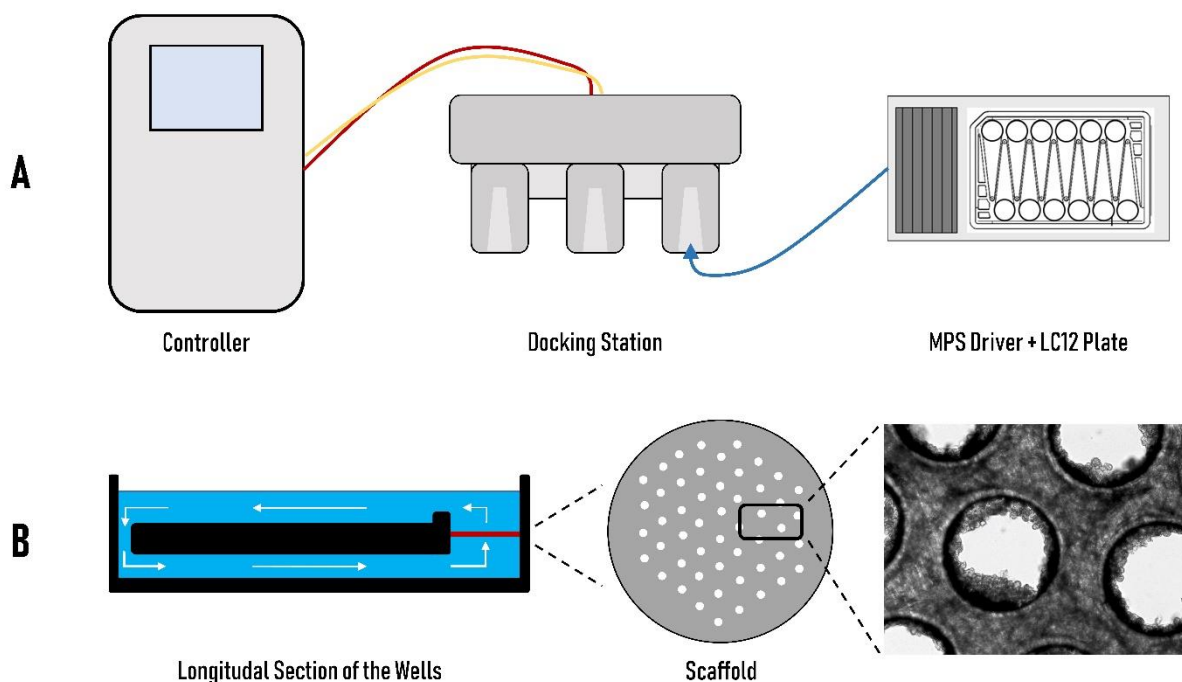


Figure 15 – Schematic of the CN Bio Liver Chip. A) Pressure and vacuum are produced in the controller by a compressor and vacuum pump. In addition, operations such as control of the fluid flow can be instructed with the controller. Docking station is linked to the controller and can house the MPS drivers. The MPS driver integrates a series of pneumatic solenoid valves to induce the flow to the incubation medium. B) Longitude section of the wells showing an up-flow of the medium (blue area) through the scaffold containing the hepatocytes (red area). The collagen-coated scaffold is shown as schematic (grey area). The microscope picture was taken in our laboratories and shows hepatocytes attached to the surface of the scaffold.

Materials and Methods

Materials

Ketoprofen (K-1751), zidovudine (A-2169), dextromethorphan (D-2531), dextrorphan (D-127), diclofenac (D-6899), repaglanide (R-9028), carbazeran (SML-0308), irinotecan (I-1406), telmisartan (T-8949), and quinidine (Q-3625) were purchased from Sigma-Aldrich (St. Louis, MO, USA). Lorazepam (L469850), naloxone (N284995), diclofenac-glucuronide (D436475), 3-hydroxy-quinidine

(H953230), 4-hydroxy-carbazeran (H884125), naloxone-glucuronide (N285010), efavirenz (E425000), telmisartan-glucuronide (T017010), and posaconazole (P689600) were purchased from Toronto Research Chemicals (Toronto, Canada). Cryopreserved hepatocyte recovery medium (CM7000), William's E medium (A12176-01), primary hepatocyte plating supplements (CM3000), primary hepatocyte maintenance supplements (CM4000), and human hepatocytes (lot: Hu8264) were purchased from ThermoFisher Scientific (Grand Island, NY, USA). Oxazepam, midazolam, and 1-hydroxymidazolam were synthesized at F. Hoffmann-La Roche Ltd. (Basel, Switzerland). All CN Bio components (controller, docking station, and drivers) and consumables (LC-12 plates) were acquired from CN Bio Innovations (Cambridge, UK).

Preparation of LC-12 Plates and Seeding of Cryopreserved Human Hepatocytes

The diagram in Figure 16 depicts the time scale of the process from plate preparation to the experiment. Detailed descriptions about the priming of the plates, the seeding process of the hepatocytes, and the media exchange program are provided in a later section ("Protocol: CN Bio" Liver Chip).

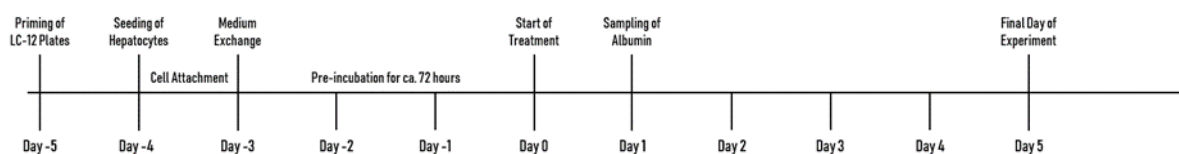


Figure 16 - Time Scale of Plate Preparation and Experiment.

Five days before the start of the treatment (Day -5), LC-12 plates were primed by flooding the microchannels with plating medium (William's E medium containing 5% fetal bovine serum, 1 μ M dexamethasone, 100 U/mL penicillin, 100 μ g/mL streptomycin, 4 μ g/mL human recombinant insulin, 2 mM GlutaMAX™, 15 mM HEPES). The day after (Day -4), hepatocytes were seeded on the scaffolds in the LC-12 plates. Briefly, primary cryopreserved hepatocytes (one vial per LC-12 plate) were thawed and suspended in cryopreserved hepatocyte recovery medium. Supernatant was aspirated after centrifugation (100 G for 10 minutes) and hepatocytes were re-suspended in 3 mL plating medium. Cells were counted with a hemocytometer (Bioswisstec Ltd., Switzerland) and seeded at between 400,000 and 650,000 hepatocytes per well. Plates were incubated at 37°C in a 5% CO₂ atmosphere overnight to allow

for the attachment of hepatocytes. The medium was changed after attachment of the cells on the scaffold (at Day -3) to maintenance medium (William's E medium containing 0.1 μM dexamethasone, 50 U/mL penicillin, 50 $\mu\text{g/mL}$ streptomycin, 6.25 $\mu\text{g/mL}$ human recombinant insulin, 6.25 $\mu\text{g/mL}$ human transferrin, 6.25 ng/mL selenous acid, 1.25 mg/mL bovine serum albumin, 5.35 $\mu\text{g/mL}$ linoleic acid, 2 mM GlutaMAX™, 15 mM HEPES) and cells were pre-incubated without media exchange for three days at 37°C in a 5% CO₂ atmosphere for three days until the first treatment day (Day 0).

In addition at Day -4 and in each experiment, the remaining hepatocyte suspension after the seeding process was used to investigate the total protein content per millions of hepatocytes, which is a relevant parameter for quantification of the cell number as described in the chapter below ("Quantification of Cell Number"). The remaining hepatocyte suspension was diluted with 20 mL PBS and centrifuged at 100G for 10 minutes. The supernatant was aspirated and the hepatocyte pellet was lysed with 5 mL PBS containing 1% Triton-X for twenty minutes. Total protein content was measured using the Pierce™ BCA Protein Assay Kit (Thermo Fisher Scientific) and correlated with the known number of cells in the remaining hepatocyte suspension (known from counting with the hemocytometer during the seeding process) to calculate the total protein yield per one million hepatocytes.

Quantification of Cell Number

The number of cells attached to the scaffold at Day 0 relative to the number of cells seeded at Day -4 (i.e. seeding efficiency) is unknown and had to be derived by using control wells in each experiment where the hepatocytes were lysed to determine the number of hepatocytes. The identified number of hepatocytes in the control wells were used to calculate an albumin production rate (APR) based on the albumin concentration in the medium of respective wells at Day 1 (24 hours after media exchange at Day 0) as depicted in Equation 1:

$$APR (\mu\text{g}_{ALB} * \text{day}^{-1} * 10^{-6} \text{cells}) = \frac{[ALB_{24h}] * V_{med}}{N_H} * 10^6 \quad (1)$$

ALB_{24h} is the concentration of albumin in the medium after 24 hours, V_{med} is the volume of medium, and N_H is the number of hepatocytes determined in the lysates from the control wells. The average APR calculated from the control wells could then be used to derive the number of hepatocytes in the

remaining wells with measured albumin concentrations in the medium of the respective wells using Equation 2:

$$N_H = \frac{[ALB_{24}] * V_{med}}{APR} * 10^6 \quad (2)$$

The albumin concentration was measured with the Human Albumin ELISA kit (Immunology Consultants Laboratory, Inc., Portland [insert where]) and total protein was measured using the Pierce™ BCA Protein Assay Kit (Thermo Fisher Scientific, what, where). A detailed protocol about the lysis of the hepatocytes in the scaffolds of the control wells is provided in the next section.

Lysis of Hepatocytes Attached on the Scaffolds

The scaffolds in the control wells were removed, washed twice in 1000 μL PBS and subsequently placed into 500 μL PBS containing 1% Triton-X. The surface of the scaffold was then thoroughly scratched with a pipette tip to ensure maximal retrieval of contained cells, and the lysing process was continued for half an hour. This process was repeated twice to ensure complete detachment and lysis of the cells. After the scaffold was washed and removed from the cell lysate, total protein content measured with the Pierce™ BCA Protein Assay Kit (Thermo Fisher Scientific), and the cell number estimated. For the measurements, it was assumed that all attached cells were alive and metabolically active, while dead cells were detached and removed from the scaffold during the washing steps.

In Vitro Intrinsic Clearance Measurements

The in vitro intrinsic clearance was determined for eleven substrates of CYP, UGT and AO enzymes (Table III). At the first treatment day (Day 0), the maintenance medium was replaced with fresh maintenance medium containing the probe substrates with a total volume of 1.8 mL medium (0.2 mL dead volume plus 1.6 mL added volume). Afterwards, no medium exchange was conducted during the time course of the experiment. The medium was first allowed to distribute into the whole well for at least half an hour before starting sampling. At respective time points, media samples were removed and quenched in acetonitrile containing internal standard (128 ng/mL D₆-Midazolam), centrifuged at 6200 G for 10 minutes at 4 °C and stored at -20 °C until preparation for measurement in liquid chromatography tandem mass spectrometry (LC-MS/MS). Compound depletion was measured in

triplicate for each drug in one occasion.

To determine the depletion of the probe substrates, the natural logarithm of the drug concentration in the incubation samples was plotted against time and linear regression analysis was applied using GraphPad Prism version 7.04 for Windows (GraphPad Software, La Jolla, CA). The *in vitro* CL_{int} was calculated from the depletion rate constant (k) of the linear regression (min^{-1}) for each well individually:

$$\text{In Vitro } CL_{int} (\mu\text{L}/\text{min}/10^6 \text{ hepatocytes}) = \frac{-k * V_{med} * 10^6}{N_H} \quad (3)$$

Where V_{med} was 1800 μL , and N_H is the number of cells estimated from the measured albumin production rate in the respective wells.

Table III – Probe Substrates and Metabolism

Compounds	Marker Enzyme(s)	Marker Reaction(s)	Product Formed	Ref.
Midazolam	CYP3A4/5	1-hydroxylation	1-hydroxy-midazolam	(197)
Dextromethorphan	CYP2D6	O-demethylation	Dextrorphan	(198)
Diclofenac	CYP2C9, UGT2B7	4-hydroxylation, O-glucuronidation	4-hydroxy-diclofenac Diclofenac-O-glucuronide	(199, 200)
Quinidine	CYP3A4/5	3-hydroxylation	3-hydroxy-quinidine	(201)
Carbazeran	AO1	4-hydroxylation	4-hydroxy-carbazeran	(202)
Repaglanide	UGT1A1, UGT1A3	O-glucuronidation	Repaglanide-O-glucuronide	(203)
Telmisartan	UGT1A3	O-glucuronidation	Telmisartan-1-O-glucuronide	(204)
Posaconazole	UGT1A4	N-glucuronidation	Posaconazole-N-glucuronide	(205)
Naloxone	UGT2B7	O-glucuronidation	Naloxone-O-glucuronide	(206)
Zidovudine	UGT2B7	O-glucuronidation	Zidovudine-O-glucuronide	(207)
Lorazepam	UGT2B7, UGT2B15	O-glucuronidation	Lorazepam-O-glucuronide	(208)

In addition, the metabolic activity in the hepatocytes was determined over the time period of four days by repeating the measurement each day with an intermediate washout step after every 24h hours. This measurement was conducted for midazolam (1-hydroxymidazolam formation via CYP3A4), diclofenac

(4-hydroxydiclofenac formation via CYP2C9 and diclofenac-glucuronide formation via UGT2B7), dextromethorphan (dextrorphan formation via CYP2D6), quinidine (3-hydroxyquinidine formation via CYP3A4), carbazeren (4-hydroxy-carbazeren formation via AO1), repaglanide (repaglanide-glucuronide formation via UGT1A1/1A3), and naloxone (naloxone-glucuronide formation via UGT2B7). The evaluation involved comparison of the depletion rate constant for the parent drugs and comparison of the area under the curve (AUC) of the concentration time profile for the metabolites.

Detailed Protocol: CN Bio Liver Chip

Device Set-Up and Priming of the LC-12 Plates

At Day -5, the LC-12 plate was primed with plating medium to avoid dry spots in the channels and to acclimatize the media and the components of the system to the incubator temperature. The LC-12 plates and the PhysioMimix™ MPS Drivers were first wiped with 70% ethanol and afterwards combined. The plating medium was pre-warmed to 37°C and was added (500 µL) to the reservoir side of the reservoir chamber (see Figure S-1). The drivers were slid into the PhysioMimix™ Docking Station to run the “Prime” Program, which induces an up-flow of 2.5 µL/s for 3 minutes to the medium in the wells. After this step, the wells were filled with 1100 µL to cover the whole surface of the well with medium. The plate was returned to the docking station to run the “Incubate” Program, which induces an up-flow of 2.5 µL/s to medium in the wells until the seeding at Day -4.

Media Exchange

The plates were removed from the incubator and the medium in the wells was aspirated until the remaining dead volume of 200 µL. Then, 400 µL of pre-warmed (37 °C) maintenance medium was added to the wells and the LC-12 plates were returned to the docking station to run the “Media Exchange” program, which induces a down-flow of 1.0 µL/s for 3 minutes. After the 3 minutes, the plates were removed from the docking station and the medium was again aspirated until the remaining dead volume of 200 µL. Then, 1400 µL of plating medium was added to each well and plates were returned to the docking station to run the “Incubate” program.

Seeding of the Cells

At Day -4, the hepatocytes were seeded on the scaffold of the wells in the LC-12 plate. For the process, the cryopreserved hepatocyte recovery medium (CHRM) and plating medium were pre-warmed to 37 °C in the water bath. Hepatocytes vial(s) were thawed and the cells were transferred and suspended into 50 mL of CHRM. The cell suspension was centrifuged at room temperature at 100G for 10 minutes, and afterwards, the supernatant was carefully aspirated. Hepatocyte pellet was loosened by gently tapping the falcon tube and re-suspended in 3.0 mL (for two vials of hepatocytes) of plating medium. 50 µL of cell suspension was transferred to 0.1% Trypan Blue for the cell count with the hemocytometer.

The primed plates were removed from the incubator and the medium in the wells was removed as described in the media exchange program, with the difference that the medium added in the last step was not 1400 µL maintenance medium, but 300 µL plating medium in order to prepare the plates for the seeding process. The prepared hepatocyte suspension was now equally distributed to the different scaffolds (100 µL for each well). Note: Important to ensure a well-mixed hepatocyte suspension and to disperse the hepatocytes over the whole scaffold to avoid inter-well variability. Afterwards, the plates were returned to the docking station to run the “Seed” program, which induces a down-flow of 1.0 µL/s for 2 minutes. The plates were removed and 1000 µL of plating medium was very slowly added to the wells to cover the surface of the wells. Finally, plates were returned to the docking station to run the remaining “Seed” program that runs for another 7 hours and 58 minutes and automatically changes to the “Incubate” program afterwards.

Results and Discussion

Quantification of the number of hepatocytes was assumed to be achieved via the use of albumin as marker that can be applied to correlate the cell number present during the incubation. Hence, first experiments were dedicated to evaluate the appropriateness of using albumin as marker and to provide a methodology in determining the hepatocyte number with sufficient confidence. Subsequent experiments tested metabolic activity of the hepatocytes incubated with the system to evaluate the potential for metabolism studies using specific probe substrates and/or marker reactions. In addition, the calculated number of cells per well was used to calculate in vitro intrinsic clearance values (in

$\mu\text{L}/\text{min}/10^6$ hepatocytes) and to reduce the inter-well variability due to differences in seeding density in the wells.

Measurement of Total Protein and Correlation with Number of Hepatocytes

Quantification of hepatocyte number in the wells was based on the albumin production rate measured in dedicated control wells, which required measurement for albumin concentrations in the medium and determination of the hepatocyte number in the control wells. Relevant for latter was the determination of the total amount of protein per one million hepatocytes. The amount of total protein determined with the BCA kit was compared to the number of cells counted on seven independent analyses and was consistent (between 1.015 and 1.078 mg / 10^6 hepatocytes) in six samples with one exceptional outlier (1.302 mg_{total protein}/ 10^6 hepatocytes). Linear regression showed a strong correlation ($R^2 = 0.995$) between the amount of total protein and the number of cells, with a mean value of 1.051 ± 0.019 mg_{total protein}/ 10^6 hepatocytes, excluding the outlier (Figure 17A). This mean value was similar to the total amount of protein per one millions hepatocytes applied in other publications (108, 209) and was applied for determination of cell number attached to the scaffold in the control wells.

Seeding Efficacy after Preincubation

Varying amounts of hepatocytes were initially seeded in the different experiment at Day -4, which was depending on the total revenue of hepatocytes per vial provided by the vendor. The measured number of hepatocytes at Day 1 in the control wells ($n = 15$) from each experiment ($n = 5$) was in average 260000 ± 25000 (CV: 9.3%) and ranged from 230000 to 310000 hepatocytes. Comparison of the number of hepatocytes measured in the control wells with the initial seeding number resulted in an average seeding efficiency of $52.0 \pm 7.1\%$ (CV: 13.6%) with values ranging from 39.0 to 66.5% (Figure 17B). Hence, about half of the cells remained attached on the scaffold after the pre-incubation. This is an important finding when considering the potential for under-prediction of DMPK properties (i.e. intrinsic clearance) based on the assumption that all seeded hepatocytes remained attached and viable during the pre-incubation and the experiment. Nevertheless, encouraging is the consistency of the seeding efficacy over

the different experiments, which increased the confidence in the methodology used for hepatocyte seeding and remaining plate manipulation procedures.

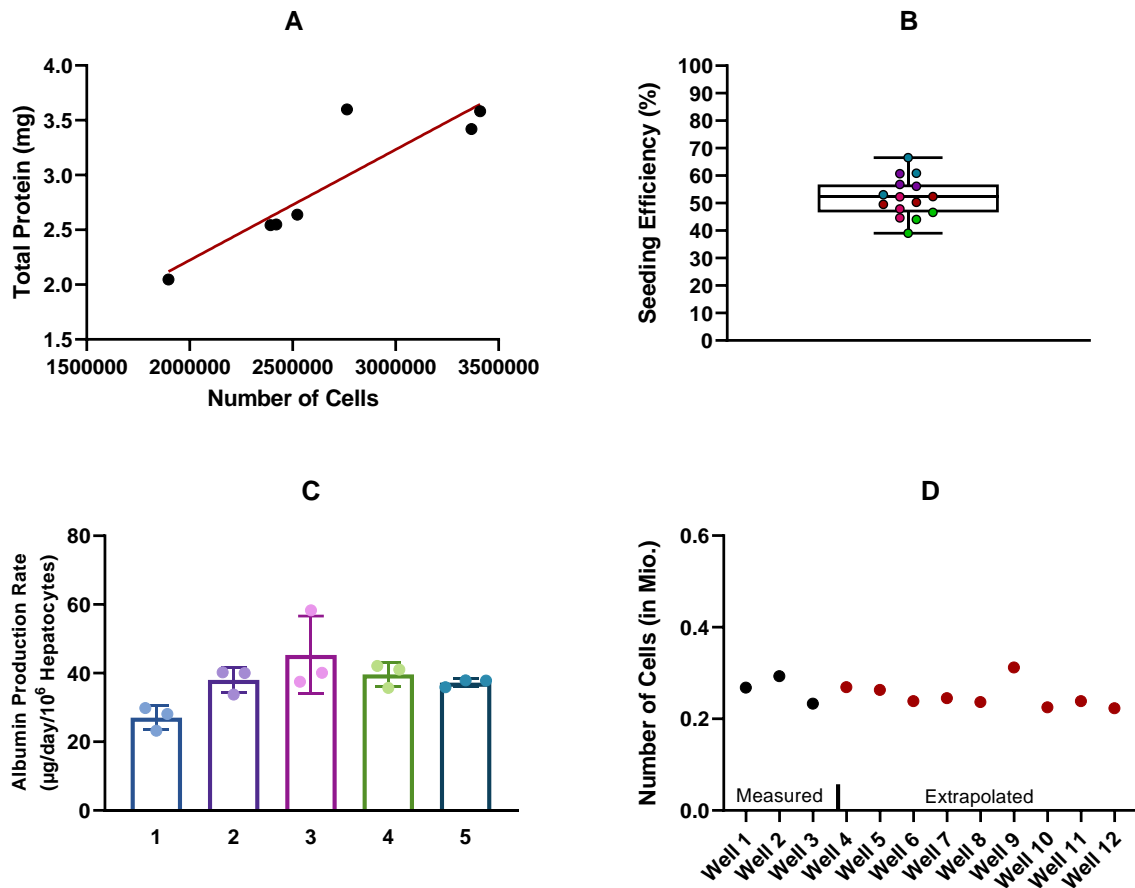


Figure 2 - Results from Total Protein Analysis and Albumin Correlation to Hepatocyte Number. A) Correlation between total protein and number of cells. B) Seeding efficiency of the experiments by comparing the initial amount of hepatocytes seeded and the measured total protein amount at Day 1 of the experiment in control wells. Different colours indicate data from different experiments. C) Albumin production rate measured in dedicated control wells in five different experiments. D) Measured (black dots) and interpolated (red dots) number of cells in different wells.

Albumin Concentration and Albumin Production Rate

The mean albumin concentration in all experiments (n = 5) and wells (n = 120) was $10.32 \pm 3.73 \mu\text{g}$ (CV: 36.1%). The mean albumin production rate (APR) was calculated using the known number of cells from protein analysis in the control wells (n = 15) and was $38.95 \pm 8.40 \mu\text{g/day}/10^6$ hepatocytes (CV: 21.6%) with values ranging from 23.2 to $58.3 \mu\text{g/day}/10^6$ hepatocytes. The mean APR differed between the experiments and was 27.0 ± 2.8 (CV: 10.4%), 38.0 ± 3.0 (CV: 7.8%), 45.3 ± 9.3 (CV: 20.4%), 39.6 ± 2.8 (CV: 7.1%), and 37.2 ± 0.9 (CV: 2.5%) $\mu\text{g/day}/10^6$ hepatocytes in the experiments 1, 2, 3, 4, and 5, respectively (Figure 17C). The APR in experiment 1 was significantly different (independent samples

T-test) from the APR in experiment 2 (p-value = 0.007), in experiment 4 (p-value = 0.008), and in experiment 5 (p-value = 0.039). Nevertheless, the overall mean APR from this study lies within the estimated albumin output of a human liver of 37 to 105 $\mu\text{g}/\text{day}/10^6$ hepatocytes as reported by Baudy and colleagues (210). Of note: It was considered to apply a global APR for all experiments that can be used to correlate the number of hepatocytes in each well. Due to the inter-experiment differences of the albumin production rate, a global APR value could not be applied. This had the disadvantage that three wells always had to be dedicated for the quantification of the cell number, but the advantage that the APR is reflecting altered incubation conditions (i.e. adaptation of the medium composition) for each experiment individually and/or other hepatocyte donors which will result in different values of APR. The measured number of hepatocytes in the control wells in combination with the albumin concentrations in the respective wells could then be used to calculate the albumin production rate. The albumin production rate could in turn be used to derive the number of hepatocytes in the remaining wells based on the albumin concentrations in the media. An exemplary depiction of extrapolated and measured values for cell numbers is shown in Figure 17D.

Compound Depletion and Calculation of In Vitro Intrinsic Clearance

In the second part of the study, the metabolic activity of major drug metabolizing enzymes was determined by measuring the depletion of four CYP substrates, six UGT substrates and one AO substrate. Depletion of the parent drug and metabolite formation was observed for all eleven drugs tested (Figure 18). Hence, the hepatocytes within the microfluidic system seem to retain their activity at least during the pre-incubation period which demonstrates the positive impact of the medium flow (i.e. shear stress) on the functionality of the hepatocytes. In comparison, a significant loss of activity is obtained for 2D-monocultured hepatocytes only 24 hours after the seeding (99).

Concentration time profiles of parent depletion were described by a linear regression curve and in vitro intrinsic clearance values were calculated based on the correlated number of cells. Rate of depletion and calculated in vitro intrinsic clearance values are summarized in Table IV. Mean intrinsic clearance values ranged from 1.81 ± 0.37 to 56.6 ± 1.3 $\mu\text{L}/\text{min}/10^6$ hepatocytes for zidovudine and naloxone, respectively. The intrinsic clearance was below 3 $\mu\text{L}/\text{min}/10^6$ hepatocytes for four compounds and

above 10 $\mu\text{L}/\text{min}/10^6$ hepatocytes for five compounds. Inter-well variability of the calculated depletion rate constant had an average CV of 12.7% (range from 2.7 to 26.9%) and was similar compared to the

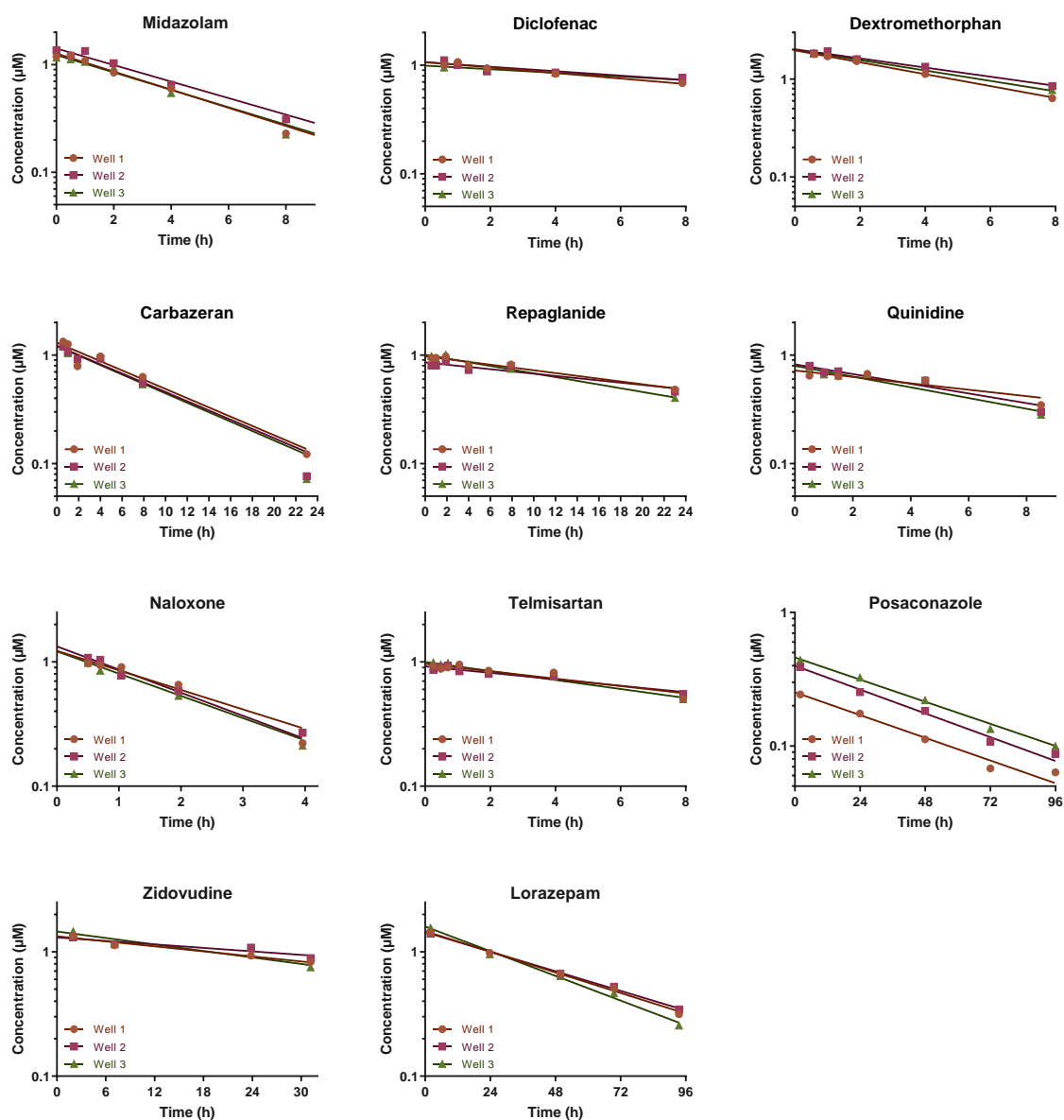


Figure 18 - Depletion of the Compounds over Time. Graphs describing the log-transformed concentrations of the compounds over time. Symbols represent the observed concentrations in the wells 1-3 and solid lines represent the linear regression curve. Parent depletion was described as the slope of the linear regression curve. Of note: differences in the experiment durations were due to differences in the metabolic stability of drugs.

mean CV of 11.8% (range from 2.3 to 21.3%) for in vitro intrinsic clearance values after normalization by the correlated cell number.

Metabolic Activity over Time

In order to determine the stability of the metabolic activity, we repeatedly measured compound depletion and metabolite formation over four days (i.e. day 0, day 1, day 2, and day 3) with an intermediate washing step before each measurement to wash out the compounds from the previous day. The measurement was conducted for seven out of eleven substrates. The stability of metabolic activity was assessed by comparing the depletion rates for the parent drugs and the area under the curve for metabolite formation at the different days (Figure 19). The rate of parent depletion at Day 4 compared to the initial depletion rate was 51.9% for midazolam, 79.9% for diclofenac, 63.7% for dextromethorphan, 48.2% for carbazeran, 84.2% for naloxone, 46.0% for repaglanide, and 42.3% for quinidine. The AUC of formed metabolites at Day 4 compared to the initial value at Day 0 was 72.1% for 1-hydroxymidazolam, 52.0% for 4-hydroxydiclofenac, 99.2% for diclofenac-O-glucuronide, 116.7% for dextroprphan, 27.0% for 4-hydroxy-carbazeran, 120.4% for repaglanide-O-glucuronide, 85.6% for naloxone-glucuronide, and 98.4% for 3-hydroxyquinidine.

Hence, the loss of activity was mainly observed for oxidative metabolism mediated by CYP enzymes and for oxidation mediated by the aldehyde oxidase. In contrast, the activity of UGT enzymes appeared to be stable over the time course of the experiment. Reasons for the loss of activity over time is most probably a combination of different factors. Firstly, the decrease in metabolic activity might be due to the loss of viable cells during the medium change or during the incubations. This was evident from total protein measurements at the final day of the experiment (data not shown) which showed a lower number of cells compared to Day 1 of the experiment in tendency. Secondly, a loss of phenotype is apparent when considering differences in decrease of metabolic activity for oxidative metabolism and glucuronidation activity. The problem might be solved by using a different hepatocyte lot or adapting the incubation conditions such as the flow rate of the medium or the medium composition.

Table IV – Parent Depletion and Bound In Vitro Intrinsic Clearance Values

Compound	Well	Decay Constant from Linear Regression in hours ⁻¹ (95% Confidence Interval)	Number of Cells	In Vitro Intrinsic Clearance (μL/min/10 ⁶ cells)	Average In Vitro CL _{int} ± SD (μL/min/10 ⁶ cells)	Inter-Well Variability (CV)
Midazolam	1	-0.2127 (-0.2400 to -0.1854)	233300	27.3	28.1 ± 2.40	8.7%
	2	-0.1908 (-0.2246 to -0.1570)	223200	25.6		
	3	-0.2133 (-0.2469 to -0.1797)	204000	31.4		
Diclofenac	1	-0.0361 (-0.0466 to -0.0256)	267800	6.45	5.10 ± 1.02	20.0%
	2	-0.0185 (-0.0322 to -0.0048)	330700	3.97		
	3	-0.0348 (-0.0403 to -0.0292)	231400	4.90		
Dextromethorphan	1	-0.1423 (-0.1487 to -0.1359)	279400	15.3	13.7 ± 1.1	8.3%
	2	-0.1090 (-0.1326 to -0.0855)	259500	12.6		
	3	-0.1212 (-0.1303 to -0.1121)	272600	13.3		
Carbazeran	1	-0.0976 (-0.1213 to -0.0739)	307900	9.5	10.0 ± 0.4	4.5%
	2	-0.1158 (-0.1308 to -0.1008)	328800	10.6		
	3	-0.1180 (-0.1360 to -0.0998)	347100	10.0		
Repaglanide	1	-0.0290 (-0.0373 to -0.0207)	452200	1.92	2.10 ± 0.47	22.4%
	2	-0.0247 (-0.0371 to -0.0123)	452100	1.64		
	3	-0.0379 (-0.0450 to -0.0308)	413900	2.75		
Quinidine	1	-0.0806 (-0.1414 to -0.0199)	304700	7.9	10.7 ± 2.3	21.3%
	2	-0.1135 (-0.1610 to -0.0660)	315300	10.8		
	3	-0.1213 (-0.1623 to -0.0803)	270000	13.5		
Telmisartan	1	-0.0763 (-0.1053 to -0.0472)	231000	9.91	9.57 ± 1.02	10.6%
	2	-0.0620 (-0.0805 to -0.0434)	227100	8.19		
	3	-0.0849 (-0.1019 to -0.0678)	240200	10.61		
Posaconazole	1	-0.0154 (-0.0209 to -0.0099)	238100	1.94	1.96 ± 0.10	4.9%
	2	-0.0163 (-0.0198 to -0.0128)	234000	2.09		
	3	-0.0163 (-0.0186 to -0.0141)	262800	1.86		
Naloxone	1	-0.4335 (-0.5670 to -0.3040)	223200	58.3	56.6 ± 1.3	2.3%
	2	-0.4000 (-0.4739 to -0.3262)	217900	55.1		
	3	-0.4457 (-0.5384 to -0.3531)	236700	56.5		
Zidovudine	1	-0.0152 (-0.0237 to -0.0066)	244700	1.86	1.81 ± 0.37	20.2%
	2	-0.0109 (-0.0237 to -0.0018)	244800	1.34		
	3	-0.0200 (-0.0353 to -0.0046)	269000	2.23		
Lorazepam	1	-0.0161 (-0.0180 to -0.0142)	250100	1.93	2.07 ± 0.13	6.2%
	2	-0.0151 (-0.0174 to -0.0129)	222000	2.04		
	3	-0.0190 (-0.0222 to -0.0158)	254500	2.24		

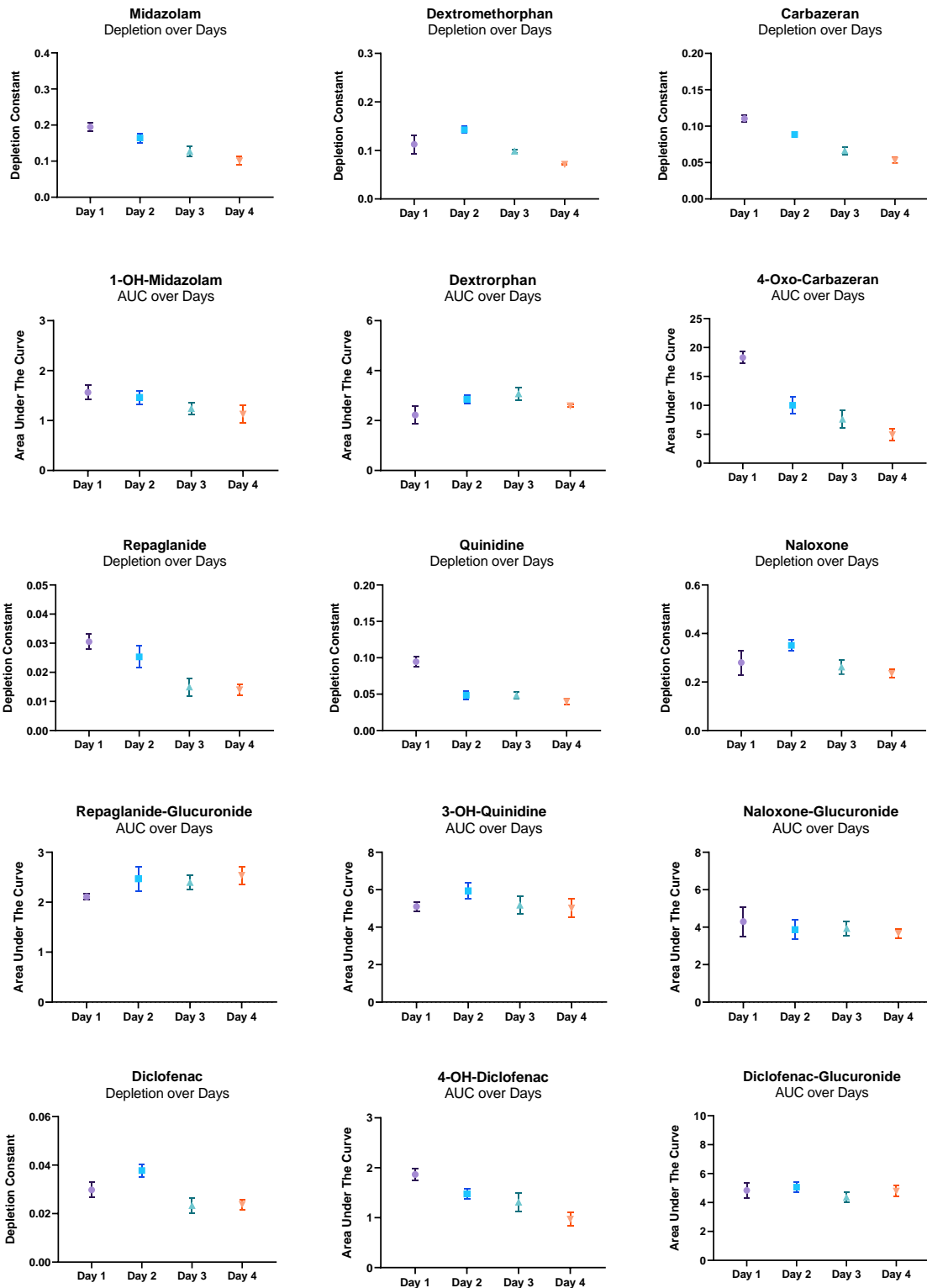


Figure 19 - Measured Metabolic Activity over Time. Change in metabolic activity over time determined via depletion rate of parent drugs and the AUC of formed metabolite. All depletion constants are given in min^{-1} and area under the curve is displayed in $\mu\text{mol}\cdot\text{hours}\cdot\text{mL}^{-1}$.

Conclusion and Preview on Modelling and Simulation

We successfully showed the approach of using albumin as a marker for the number of hepatocytes within the wells and could use the methodology for calculation of the in vitro intrinsic clearance. Metabolic activity was measured for the clinically relevant metabolizing enzymes which increases the confidence in the system for the application of DMPK assessments during the drug development. However, the activity did not remain stable mainly for oxidative metabolism and incubation conditions might be optimized and/or hepatocyte donors might be identified that demonstrate improved stability of the metabolic activity. Finally, the combination of the in vitro investigations with modelling and simulation techniques is key to the current work, but was not included in this manuscript yet, since the models require finalization. However, data indicate that the quality of the calculated in vitro intrinsic clearance was substantially improved by the application of a non-linear model that accounts for loss of activity during the incubation time due to evaporation and sampling. In addition, fraction metabolized values were derived for diclofenac ($f_{m,CYP}$ and $f_{m,UGT}$) and oxazepam ($f_{m,UGT2B15}$ and $f_{m,UGT1A9}$) that compare well with reported mass balance studies in vivo.

7 SUMMARY AND FUTURE INVESTIGATIONS

The publication with the title “In Vitro to In Vivo Extrapolation of Metabolic Clearance for UGT Substrates Using Short-Term Suspension and Long-Term Co-Cultured Human Hepatocytes” (211) investigated the accuracy and precision of the hepatic clearance for UGT substrates. Based on recent literature and research, we hypothesized that we could achieve improved prediction accuracy of the metabolic clearance using the HepatoPac system compared to suspended hepatocytes. Previous studies that used HepatoPac for IVIVE were quite specific on CYP-mediated metabolism, whilst disregarding generalization to other DMEs like UGT enzymes. Our investigations aimed to extend the previous work to the prediction of hepatic clearance for UGT-mediated metabolism. The results successfully proved the hypothesis by conducting an array of extensive in vitro experiments to investigate the in vitro clearance and by scaling and comparing the results to observed in vivo clearance, which showed improved predictions of the hepatic clearance using the hepatocyte co-culture. This was an important gap to fill and will have a positive impact on the confidence in the application of the system during drug development for UGT substrates. In addition, we clearly defined the protein binding and high inter-study variability as sources for uncertainty of the predictions and discussed potential reasons for the outlier behavior mainly regarding non-metabolic routes of clearances and/or other sites of metabolism (i.e. renal and intestinal tissues). The aspects are discussed in more depth in the manuscript.

We extended the work about the evaluation of UGT-mediated clearance further by generating and evaluating PBPK models for four of the substrates used in the clearance scaling publication. The work aimed to address previous reports that noticed low confidence in the application of PBPK modelling and simulation for UGT substrates. Hence, the aim of the study was to investigate current possibilities and limitations of PBPK modelling for UGT substrates, which is addressed in the publication with the title “Construction and Verification of Physiologically Based Pharmacokinetic Models for Four Drugs Majorly Cleared by Glucuronidation: Lorazepam, Oxazepam, Naloxone, and Zidovudine” (212). We successfully generated well-verified models for all of the UGT substrates and were able to simulate the PK profile of the parent drugs and their metabolites. Importantly, the systemic clearance was predicted within 1.5-fold of observed systemic clearance, while almost all of the remaining PK parameters (AUC_0

t_{inf} , C_{max} , T_{max} , V_{ss}) were predicted within 2-fold. By using these generated and validated PBPK models, we defined areas that require improvement to reach higher confidence in the application of PBPK modelling for UGT substrates. Major gaps that we identified were the estimation of fraction metabolized values for specific isoforms, the prediction of intestinal glucuronidation, and the prediction of the clearance of glucuronide metabolites. In addition, we related the importance of high quality input for UGT expression levels in different tissues and the identification of specific substrates and inhibitors of UGT isoforms to the uncertainty and variability reported in the literature. We finally concluded that The uncertainty of these parameters have to be improved in order to allow for higher confidence in bottom-up simulations of drug metabolism and pharmacokinetics using PBPK modelling and simulation. These and more limitations regarding UGT-mediated metabolism are reported in more detail in the publication.

Taken the two studies together, we could increase the confidence in translating UGT-mediated clearance based on the HepatoPac system and PBPK modelling and simulation. Yet, knowledge gaps remain for UGT enzymes and prediction of the metabolism in human. In the clearance scaling publication, a relatively low number of compounds ($n = 13$) was used for the investigations, which had the advantage that the quality of the generated data was high and that we could gain a mechanistic understanding about each of the drugs involved. This allowed us to assess the prediction accuracy for each of the compound and to discuss potential reasons for miss-predictions. The disadvantage of the approach was that the reduced number of drugs prevents a trend analysis to find statistical regularities for the success or failure of IVIVE. A high number of substrates can be applied to determine a more apparent impact on IVIVE from the uncertainty of protein binding values, from the physico-chemical properties, from the ECCS classification, and/or from the rate of hepatic extraction observed in vivo. Nevertheless, these types of studies have already been conducted in recent publication and was not in the scope of the study (137, 213, 214). More interesting and at the same time a suggestion for a future study is to correlate the bias of the IVIVE prediction for substrates of renally expressed UGT enzymes to determine the impact of extra-hepatic glucuronidation with a wider set of UGT substrates which might have an impact on the success of IVIVE as discussed in the publication. The challenge for this analysis would be to select an appropriate set of drugs since most UGT enzymes are metabolized by multiple UGT isoforms and significant renal glucuronidation is only expected for substrates of UGT1A9, UGT2B7, and UGT1A6.

Furthermore, the prediction bias seen with hepatocyte suspension could be improved by the use of the hepatocyte co-culture, nevertheless, a general bias towards under-prediction of the clearance remains. The general under-prediction of hepatic clearance is not only obtained in the current study, but has been reported in several studies beforehand (109, 215, 216). Two recent reviews addressed and discussed this limitation further (213, 217). Benet and Sodhi (217) discussed potential reasons for the poor predictions of metabolic clearance and declared three relevant factors that negatively impact the success of the predictions, which are: poor assay conditions for in vitro intrinsic clearance determinations, the assumption that the in vitro cells can be regarded as equivalent to in vivo hepatocytes, and poor methodology for the determination of fraction unbound. Importantly and related to their second point, we assumed that the pooled in vitro hepatocytes in both cellular tools have a comparable enzyme expression level to hepatocytes in vivo which, however, was not determined with quantitative proteomics in the hepatocyte co-culture due to the missing reference expression levels from the clinical studies and due to the difficulties of determining UGT enzyme expression levels.

The studies about PBPK modelling for UGT substrates could be extended by further investigating the potential and prediction of drug-drug interactions for UGT substrates. In fact, induction of CYP enzymes mainly via activation of PXR (e.g. rifampicin), AhR (e.g. omeprazole), and CAR (e.g. phenobarbital) is widely assessed. Although in vivo induction of the UGT enzymes is reported, the effect of inducers on the glucuronidation tend to be smaller than on CYP mediated clearance. This is also true for in vivo inhibition of the UGTs with an area under the curve (AUC) ratio typically of less than 2 when comparing the pharmacokinetics with and without concomitant administration of the inhibitor. Reasons for the weaker DDI effect for UGT enzymes might be 1) the metabolism, which is mediated by several UGT isoforms, leading to less weight of inhibition/induction of an individual UGT isoform, 2) the inhibitor concentration which is well below the K_I (inhibition constant) leading to a weak inhibition effect, 3) low hepatic extraction of the drug, or 4) a much higher K_M compared to intracellular concentrations in the liver at the site of metabolism (218). In order to increase the confidence in the prediction of DDIs, more examples showing successful predictions of DDI mediated by UGT enzymes have to be reported and current lines have to be drawn where the field is currently limited.

In addition to DDIs, an increasing amount of data is available about inter-individual variability of

metabolic clearance due to UGT enzymes and can be combined with PBPK modelling in order to improve the confidence in the approach and to strengthen the regulatory impact (161). Badé and colleagues (219) thoroughly investigated age-dependent changes in glucuronidation activity of ten different hepatic UGT isoforms (UGT1A1, 1A3, 1A4, 1A6, 1A9, 2B4, 2B7, 2B10, and 2B15) from pediatric to adult donors which was an important study due to the limited knowledge about the postnatal ontogeny of individual UGT enzymes. The newly generated data can be integrated into PBPK modelling and potentially improve the dosing recommendation and study designs in children (220). Finally, inter-individual variability due to polymorphisms are known and described for UGT enzymes. However, generation and validation of PBPK models describing differences in PK due to genetic polymorphisms is only poorly reflected in the literature.

Besides the HepatoPac co-culture, numerous in vitro systems are currently introduced in the pharmaceutical industry. The cultivation techniques might differ between the in vitro system, but the general promise for all the new systems is to prolong the cultivation period and to extend the possibilities which are limited by the current in vitro tools. These newly emerging systems (e.g. HepatoPac, spheroids, MPS) together with the well-established and routinely applied in vitro screening tools (e.g. HLM, suspended/plated hepatocytes) provide a plethora of in vitro test systems that can be applied during the drug development. However, deployment of the individual systems have to be reasonable and tailored to the respective development stages due to the distinct demands for data quality and throughput rate. The review with the title “Application of New Cellular and Microphysiological Systems to Drug Metabolism Optimization and Their Positioning Respective to In Silico Tools” (195) sorted out the value of advanced and conventional in vitro cultivation techniques for DMPK assessments during drug discovery and development. We accessorized the statements with results generated in the laboratory to show the improvement that comes from the application of the hepatocyte co-culture over suspended/plated hepatocytes for the determination of in vitro intrinsic clearance of metabolically stable drugs and for the study of drug-drug interactions due to time-dependent inhibition and induction. In addition, we reviewed other promising in vitro systems and in silico tools for DMPK assessments with the focus on applications where the systems can offer a merit over conventional tools. Importantly, we discussed that the adoption of new experimental systems is driven by the demonstration of clear added

value by 1) increasing the experimental capacity, 2) improving the quality of the measurements for ADME properties, and 3) enabling measurements that were not previously possible.

This was also a relevant consideration for the adoption of a novel micro-physiological system that we aimed to introduce to Roche. Basic evaluation of the system for minimal prerequisites had to be done first in order to demonstrate the appropriateness of the system. The last manuscript with the title “Optimization of a Liver-on-Chip System for DMPK Application and Combination with Modelling and Simulations” describes an evaluation of an MPS (CN Bio Liver Chip) that might be applied for more complex DMPK assessments. We achieved to exploit the albumin production rate as a marker for the cell number and demonstrated the presence of clinically relevant metabolizing enzymes. In addition, we calculated in vitro intrinsic clearance values based on the correlated number of hepatocytes. Hence, the work showed promising results for the application of the MPS for determinations of the metabolic clearance. Nevertheless, the system is currently limited by the apparent decrease in metabolic activity over the incubation time. This decrease in metabolic activity has to be addressed in an additional evaluation step in which 1) the incubation conditions (e.g. medium composition, medium flow rate, seeding density) are optimized and/or 2) more suitable hepatocyte donors are identified that remain a stable metabolic activity.

After the optimization of the metabolic stability in the hepatocytes, subsequent investigations need to include an in vitro to in vivo scaling of the measured intrinsic clearance to assess translatability to human clearance. This was not conducted because we used a single donor that hinders a reasonable comparison of the predicted clearance to observed clearance measured in a clinical study within a population. Instead, a pool of hepatocytes or multiple single donors should be applied for a proper IVIVE study like demonstrated in the publication describing the IVIVE of metabolic clearance for UGT substrates (211). The promise of the system is to combine multiple endpoints, describing different DMPK properties of a drug in one experiment. For example, simultaneous assessments of drug metabolism, active transport, and drug-drug interactions as demonstrated by Kratochwil and colleagues using HepatoPac (110) must be demonstrated. In addition, DMPK assessment can also be combined with safety risk assessments as investigated by Sarkar and colleagues (25) that simultaneously assess biotransformation and toxicity of diclofenac and its metabolites. However, in order to enable these types of studies, the MPS model needs

further characterization (i.e. mitochondrial and biochemical synthesis, mRNA expression of ADME genes, etc.) and requires to meet pre-defined specifications (196).

Finally, the medium flow has a positive effect on the hepatocytes (97), but can further be exploited by combining multiple tissues. In the longer term, the combination between liver and gut tissue is appealing because it offers the opportunity to assess the continuous communication between the tissues and to investigate the PK process after oral drug administration (120). Such applications have the potential to reduce the usage of preclinical animal models which are costly and unethical and might be, in combination with modelling and simulation, a powerful tool that find broad applicability in pre-clinical drug development (128).

8 CONCLUSION

The PhD project aimed to evaluate hepatocyte in vitro systems and PBPK modelling and simulation with a strong focus on UGT-mediated clearance. We demonstrated for the first time that an improvement is achieved upon the application of the HepatoPac co-culture for the in vitro to in vivo extrapolation of metabolic clearance for UGT substrates. We also identified and discussed current limitations in PBPK modelling and simulation based on well-constructed PBPK models regarding the bottom-up prediction of hepatic and extra-hepatic glucuronidation. Taken these studies together, we could increase the confidence in the development of UGT substrates when it comes to the static and mechanistic translation of metabolic clearance. The number of compounds undergoing metabolism via UGT enzymes is increasing and assessments as well as optimization of the current and also future test systems for UGT mediated metabolism is substantial for a successful drug development. Hence, the studies have a positive impact on the decision-making process in the pre-clinical drug development and, in addition, for dose predictions in first-in-human studies.

The review discussed the state of the art for the application of conventional and advanced hepatocyte systems, which were placed within the value chain of drug development and in relation to supporting computational approaches. Furthermore, we aimed to adopt a liver-on-chip device for the determination of DMPK properties ourselves. As demonstrated, the application of the systems in the pharmaceutical industry is yet in a relatively exploratory phase and more assessments and optimization have to be made before definite incorporation into the drug development.

The studies conducted during the PhD project can be complemented with additional assessments regarding the general improvement of the clearance scaling approach, as well as the prediction of drug-drug interactions, polymorphisms, and/or ontogeny based on UGT-mediated metabolism. Current and future in vitro systems and PBPK modelling and simulation can yet be improved to allow for mechanistic bottom-up modelling to describe the ADME behavior of a drug in human already in the pre-clinical phase of the drug development. Ultimately, this will be a step forward that accelerates the drug development process and that can potentially reduce the costly and unethical animal studies.

9 REFERENCES

1. Boyer S BC, Davis AM. Attrition in Drug Discovery and Development. In: Alex A HC, Smith DA editor. Attrition in the Pharmaceutical Industry 2015. p. 5-45.
2. Prentis RA, Lis Y, Walker SR. Pharmaceutical innovation by the seven UK-owned pharmaceutical companies (1964-1985). *Br J Clin Pharmacol*. 1988;25(3):387-96.
3. Kola I, Landis J. Can the pharmaceutical industry reduce attrition rates? *Nature Reviews Drug Discovery*. 2004;3(8):711-6.
4. Zhang D, Luo G, Ding X, Lu C. Preclinical experimental models of drug metabolism and disposition in drug discovery and development. *Acta Pharmaceutica Sinica B*. 2012;2(6):549-61.
5. Kassel DB. Applications of high-throughput ADME in drug discovery. *Curr Opin Chem Biol*. 2004;8(3):339-45.
6. Roberts SA. High-throughput screening approaches for investigating drug metabolism and pharmacokinetics. *Xenobiotica*. 2001;31(8-9):557-89.
7. Singh SS. Preclinical pharmacokinetics: an approach towards safer and efficacious drugs. *Curr Drug Metab*. 2006;7(2):165-82.
8. Chien JY, Friedrich S, Heathman MA, de Alwis DP, Sinha V. Pharmacokinetics/Pharmacodynamics and the stages of drug development: role of modeling and simulation. *Aaps j*. 2005;7(3):E544-59.
9. Dickson M, Gagnon JP. Key factors in the rising cost of new drug discovery and development. *Nature Reviews Drug Discovery*. 2004;3(5):417-29.
10. Paul SM, Mytelka DS, Dunwiddie CT, Persinger CC, Munos BH, Lindborg SR, et al. How to improve R&D productivity: the pharmaceutical industry's grand challenge. *Nature Reviews Drug Discovery*. 2010;9(3):203-14.
11. Mohs RC, Greig NH. Drug discovery and development: Role of basic biological research. *Alzheimer's & Dementia: Translational Research & Clinical Interventions*. 2017;3(4):651-7.
12. Cao X, Gibbs ST, Fang L, Miller HA, Landowski CP, Shin H-C, et al. Why is it Challenging to Predict Intestinal Drug Absorption and Oral Bioavailability in Human Using Rat Model. *Pharm Res*. 2006;23(8):1675-86.

13. Akabane T, Tabata K, Kadono K, Sakuda S, Terashita S, Teramura T. A Comparison of Pharmacokinetics between Humans and Monkeys. *Drug Metab Disposition*. 2010;38(2):308-16.
14. Di L. The role of drug metabolizing enzymes in clearance. *Expert Opin Drug Metab Toxicol*. 2014;10(3):379-93.
15. van Dorp EL, Morariu A, Dahan A. Morphine-6-glucuronide: potency and safety compared with morphine. *Expert Opin Pharmacother*. 2008;9(11):1955-61.
16. Pumford NR, Myers TG, Davila JC, Highet RJ, Pohl LR. Immunochemical detection of liver protein adducts of the nonsteroidal antiinflammatory drug diclofenac. *Chem Res Toxicol*. 1993;6(2):147-50.
17. Allison AC. Mechanisms of action of mycophenolate mofetil. *Lupus*. 2005;14(3_suppl):2-8.
18. Allison AC, Almquist SJ, Muller CD, Eugui EM. In vitro immunosuppressive effects of mycophenolic acid and an ester pro-drug, RS-61443. *Transplant Proc*. 1991;23(2 Suppl 2):10-4.
19. Fujiyama N, Miura M, Kato S, Sone T, Isobe M, Satoh S. Involvement of Carboxylesterase 1 and 2 in the Hydrolysis of Mycophenolate Mofetil. *Drug Metab Disposition*. 2010;38(12):2210.
20. McQueen CA, Bond J, Ramos K, Lamb J, Guengerich FP, Lawrence D, et al. *Comprehensive Toxicology, Volumes 1-14 (2nd Edition)*. Elsevier.
21. Nebert DW, Wikvall K, Miller WL. Human cytochromes P450 in health and disease. *Philosophical transactions of the Royal Society of London Series B, Biological sciences*. 2013;368(1612):20120431-.
22. Nelson DR, Koymans L, Kamataki T, Stegeman JJ, Feyereisen R, Waxman DJ, et al. P450 superfamily: update on new sequences, gene mapping, accession numbers and nomenclature. *Pharmacogenet Genomics*. 1996;6(1):1-42.
23. Wijnen PAHM, Op Den Buijsch RAM, Drent M, Kuipers PMJC, Neef C, Bast A, et al. Review article: the prevalence and clinical relevance of cytochrome P450 polymorphisms. *Aliment Pharmacol Ther*. 2007;26(s2):211-9.
24. Yu A, Haining RL. Comparative contribution to dextromethorphan metabolism by cytochrome P450 isoforms in vitro: can dextromethorphan be used as a dual probe for both CYP2D6 and CYP3A activities? *Drug Metab Dispos*. 2001;29(11):1514-20.
25. Sarkar U, Ravindra KC, Large E, Young CL, Rivera-Burgos D, Yu J, et al. Integrated Assessment of Diclofenac Biotransformation, Pharmacokinetics, and Omics-Based Toxicity in a Three-

- Dimensional Human Liver-Immunocompetent Coculture System. *Drug Metab Dispos.* 2017;45(7):855-66.
26. Gong L, Stamer UM, Tzvetkov MV, Altman RB, Klein TE. PharmGKB summary: tramadol pathway. *Pharmacogenet Genomics.* 2014;24(7):374-80.
 27. Hua L, Chiang CW, Cong W, Li J, Wang X, Cheng L, et al. The Cancer Drug Fraction of Metabolism Database. *CPT Pharmacometrics Syst Pharmacol.* 2019;8(7):511-9.
 28. Fowler S, Zhang H. In vitro evaluation of reversible and irreversible cytochrome P450 inhibition: current status on methodologies and their utility for predicting drug-drug interactions. *The AAPS journal.* 2008;10(2):410-24.
 29. Bauman JL. The role of pharmacokinetics, drug interactions and pharmacogenetics in the acquired long QT syndrome. *Eur Heart J Suppl.* 2001;3(suppl_K):K93-K100.
 30. Woosley RL, Chen Y, Freiman JP, Gillis RA. Mechanism of the Cardiotoxic Actions of Terfenadine. *JAMA.* 1993;269(12):1532-6.
 31. Hewitt NJ, Lecluyse EL, Ferguson SS. Induction of hepatic cytochrome P450 enzymes: methods, mechanisms, recommendations, and in vitro-in vivo correlations. *Xenobiotica.* 2007;37(10-11):1196-224.
 32. Fromm MF, Busse D, Kroemer HK, Eichelbaum M. Differential induction of prehepatic and hepatic metabolism of verapamil by rifampin. *Hepatology.* 1996;24(4):796-801.
 33. Shenfield GM. Genetic polymorphisms, drug metabolism and drug concentrations. *The Clinical biochemist Reviews.* 2004;25(4):203-6.
 34. McGraw J, Waller D. Cytochrome P450 variations in different ethnic populations. *Expert Opin Drug Metab Toxicol.* 2012;8(3):371-82.
 35. Ingelman-Sundberg M. Genetic polymorphisms of cytochrome P450 2D6 (CYP2D6): clinical consequences, evolutionary aspects and functional diversity. *The Pharmacogenomics Journal.* 2005;5(1):6-13.
 36. Xie HG, Kim RB, Wood AJ, Stein CM. Molecular basis of ethnic differences in drug disposition and response. *Annu Rev Pharmacol Toxicol.* 2001;41:815-50.
 37. Kirchheiner J, Schmidt H, Tzvetkov M, Keulen JT, Lötsch J, Roots I, et al. Pharmacokinetics of codeine and its metabolite morphine in ultra-rapid metabolizers due to CYP2D6 duplication. *The Pharmacogenomics Journal.* 2007;7(4):257-65.

38. Sistonen J, Fuselli S, Palo JU, Chauhan N, Padh H, Sajantila A. Pharmacogenetic variation at CYP2C9, CYP2C19, and CYP2D6 at global and microgeographic scales. *Pharmacogenet Genomics*. 2009;19(2):170-9.
39. Tanaka E. Update: genetic polymorphism of drug metabolizing enzymes in humans. *J Clin Pharm Ther*. 1999;24(5):323-9.
40. Brian W, Tremaine LM, Arefayene M, de Kanter R, Evers R, Guo Y, et al. Assessment of drug metabolism enzyme and transporter pharmacogenetics in drug discovery and early development: perspectives of the I-PWG. *Pharmacogenomics*. 2016;17(6):615-31.
41. Guillemette C, Lévesque É, Rouleau M. Pharmacogenomics of human uridine diphospho-glucuronosyltransferases and clinical implications. *Clin Pharmacol Ther*. 2014;96(3):324-39.
42. Thummel KE, Lin YS. Sources of Interindividual Variability. In: Nagar S, Argikar UA, Tweedie DJ, editors. *Enzyme Kinetics in Drug Metabolism: Fundamentals and Applications*. Totowa, NJ: Humana Press; 2014. p. 363-415.
43. Yang L, Price ET, Chang C-W, Li Y, Huang Y, Guo L-W, et al. Gene Expression Variability in Human Hepatic Drug Metabolizing Enzymes and Transporters. *PLoS One*. 2013;8(4):e60368.
44. Huang S-M, Temple R. Is This the Drug or Dose for You?: Impact and Consideration of Ethnic Factors in Global Drug Development, Regulatory Review, and Clinical Practice. *Clin Pharmacol Ther*. 2008;84(3):287-94.
45. Thompson TN. Optimization of metabolic stability as a goal of modern drug design. *Med Res Rev*. 2001;21(5):412-49.
46. Argikar UA, Potter PM, Hutzler JM, Marathe PH. Challenges and Opportunities with Non-CYP Enzymes Aldehyde Oxidase, Carboxylesterase, and UDP-Glucuronosyltransferase: Focus on Reaction Phenotyping and Prediction of Human Clearance. *Aaps j*. 2016;18(6):1391-405.
47. Walia G, Smith AD, Riches Z, Collier AC, Coughtrie MWH. The effects of UDP-sugars, UDP and Mg²⁺ on uridine diphosphate glucuronosyltransferase activity in human liver microsomes. *Xenobiotica*. 2018;48(9):882-90.
48. Zamek-Gliszczynski MJ, Taub ME, Chothe PP, Chu X, Giacomini KM, Kim RB, et al. Transporters in Drug Development: 2018 ITC Recommendations for Transporters of Emerging Clinical Importance. *Clin Pharmacol Ther*. 2018;104(5):890-9.

49. Guillemette C. Pharmacogenomics of human UDP-glucuronosyltransferase enzymes. *The Pharmacogenomics Journal*. 2003;3(3):136-58.
50. Meech R, Hu DG, McKinnon RA, Mubarakah SN, Haines AZ, Nair PC, et al. The UDP-Glycosyltransferase (UGT) Superfamily: New Members, New Functions, and Novel Paradigms. *Physiol Rev*. 2019;99(2):1153-222.
51. Radomska-Pandya A, Bratton SM, Redinbo MR, Miley MJ. The crystal structure of human UDP-glucuronosyltransferase 2B7 C-terminal end is the first mammalian UGT target to be revealed: the significance for human UGTs from both the 1A and 2B families. *Drug Metab Rev*. 2010;42(1):133-44.
52. Fujiwara R, Yokoi T, Nakajima M. Structure and Protein-Protein Interactions of Human UDP-Glucuronosyltransferases. *Front Pharmacol*. 2016;7:388-.
53. Liu Y, Coughtrie MWH. Revisiting the Latency of Uridine Diphosphate-Glucuronosyltransferases (UGTs)-How Does the Endoplasmic Reticulum Membrane Influence Their Function? *Pharmaceutics*. 2017;9(3):32.
54. Miners JO, Rowland A, Novak JJ, Lapham K, Goosen TC. Evidence-based strategies for the characterisation of human drug and chemical glucuronidation in vitro and UDP-glucuronosyltransferase reaction phenotyping. *Pharmacol Ther*. 2020:107689.
55. Allain EP, Rouleau M, Lévesque E, Guillemette C. Emerging roles for UDP-glucuronosyltransferases in drug resistance and cancer progression. *Br J Cancer*. 2020;122(9):1277-87.
56. Oda S, Fukami T, Yokoi T, Nakajima M. A comprehensive review of UDP-glucuronosyltransferase and esterases for drug development. *Drug Metab Pharmacokinet*. 2015;30(1):30-51.
57. Rowland A, Miners JO, Mackenzie PI. The UDP-glucuronosyltransferases: their role in drug metabolism and detoxification. *Int J Biochem Cell Biol*. 2013;45(6):1121-32.
58. Vergara AG, Watson CJW, Chen G, Lazarus P. UDP-glycosyltransferase 3A (UGT3A) metabolism of polycyclic aromatic hydrocarbons: potential importance in aerodigestive tract tissues. *Drug Metab Disposition*. 2019:dmd.119.089284.
59. Tukey RH, Strassburg CP. Human UDP-Glucuronosyltransferases: Metabolism, Expression, and Disease. *Annu Rev Pharmacol Toxicol*. 2000;40(1):581-616.

60. Lv X, Zhang J-B, Hou J, Dou T-Y, Ge G-B, Hu W-Z, et al. Chemical Probes for Human UDP-Glucuronosyltransferases: A Comprehensive Review. *Biotechnol J*. 2019;14(1):1800002.
61. Hadžiabdić J, Elezovic A, Imamović B, Becic E. The Improvement of Lorazepam Solubility by Cosolvency, Micellization and Complexation 2012.
62. Ladumor MK, Thakur A, Sharma S, Rachapally A, Mishra S, Bobe P, et al. A repository of protein abundance data of drug metabolizing enzymes and transporters for applications in physiologically based pharmacokinetic (PBPK) modelling and simulation. *Sci Rep*. 2019;9(1):9709.
63. Sato Y, Nagata M, Tetsuka K, Tamura K, Miyashita A, Kawamura A, et al. Optimized methods for targeted peptide-based quantification of human uridine 5'-diphosphate-glucuronosyltransferases in biological specimens using liquid chromatography-tandem mass spectrometry. *Drug Metab Dispos*. 2014;42(5):885-9.
64. Court MH. Isoform-Selective Probe Substrates for In Vitro Studies of Human UDP-Glucuronosyltransferases. *Methods Enzymol*. 400: Academic Press; 2005. p. 104-16.
65. Hiraoka H, Yamamoto K, Miyoshi S, Morita T, Nakamura K, Kadoi Y, et al. Kidneys contribute to the extrahepatic clearance of propofol in humans, but not lungs and brain. *Br J Clin Pharmacol*. 2005;60(2):176-82.
66. Ohno S, Nakajin S. Determination of mRNA expression of human UDP-glucuronosyltransferases and application for localization in various human tissues by real-time reverse transcriptase-polymerase chain reaction. *Drug Metab Dispos*. 2009;37(1):32-40.
67. Zhang H, Wolford C, Basit A, Li AP, Fan PW, Takahashi RH, et al. Regional proteomic quantification of clinically relevant non-cytochrome P450 enzymes along the human small intestine. *Drug Metab Disposition*. 2020;dmd.120.090738.
68. Heringa M. Review on raloxifene: profile of a selective estrogen receptor modulator. *Int J Clin Pharmacol Ther*. 2003;41(8):331-45.
69. Mizuma T. Intestinal glucuronidation metabolism may have a greater impact on oral bioavailability than hepatic glucuronidation metabolism in humans: a study with raloxifene, substrate for UGT1A1, 1A8, 1A9, and 1A10. *Int J Pharm*. 2009;378(1-2):140-1.
70. Achour B, Rostami-Hodjegan A, Barber J. Protein expression of various hepatic uridine 5'-diphosphate glucuronosyltransferase (UGT) enzymes and their inter-correlations: a meta-analysis. *Biopharm Drug Dispos*. 2014;35(6):353-61.

71. Achour B, Dantonio A, Niosi M, Novak JJ, Al-Majdoub ZM, Goosen TC, et al. Data Generated by Quantitative Liquid Chromatography-Mass Spectrometry Proteomics Are Only the Start and Not the Endpoint: Optimization of Quantitative Concatemer-Based Measurement of Hepatic Uridine-5'-Diphosphate-Glucuronosyltransferase Enzymes with Reference to Catalytic Activity. *Drug Metab Dispos.* 2018;46(6):805-12.
72. Stingl JC, Bartels H, Viviani R, Lehmann ML, Brockmoller J. Relevance of UDP-glucuronosyltransferase polymorphisms for drug dosing: A quantitative systematic review. *Pharmacol Ther.* 2014;141(1):92-116.
73. Strassburg CP, Lankisch TO, Manns MP, Ehmer U. Family 1 uridine-5'-diphosphate glucuronosyltransferases (UGT1A): from Gilbert's syndrome to genetic organization and variability. *Arch Toxicol.* 2008;82(7):415-33.
74. Ramesh M, Ahlawat P, Srinivas NR. Irinotecan and its active metabolite, SN-38: review of bioanalytical methods and recent update from clinical pharmacology perspectives. *Biomed Chromatogr.* 2010;24(1):104-23.
75. Iyer L, Das S, Janisch L, Wen M, Ramírez J, Karrison T, et al. UGT1A1*28 polymorphism as a determinant of irinotecan disposition and toxicity. *The Pharmacogenomics Journal.* 2002;2(1):43-7.
76. Lu CY, Huang CW, Wu IC, Tsai HL, Ma CJ, Yeh YS, et al. Clinical Implication of UGT1A1 Promoter Polymorphism for Irinotecan Dose Escalation in Metastatic Colorectal Cancer Patients Treated with Bevacizumab Combined with FOLFIRI in the First-line Setting. *Transl Oncol.* 2015;8(6):474-9.
77. Guillemette C, Ritter JK, Auyeung DJ, Kessler FK, Housman DE. Structural heterogeneity at the UDP-glucuronosyltransferase 1 locus: functional consequences of three novel missense mutations in the human UGT1A7 gene. *Pharmacogenet Genomics.* 2000;10(7):629-44.
78. Reimers A, Sjursen W, Helde G, Brodtkorb E. Frequencies of UGT1A4*2 (P24T) and *3 (L48V) and their effects on serum concentrations of lamotrigine. *Eur J Drug Metab Pharmacokinet.* 2016;41(2):149-55.
79. He X, Hesse LM, Hazarika S, Masse G, Harmatz JS, Greenblatt DJ, et al. Evidence for oxazepam as an in vivo probe of UGT2B15: oxazepam clearance is reduced by UGT2B15 D85Y polymorphism but unaffected by UGT2B17 deletion. *Br J Clin Pharmacol.* 2009;68(5):721-30.

80. Fowler S, Kletzl H, Finel M, Manevski N, Schmid P, Tuerck D, et al. A UGT2B10 Splicing Polymorphism Common in African Populations May Greatly Increase Drug Exposure. *J Pharmacol Exp Ther.* 2015;352(2):358-67.
81. Glatard A, Guidi M, Dobrinas M, Cornuz J, Csajka C, Eap CB. Influence of body weight and UGT2B7 polymorphism on varenicline exposure in a cohort of smokers from the general population. *Eur J Clin Pharmacol.* 2019;75(7):939-49.
82. Holthe M, Rakvåg TN, Klepstad P, Idle JR, Kaasa S, Krokan HE, et al. Sequence variations in the UDP-glucuronosyltransferase 2B7 (UGT2B7) gene: identification of 10 novel single nucleotide polymorphisms (SNPs) and analysis of their relevance to morphine glucuronidation in cancer patients. *The Pharmacogenomics Journal.* 2003;3(1):17-26.
83. Wang P, Lin X-Q, Cai W-K, Xu G-L, Zhou M-D, Yang M, et al. Effect of UGT2B7 genotypes on plasma concentration of valproic acid: a meta-analysis. *Eur J Clin Pharmacol.* 2018;74(4):433-42.
84. Wang YH, Trucksis M, McElwee JJ, Wong PH, Maciolek C, Thompson CD, et al. UGT2B17 genetic polymorphisms dramatically affect the pharmacokinetics of MK-7246 in healthy subjects in a first-in-human study. *Clin Pharmacol Ther.* 2012;92(1):96-102.
85. FDA. Drug Development and Drug Interactions: Table of Substrates, Inhibitors and Inducers. 2020.
86. Zientek MA, Youdim K. Reaction phenotyping: advances in the experimental strategies used to characterize the contribution of drug-metabolizing enzymes. *Drug Metab Dispos.* 2015;43(1):163-81.
87. Badee J, Qiu N, Parrott NJ, Collier AC, Schmidt S, Fowler S. Optimization of Experimental Conditions of Automated Glucuronidation Assays in Human Liver Microsomes using a Cocktail Approach and Ultra-High Performance Liquid Chromatography-Tandem Mass Spectrometry. *Drug Metab Disposition.* 2018;dmd.118.084301.
88. Busse D, Leandersson S, Amberntsson S, Darnell M, Hilgendorf C. Industrial Approach to Determine the Relative Contribution of Seven Major UGT Isoforms to Hepatic Glucuronidation. *J Pharm Sci.* 2020;109(7):2309-20.
89. Walsky RL, Bauman JN, Bourcier K, Giddens G, Lapham K, Negahban A, et al. Optimized Assays for Human UDP-Glucuronosyltransferase (UGT) Activities: Altered Alamethicin

- Concentration and Utility to Screen for UGT Inhibitors. *Drug Metab Disposition*. 2012;40(5):1051-65.
90. Uchaipichat V, Mackenzie PI, Elliot DJ, Miners JO. Selectivity of substrate (trifluoperazine) and inhibitor (amitriptyline, androsterone, canrenoic acid, hecogenin, phenylbutazone, quinidine, quinine, and sulfinpyrazone) "probes" for human udp-glucuronosyltransferases. *Drug Metab Dispos*. 2006;34(3):449-56.
 91. Uchaipichat V, Winner LK, Mackenzie PI, Elliot DJ, Williams JA, Miners JO. Quantitative prediction of in vivo inhibitory interactions involving glucuronidated drugs from in vitro data: the effect of fluconazole on zidovudine glucuronidation. *Br J Clin Pharmacol*. 2006;61(4):427-39.
 92. Miners JO, Bowalgaha K, Elliot DJ, Baranczewski P, Knights KM. Characterization of niflumic acid as a selective inhibitor of human liver microsomal UDP-glucuronosyltransferase 1A9: application to the reaction phenotyping of acetaminophen glucuronidation. *Drug Metab Dispos*. 2011;39(4):644-52.
 93. Fisher MB, Campanale K, Ackermann BL, VandenBranden M, Wrighton SA. In vitro glucuronidation using human liver microsomes and the pore-forming peptide alamethicin. *Drug Metab Dispos*. 2000;28(5):560-6.
 94. Manevski N, Moreolo PS, Yli-Kauhaluoma J, Finel M. Bovine Serum Albumin Decreases Km Values of Human UDP-Glucuronosyltransferases 1A9 and 2B7 and Increases Vmax Values of UGT1A9. *Drug Metab Disposition*. 2011;39(11):2117.
 95. Asha S, Vidyavathi M. Role of Human Liver Microsomes in In Vitro Metabolism of Drugs—A Review. *Appl Biochem Biotechnol*. 2010;160(6):1699-722.
 96. Crespi CL, Miller VP. The use of heterologously expressed drug metabolizing enzymes— state of the art and prospects for the future. *Pharmacol Ther*. 1999;84(2):121-31.
 97. Godoy P, Hewitt NJ, Albrecht U, Andersen ME, Ansari N, Bhattacharya S, et al. Recent advances in 2D and 3D in vitro systems using primary hepatocytes, alternative hepatocyte sources and non-parenchymal liver cells and their use in investigating mechanisms of hepatotoxicity, cell signaling and ADME. *Arch Toxicol*. 2013;87(8):1315-530.
 98. McGinnity DF, Soars MG, Urbanowicz RA, Riley RJ. Evaluation of fresh and cryopreserved hepatocytes as in vitro drug metabolism tool for the prediction of metabolic clearance. *Drug Metab Disposition*. 2004;32(11):1247-53.

99. Smith CM, Nolan CK, Edwards MA, Hatfield JB, Stewart TW, Ferguson SS, et al. A comprehensive evaluation of metabolic activity and intrinsic clearance in suspensions and monolayer cultures of cryopreserved primary human hepatocytes. *J Pharm Sci.* 2012;101(10):3989-4002.
100. Olsavsky Goyak KM, Laurenzana EM, Omiecinski CJ. Hepatocyte differentiation. *Methods in molecular biology (Clifton, NJ).* 2010;640:115-38.
101. Vinken M, Hengstler JG. Characterization of hepatocyte-based in vitro systems for reliable toxicity testing. *Arch Toxicol.* 2018;92(10):2981-6.
102. Li AP. Human hepatocytes: Isolation, cryopreservation and applications in drug development. *Chem Biol Interact.* 2007;168(1):16-29.
103. Richert L, Liguori MJ, Abadie C, Heyd B, Manton G, Halkic N, et al. Gene expression in human hepatocytes in suspension after isolation is similar to the liver of origin, is not affected by hepatocyte cold storage and cryopreservation, but is strongly changed after hepatocyte plating. *Drug Metab Dispos.* 2006;34(5):870-9.
104. Hultman I, Vedin C, Abrahamsson A, Winiwarter S, Darnell M. Use of H μ REL Human Coculture System for Prediction of Intrinsic Clearance and Metabolite Formation for Slowly Metabolized Compounds. *Mol Pharm.* 2016;13(8):2796-807.
105. Khetani SR, Bhatia SN. Microscale culture of human liver cells for drug development. *Nat Biotechnol.* 2007;26:120.
106. Andersson TB. Evolution of Novel 3D Culture Systems for Studies of Human Liver Function and Assessments of the Hepatotoxicity of Drugs and Drug Candidates. *Basic Clin Pharmacol Toxicol.* 2017;121(4):234-8.
107. Bell CC, Hendriks DF, Moro SM, Ellis E, Walsh J, Renblom A, et al. Characterization of primary human hepatocyte spheroids as a model system for drug-induced liver injury, liver function and disease. *Sci Rep.* 2016;6:25187.
108. Kratochwil NA, Meille C, Fowler S, Klammers F, Ekiciler A, Molitor B, et al. Metabolic Profiling of Human Long-Term Liver Models and Hepatic Clearance Predictions from In Vitro Data Using Nonlinear Mixed-Effects Modeling. *The AAPS Journal.* 2017;19(2):534-50.
109. Lin C, Shi J, Moore A, Khetani SR. Prediction of Drug Clearance and Drug-Drug Interactions in Microscale Cultures of Human Hepatocytes. *Drug Metab Dispos.* 2016;44(1):127-36.

110. Kratochwil NA, Triyatni M, Mueller MB, Klammers F, Leonard B, Turley D, et al. Simultaneous Assessment of Clearance, Metabolism, Induction, and Drug-Drug Interaction Potential Using a Long-Term In Vitro Liver Model for a Novel Hepatitis B Virus Inhibitor. *J Pharmacol Exp Ther*. 2018;365(2):237-48.
111. Mizoi K, Hosono M, Kojima H, Ogihara T. Establishment of a primary human hepatocyte spheroid system for evaluating metabolic toxicity using dacarbazine under conditions of CYP1A2 induction. *Drug Metab Pharmacokinet*. 2020;35(2):201-6.
112. Huh D, Hamilton GA, Ingber DE. From 3D cell culture to organs-on-chips. *Trends Cell Biol*. 2011;21(12):745-54.
113. Nakao Y, Kimura H, Sakai Y, Fujii T. Bile canaliculi formation by aligning rat primary hepatocytes in a microfluidic device. *Biomicrofluidics*. 2011;5(2):022212.
114. Allen JW, Khetani SR, Bhatia SN. In Vitro Zonation and Toxicity in a Hepatocyte Bioreactor. *Toxicol Sci*. 2004;84(1):110-9.
115. Imura Y, Sato K, Yoshimura E. Micro Total Bioassay System for Ingested Substances: Assessment of Intestinal Absorption, Hepatic Metabolism, and Bioactivity. *Anal Chem*. 2010;82(24):9983-8.
116. Imura Y, Asano Y, Sato K, Yoshimura E. A microfluidic system to evaluate intestinal absorption. *Anal Sci*. 2009;25(12):1403-7.
117. Sung KE, Yang N, Pehlke C, Keely PJ, Eliceiri KW, Friedl A, et al. Transition to invasion in breast cancer: a microfluidic in vitro model enables examination of spatial and temporal effects. *Integrative Biology*. 2010;3(4):439-50.
118. Puleo CM, McIntosh Ambrose W, Takezawa T, Elisseff J, Wang T-H. Integration and application of vitrified collagen in multilayered microfluidic devices for corneal microtissue culture. *Lab on a Chip*. 2009;9(22):3221-7.
119. Dehne E-M, Hasenberg T, Marx U. The ascendance of microphysiological systems to solve the drug testing dilemma. *Future Science OA*. 2017;3(2):FSO0185.
120. Tsamandouras N, Chen WLK, Edington CD, Stokes CL, Griffith LG, Cirit M. Integrated Gut and Liver Microphysiological Systems for Quantitative In Vitro Pharmacokinetic Studies. *The AAPS Journal*. 2017;19(5):1499-512.

121. Tsamandouras N, Kostrzewski T, Stokes CL, Griffith LG, Hughes DJ, Cirit M. Quantitative Assessment of Population Variability in Hepatic Drug Metabolism Using a Perfused Three-Dimensional Human Liver Microphysiological System. *J Pharmacol Exp Ther*. 2017;360(1):95-105.
122. Bae M, Yi HG, Jang J, Cho DW. Microphysiological Systems for Neurodegenerative Diseases in Central Nervous System. *Micromachines (Basel)*. 2020;11(9).
123. Özkan A, Stolley D, Cressman ENK, McMillin M, DeMorrow S, Yankeelov TE, et al. The Influence of Chronic Liver Diseases on Hepatic Vasculature: A Liver-on-a-chip Review. *Micromachines*. 2020;11(5):487.
124. Ryan H, Simmons CS. Potential Applications of Microfluidics to Acute Kidney Injury Associated with Viral Infection. *Cell Mol Bioeng*. 2020;13(4):1-7.
125. Low LA, Giulianotti MA. Tissue Chips in Space: Modeling Human Diseases in Microgravity. *Pharm Res*. 2019;37(1):8.
126. Fowler S, Chen WLK, Duignan DB, Gupta A, Hariparsad N, Kenny JR, et al. Microphysiological systems for ADME-related applications: current status and recommendations for system development and characterization. *Lab on a Chip*. 2020;20(3):446-67.
127. Hughes DJ, Kostrzewski T, Sceats EL. Opportunities and challenges in the wider adoption of liver and interconnected microphysiological systems. *Exp Biol Med*. 2017;242(16):1593-604.
128. Sung JH, Wang Y, Shuler ML. Strategies for using mathematical modeling approaches to design and interpret multi-organ microphysiological systems (MPS). *APL Bioengineering*. 2019;3(2):021501.
129. Wang YI, Carmona C, Hickman JJ, Shuler ML. Multiorgan Microphysiological Systems for Drug Development: Strategies, Advances, and Challenges. *Adv Healthc Mater*. 2018;7(2).
130. Low LA, Tagle DA. Organs-on-chips: Progress, challenges, and future directions. *Exp Biol Med (Maywood)*. 2017;242(16):1573-8.
131. Maass C, Stokes CL, Griffith LG, Cirit M. Multi-functional scaling methodology for translational pharmacokinetic and pharmacodynamic applications using integrated microphysiological systems (MPS). *Integr Biol (Camb)*. 2017;9(4):290-302.
132. Abaci HE, Shuler ML. Human-on-a-chip design strategies and principles for physiologically based pharmacokinetics/pharmacodynamics modeling. *Integr Biol (Camb)*. 2015;7(4):383-91.

133. Oleaga C, Riu A, Rothmund S, Lavado A, McAleer CW, Long CJ, et al. Investigation of the effect of hepatic metabolism on off-target cardiotoxicity in a multi-organ human-on-a-chip system. *Biomaterials*. 2018;182:176-90.
134. Ouattara DA, Choi S-H, Sakai Y, Péry ARR, Brochot C. Kinetic modelling of in vitro cell-based assays to characterize non-specific bindings and ADME processes in a static and a perfused fluidic system. *Toxicol Lett*. 2011;205(3):310-9.
135. Prot JM, Maciel L, Bricks T, Merlier F, Cotton J, Paullier P, et al. First pass intestinal and liver metabolism of paracetamol in a microfluidic platform coupled with a mathematical modeling as a means of evaluating ADME processes in humans. *Biotechnol Bioeng*. 2014;111(10):2027-40.
136. Varma MV, El-Kattan AF, Feng B, Steyn SJ, Maurer TS, Scott DO, et al. Extended Clearance Classification System (ECCS) informed approach for evaluating investigational drugs as substrates of drug transporters. *Clin Pharmacol Ther*. 2017;102(1):33-6.
137. Varma MV, Steyn SJ, Allerton C, El-Kattan AF. Predicting Clearance Mechanism in Drug Discovery: Extended Clearance Classification System (ECCS). *Pharm Res*. 2015;32(12):3785-802.
138. Amidon GL, Lennernäs H, Shah VP, Crison JR. A Theoretical Basis for a Biopharmaceutic Drug Classification: The Correlation of in Vitro Drug Product Dissolution and in Vivo Bioavailability. *Pharm Res*. 1995;12(3):413-20.
139. Lennernäs H, Abrahamsson B. The use of biopharmaceutic classification of drugs in drug discovery and development: current status and future extension. *J Pharm Pharmacol*. 2005;57(3):273-85.
140. Réda C, Kaufmann E, Delahaye-Duriez A. Machine learning applications in drug development. *Computational and Structural Biotechnology Journal*. 2020;18:241-52.
141. Kar S, Leszczynski J. Recent Advances of Computational Modeling for Predicting Drug Metabolism: A Perspective. *Curr Drug Metab*. 2017;18(12):1106-22.
142. Wu F, Zhou Y, Li L, Shen X, Chen G, Wang X, et al. Computational Approaches in Preclinical Studies on Drug Discovery and Development. *Frontiers in Chemistry*. 2020;8(726).
143. Zhang H, Xiang M-L, Ma C-Y, Huang Q, Li W, Xie Y, et al. Three-class classification models of logS and logP derived by using GA–CG–SVM approach. *Mol Divers*. 2009;13(2):261.

144. Paine SW, Barton P, Bird J, Denton R, Menochet K, Smith A, et al. A rapid computational filter for predicting the rate of human renal clearance. *J Mol Graph Model*. 2010;29(4):529-37.
145. Administration USDoHaHS-FaD. Challenge and Opportunity on the Critical Path to New Medical Technologies. 2004.
146. Lalonde RL, Kowalski KG, Hutmacher MM, Ewy W, Nichols DJ, Milligan PA, et al. Model-based drug development. *Clin Pharmacol Ther*. 2007;82(1):21-32.
147. Kim TH, Shin S, Shin BS. Model-based drug development: application of modeling and simulation in drug development. *Journal of Pharmaceutical Investigation*. 2018;48(4):431-41.
148. Bonate PL. Pharmacokinetic-pharmacodynamic modeling and simulation: Springer; 2011.
149. Mould DR, Upton RN. Basic concepts in population modeling, simulation, and model-based drug development. *CPT: pharmacometrics & systems pharmacology*. 2012;1(9):e6-e.
150. Mould DR, Upton RN. Basic concepts in population modeling, simulation, and model-based drug development-part 2: introduction to pharmacokinetic modeling methods. *CPT Pharmacometrics Syst Pharmacol*. 2013;2(4):e38.
151. Upton RN, Mould DR. Basic concepts in population modeling, simulation, and model-based drug development: part 3-introduction to pharmacodynamic modeling methods. *CPT: pharmacometrics & systems pharmacology*. 2014;3(1):e88-e.
152. Johan Gabrielsson DW. Pharmacokinetic and Pharmacodynamic Data Analysis - Concepts and Applications. Swedish Pharmaceutical Press. 2016.
153. Jones HM, Parrott N, Jorga K, Lavé T. A novel strategy for physiologically based predictions of human pharmacokinetics. *Clin Pharmacokinet*. 2006;45(5):511-42.
154. Jones HM, Mayawala K, Poulin P. Dose selection based on physiologically based pharmacokinetic (PBPK) approaches. *The AAPS journal*. 2013;15(2):377-87.
155. Peters SA, Petersson C, Blaukat A, Halle J-P, Dolgos H. Prediction of active human dose: learnings from 20 years of Merck KGaA experience, illustrated by case studies. *Drug Discov Today*. 2020;25(5):909-19.
156. Zou P, Yu Y, Zheng N, Yang Y, Paholak HJ, Yu LX, et al. Applications of human pharmacokinetic prediction in first-in-human dose estimation. *Aaps j*. 2012;14(2):262-81.

157. Miller NA, Reddy MB, Heikkinen AT, Lukacova V, Parrott N. Physiologically Based Pharmacokinetic Modelling for First-In-Human Predictions: An Updated Model Building Strategy Illustrated with Challenging Industry Case Studies. *Clin Pharmacokinet.* 2019;58(6):727-46.
158. Weber O, Willmann S, Bischoff H, Li V, Vakalopoulos A, Lustig K, et al. Prediction of a potentially effective dose in humans for BAY 60-5521, a potent inhibitor of cholesteryl ester transfer protein (CETP) by allometric species scaling and combined pharmacodynamic and physiologically-based pharmacokinetic modelling. *Br J Clin Pharmacol.* 2012;73(2):219-31.
159. Boettcher MF, Heinig R, Schmeck C, Kohlsdorfer C, Ludwig M, Schaefer A, et al. Single dose pharmacokinetics, pharmacodynamics, tolerability and safety of BAY 60-5521, a potent inhibitor of cholesteryl ester transfer protein. *Br J Clin Pharmacol.* 2012;73(2):210-8.
160. Zhuang X, Lu C. PBPK modeling and simulation in drug research and development. *Acta Pharmaceutica Sinica B.* 2016;6(5):430-40.
161. Jones HM, Chen Y, Gibson C, Heimbach T, Parrott N, Peters SA, et al. Physiologically based pharmacokinetic modeling in drug discovery and development: a pharmaceutical industry perspective. *Clin Pharmacol Ther.* 2015;97(3):247-62.
162. Shebley M, Sandhu P, Emami Riedmaier A, Jamei M, Narayanan R, Patel A, et al. Physiologically Based Pharmacokinetic Model Qualification and Reporting Procedures for Regulatory Submissions: A Consortium Perspective. *Clin Pharmacol Ther.* 2018;104(1):88-110.
163. Tsamandouras N, Rostami-Hodjegan A, Aarons L. Combining the 'bottom up' and 'top down' approaches in pharmacokinetic modelling: fitting PBPK models to observed clinical data. *Br J Clin Pharmacol.* 2015;79(1):48-55.
164. Grimstein M, Yang Y, Zhang X, Grillo J, Huang SM, Zineh I, et al. Physiologically Based Pharmacokinetic Modeling in Regulatory Science: An Update From the U.S. Food and Drug Administration's Office of Clinical Pharmacology. *J Pharm Sci.* 2019;108(1):21-5.
165. Lin L, Wong H. Predicting Oral Drug Absorption: Mini Review on Physiologically-Based Pharmacokinetic Models. *Pharmaceutics.* 2017;9(4).
166. Peters SA. Physiological Model for Absorption. *Physiologically-Based Pharmacokinetic (PBPK) Modeling and Simulations* 2012. p. 43-88.

167. Stillhart C, Pepin X, Tistaert C, Good D, Van Den Bergh A, Parrott N, et al. PBPK Absorption Modeling: Establishing the In Vitro–In Vivo Link—Industry Perspective. *The AAPS Journal*. 2019;21(2):19.
168. Chung J, Kesisoglou F. Physiologically Based Oral Absorption Modelling to Study Gut-Level Drug Interactions. *J Pharm Sci*. 2018;107(1):18-23.
169. Tistaert C, Heimbach T, Xia B, Parrott N, Samant TS, Kesisoglou F. Food Effect Projections via Physiologically Based Pharmacokinetic Modeling: Predictive Case Studies. *J Pharm Sci*. 2019;108(1):592-602.
170. Heikkinen AT, Baneyx G, Caruso A, Parrott N. Application of PBPK modeling to predict human intestinal metabolism of CYP3A substrates - an evaluation and case study using GastroPlus. *Eur J Pharm Sci*. 2012;47(2):375-86.
171. Peters SA. Physiological Model for Distribution. *Physiologically-Based Pharmacokinetic (PBPK) Modeling and Simulations* 2012. p. 89-117.
172. Berezhkovskiy LM. Volume of Distribution at Steady State for a Linear Pharmacokinetic System with Peripheral Elimination. *J Pharm Sci*. 2004;93(6):1628-40.
173. Rodgers T, Leahy D, Rowland M. Physiologically based pharmacokinetic modeling 1: predicting the tissue distribution of moderate-to-strong bases. *J Pharm Sci*. 2005;94(6):1259-76.
174. Rodgers T, Rowland M. Physiologically based pharmacokinetic modelling 2: Predicting the tissue distribution of acids, very weak bases, neutrals and zwitterions. *J Pharm Sci*. 2006;95(6):1238-57.
175. Poulin P, Theil FP. Prediction of pharmacokinetics prior to in vivo studies. 1. Mechanism-based prediction of volume of distribution. *J Pharm Sci*. 2002;91(1):129-56.
176. Li R, Ghosh A, Maurer TS, Kimoto E, Barton HA. Physiologically Based Pharmacokinetic Prediction of Telmisartan in Human. *Drug Metab Disposition*. 2014;42(10):1646.
177. Plaa GL. The Enterohepatic Circulation. In: Gillette JR, Mitchell JR, editors. *Concepts in Biochemical Pharmacology: Part 3*. Berlin, Heidelberg: Springer Berlin Heidelberg; 1975. p. 130-49.
178. Guo Y, Chu X, Parrott NJ, Brouwer KLR, Hsu V, Nagar S, et al. Advancing Predictions of Tissue and Intracellular Drug Concentrations Using In Vitro, Imaging and Physiologically Based Pharmacokinetic Modeling Approaches. *Clin Pharmacol Ther*. 2018;104(5):865-89.

179. Rose RH, Neuhoff S, Abduljalil K, Chetty M, Rostami-Hodjegan A, Jamei M. Application of a Physiologically Based Pharmacokinetic Model to Predict OATP1B1-Related Variability in Pharmacodynamics of Rosuvastatin. *CPT Pharmacometrics Syst Pharmacol*. 2014;3(7):e124.
180. Chapy H, Klieber S, Brun P, Gerbal-Chaloin S, Boulenc X, Nicolas O. PBPK modeling of irbesartan: incorporation of hepatic uptake. *Biopharm Drug Dispos*. 2015;36(8):491-506.
181. Sato M, Toshimoto K, Tomaru A, Yoshikado T, Tanaka Y, Hisaka A, et al. Physiologically Based Pharmacokinetic Modeling of Bosentan Identifies the Saturable Hepatic Uptake As a Major Contributor to Its Nonlinear Pharmacokinetics. *Drug Metab Disposition*. 2018;46(5):740-8.
182. Li Z, Gao Y, Yang C, Xiang Y, Zhang W, Zhang T, et al. Assessment and Confirmation of Species Difference in Nonlinear Pharmacokinetics of Atipamezole with Physiologically Based Pharmacokinetic Modeling. *Drug Metab Disposition*. 2019;dmd.119.089151.
183. Fowler S, Morcos PN, Cleary Y, Martin-Facklam M, Parrott N, Gertz M, et al. Progress in Prediction and Interpretation of Clinically Relevant Metabolic Drug-Drug Interactions: a Minireview Illustrating Recent Developments and Current Opportunities. *Current Pharmacology Reports*. 2017;3(1):36-49.
184. Chen Y, Mao J, Hop CE. Physiologically based pharmacokinetic modeling to predict drug-drug interactions involving inhibitory metabolite: a case study of amiodarone. *Drug Metab Dispos*. 2015;43(2):182-9.
185. Yee KL, Cabalu TD, Kuo Y, Fillgrove KL, Liu Y, Triantafyllou I, et al. Physiologically Based Pharmacokinetic Modeling of Doravirine and Its Major Metabolite to Support Dose Adjustment With Rifabutin. *The Journal of Clinical Pharmacology*.n/a(n/a).
186. Asaumi R, Toshimoto K, Tobe Y, Hashizume K, Nunoya K-I, Imawaka H, et al. Comprehensive PBPK Model of Rifampicin for Quantitative Prediction of Complex Drug-Drug Interactions: CYP3A/2C9 Induction and OATP Inhibition Effects. *CPT: pharmacometrics & systems pharmacology*. 2018;7(3):186-96.
187. Zhou L, Sharma P, Yeo KR, Higashimori M, Xu H, Al-Huniti N, et al. Assessing pharmacokinetic differences in Caucasian and East Asian (Japanese, Chinese and Korean) populations driven by CYP2C19 polymorphism using physiologically-based pharmacokinetic modelling. *Eur J Pharm Sci*. 2019;139:105061.
188. Ye L, Ke M, You X, Huang P, Lin C. A Physiologically Based Pharmacokinetic Model of Ertapenem in Pediatric Patients With Renal Impairment. *J Pharm Sci*. 2020;109(9):2909-18.

189. Johnson TN, Cleary Y, Parrott N, Reigner B, Smith JR, Toovey S. Development of a physiologically based pharmacokinetic model for mefloquine and its application alongside a clinical effectiveness model to select an optimal dose for prevention of malaria in young Caucasian children. *Br J Clin Pharmacol*. 2019;85(1):100-13.
190. Morcos PN, Cleary Y, Sturm-Pellanda C, Guerini E, Abt M, Donzelli M, et al. Effect of Hepatic Impairment on the Pharmacokinetics of Alectinib. *The Journal of Clinical Pharmacology*. 2018;58(12):1618-28.
191. Chetty M, Rose RH, Abduljalil K, Patel N, Lu G, Cain T, et al. Applications of linking PBPK and PD models to predict the impact of genotypic variability, formulation differences, differences in target binding capacity and target site drug concentrations on drug responses and variability. *Front Pharmacol*. 2014;5(258).
192. Bhatia SN, Ingber DE. Microfluidic organs-on-chips. *Nat Biotechnol*. 2014;32(8):760-72.
193. Esch EW, Bahinski A, Huh D. Organs-on-chips at the frontiers of drug discovery. *Nature Reviews Drug Discovery*. 2015;14(4):248-60.
194. Sutherland ML, Fabre KM, Tagle DA. The National Institutes of Health Microphysiological Systems Program focuses on a critical challenge in the drug discovery pipeline. *Stem Cell Res Ther*. 2013;4 Suppl 1(Suppl 1):I1.
195. Docci L, Parrott N, Krahenbuhl S, Fowler S. Application of New Cellular and Microphysiological Systems to Drug Metabolism Optimization and Their Positioning Respective to In Silico Tools. *SLAS Discov*. 2019;24(5):523-36.
196. Baudy AR, Otieno MA, Hewitt P, Gan J, Roth A, Keller D, et al. Liver microphysiological systems development guidelines for safety risk assessment in the pharmaceutical industry. *Lab Chip*. 2019.
197. Wandel C, Böcker R, Böhrer H, Browne A, Rügheimer E, Martin E. Midazolam is metabolized by at least three different cytochrome P450 enzymes. *Br J Anaesth*. 1994;73(5):658-61.
198. Kerry NL, Somogyi AA, Bochner F, Mikus G. The role of CYP2D6 in primary and secondary oxidative metabolism of dextromethorphan: in vitro studies using human liver microsomes. *Br J Clin Pharmacol*. 1994;38(3):243-8.
199. Wei T. The Metabolism of Diclofenac - Enzymology and Toxicology Perspectives. *Curr Drug Metab*. 2003;4(4):319-29.

200. King C, Tang W, Ngui J, Tephly T, Braun M. Characterization of Rat and Human UDP-Glucuronosyltransferases Responsible for the in Vitro Glucuronidation of Diclofenac. *Toxicol Sci.* 2001;61(1):49-53.
201. Nielsen TL, Rasmussen BB, Flinois J-P, Beaune P, Brøsen K. In Vitro Metabolism of Quinidine: The (3S)-3-Hydroxylation of Quinidine Is a Specific Marker Reaction for Cytochrome P-4503A4 Activity in Human Liver Microsomes. *J Pharmacol Exp Ther.* 1999;289(1):31.
202. Uehara S, Yoneda N, Higuchi Y, Yamazaki H, Suemizu H. Human Aldehyde Oxidase 1–Mediated Carbazeren Oxidation in Chimeric TK-NOG Mice Transplanted with Human Hepatocytes. *Drug Metab Disposition.* 2020;48(7):580-6.
203. Säll C, Houston JB, Galetin A. A Comprehensive Assessment of Repaglinide Metabolic Pathways: Impact of Choice of In Vitro System and Relative Enzyme Contribution to In Vitro Clearance. *Drug Metab Disposition.* 2012;40(7):1279-89.
204. Yamada A, Maeda K, Ishiguro N, Tsuda Y, Igarashi T, Ebner T, et al. The impact of pharmacogenetics of metabolic enzymes and transporters on the pharmacokinetics of telmisartan in healthy volunteers. *Pharmacogenet Genomics.* 2011;21(9):523-30.
205. Ghosal A, Hapangama N, Yuan Y, Achanfuo-Yeboah J, Iannucci R, Chowdhury S, et al. Identification of human UDP-glucuronosyltransferase enzyme(s) responsible for the glucuronidation of posaconazole (Noxafil). *Drug Metab Dispos.* 2004;32(2):267-71.
206. Di Marco A, D'Antoni M, Attaccalite S, Carotenuto P, Laufer R. Determination of drug glucuronidation and UDP-glucuronosyltransferase selectivity using a 96-well radiometric assay. *Drug Metab Dispos.* 2005;33(6):812-9.
207. Barbier O, Turgeon D, Girard C, Green MD, Tephly TR, Hum DW, et al. 3'-azido-3'-deoxythymidine (AZT) is glucuronidated by human UDP-glucuronosyltransferase 2B7 (UGT2B7). *Drug Metab Dispos.* 2000;28(5):497-502.
208. Uchaipichat V, Suthisisang C, Miners JO. The Glucuronidation of R- and S-Lorazepam: Human Liver Microsomal Kinetics, UDP-Glucuronosyltransferase Enzyme Selectivity, and Inhibition by Drugs. *Drug Metab Disposition.* 2013;41(6):1273.
209. Li R, Kimoto E, Niosi M, Tess DA, Lin J, Tremaine LM, et al. A Study on Pharmacokinetics of Bosentan with Systems Modeling, Part 2: Prospectively Predicting Systemic and Liver Exposure in Healthy Subjects. *Drug Metab Dispos.* 2018;46(4):357-66.

210. Baudy AR, Otieno MA, Hewitt P, Gan J, Roth A, Keller D, et al. Liver microphysiological systems development guidelines for safety risk assessment in the pharmaceutical industry. *Lab on a Chip*. 2020;20(2):215-25.
211. Docci L, Klammers F, Ekiciler A, Molitor B, Umehara K, Walter I, et al. In Vitro to In Vivo Extrapolation of Metabolic Clearance for UGT Substrates Using Short-Term Suspension and Long-Term Co-cultured Human Hepatocytes. *The AAPS Journal*. 2020;22(6):131.
212. Docci L, Umehara K, Krähenbühl S, Fowler S, Parrott N. Construction and Verification of Physiologically Based Pharmacokinetic Models for Four Drugs Majorly Cleared by Glucuronidation: Lorazepam, Oxazepam, Naloxone, and Zidovudine. *The AAPS Journal*. 2020;22(6):128.
213. Wood FL, Houston JB, Hallifax D. Clearance Prediction Methodology Needs Fundamental Improvement: Trends Common to Rat and Human Hepatocytes/Microsomes and Implications for Experimental Methodology. *Drug Metab Dispos*. 2017;45(11):1178-88.
214. Riccardi KA, Tess DA, Lin J, Patel R, Ryu S, Atkinson K, et al. A Novel Unified Approach to Predict Human Hepatic Clearance for Both Enzyme- and Transporter-Mediated Mechanisms Using Suspended Human Hepatocytes. *Drug Metab Disposition*. 2019;dmd.118.085639.
215. Chan TS, Yu H, Moore A, Khetani SR, Tweedie D. Meeting the challenge of predicting hepatic clearance of compounds slowly metabolized by cytochrome P450 using a novel hepatocyte model, HepatoPac. *Drug Metab Dispos*. 2013;41(12):2024-32.
216. Da-Silva F, Boulenc X, Vermet H, Compigne P, Gerbal-Chaloin S, Daujat-Chavanieu M, et al. Improving Prediction of Metabolic Clearance Using Quantitative Extrapolation of Results Obtained From Human Hepatic Micropatterned Cocultures Model and by Considering the Impact of Albumin Binding. *J Pharm Sci*. 2018;107(7):1957-72.
217. Benet LZ, Sodhi JK. Investigating the Theoretical Basis for In Vitro–In Vivo Extrapolation (IVIVE) in Predicting Drug Metabolic Clearance and Proposing Future Experimental Pathways. *The AAPS Journal*. 2020;22(5):120.
218. Williams JA, Hyland R, Jones BC, Smith DA, Hurst S, Goosen TC, et al. Drug-drug interactions for UDP-glucuronosyltransferase substrates: a pharmacokinetic explanation for typically observed low exposure (AUC_i/AUC) ratios. *Drug Metab Dispos*. 2004;32(11):1201-8.

219. Badee J, Qiu N, Collier AC, Takahashi RH, Forrest WF, Parrott N, et al. Characterization of the Ontogeny of Hepatic UDP-Glucuronosyltransferase Enzymes Based on Glucuronidation Activity Measured in Human Liver Microsomes. *J Clin Pharmacol.* 2019;59 Suppl 1:S42-s55.
220. Badée J, Fowler S, de Wildt SN, Collier AC, Schmidt S, Parrott N. The Ontogeny of UDP-glucuronosyltransferase Enzymes, Recommendations for Future Profiling Studies and Application Through Physiologically Based Pharmacokinetic Modelling. *Clin Pharmacokinet.* 2018.